ABSTRACT

In digital transmission systems the nonideal channel introduces distortion that must be compensated for to provide reliable communication, a process known as *equalization*. Recently there has been a great interest in the problem of *blind* equalization of digital communication channels, in which the equalizer is computed by the receiver without aid from the transmitter. This disposes of the need for sending training signals, leading to higher bandwidth efficiency.

Many real world channels distort signals in a nonlinear fashion. However, most of the literature on blind equalization is devoted to the linear case. This thesis addresses the blind equalization problem for nonlinear single-input multiple-output digital communication channels, based on the second order statistics (SOS) of the received signal. The required channel diversity can be obtained by using several sensors and/or by oversampling the received signal. In the latter case, the overall system can be cast in a multirate framework. We provide the basic elements of a theory of multirate nonlinear systems.

We consider the class of 'linear in the parameters' channels, which can be seen as multiple-input systems in which the additional inputs are nonlinear functions of the signal of interest. These models include (but are not limited to) polynomial approximations of nonlinear systems. Although any SOS-based method can only identify the channel to within a mixing matrix (at best), sufficient conditions are given to ensure that the ambiguity is at a level that still allows for the computation of linear finite impulse response equalizers from the received signal SOS, should such equalizers exist. These conditions involve only statistical characteristics of the input signal and the channel nonlinearities and can therefore be checked *a priori*. Based on these conditions, blind algorithms are developed for the computation of the linear equalizers in the case of independent sources. For correlated sources, a novel algorithm is also given for the linear channel case. The new algorithms compare favorably to previous approaches which do not fully exploit all the information available at the receiver.

Abstract approved: ______________________
Thesis supervisor

____
Title and department

____
Date

BLIND EQUALIZATION OF LINEAR AND NONLINEAR DIGITAL COMMUNICATION CHANNELS FROM SECOND ORDER STATISTICS

by

Roberto López-Valcarce

An Abstract

Of a thesis submitted in partial fulfillment of the
requirements for the Doctor of Philosophy degree
in Electrical and Computer Engineering
in the Graduate College of
The University of Iowa

December 2000

Thesis supervisor: Professor Soura Dasgupta

BLIND EQUALIZATION OF LINEAR AND NONLINEAR DIGITAL COMMUNICATION CHANNELS FROM SECOND ORDER STATISTICS

by

Roberto López-Valcarce

A thesis submitted in partial fulfillment of the
requirements for the Doctor of Philosophy degree
in Electrical and Computer Engineering
in the Graduate College of
The University of Iowa

December 2000

Thesis supervisor: Professor Soura Dasgupta

Graduate College
The University of Iowa
Iowa City, Iowa

CERTIFICATE OF APPROVAL

PH.D. THESIS

This is to certify that the Ph.D. thesis of

Roberto López-Valcarce

has been approved by the Examining Committee
for the thesis requirement for the Doctor of Philosophy
degree in Electrical and Computer Engineering at
the December 2000 graduation.

Thesis committee: ______________________
Thesis supervisor

____
Member

____
Member

____
Member

____
Member

ACKNOWLEDGMENTS

I would like to express my appreciation and gratitude to my thesis advisor, Dr. Soura Dasgupta, for his guidance throughout the course of this project and his patience with this student who never got it right at the first time.

I am also grateful to the rest of my thesis committee, Dr. Mark Andersland, Dr. Erwei Bai, Dr. Gary Christensen and Dr. Witold Krajewski for their valuable time and effort. Thanks also to Dr. Zhi Ding for his constructive suggestions in this and other projects.

I am also indebted to my fellow students, Chris Schwarz, Ashish Pandharipande and Jing Liang, for their friendship and many fruitful discussions.

“La libélula” had to put up with me and my habits during these two and a half years. Thanks for all the great cooking, for your encouragement and for being a wonderful friend. I love you.

Most importantly I would like to thank my parents, sister, and grandparents, because it is to them that I owe it all. What they have given me is far more than I will ever be able to return.

TABLE OF CONTENTS

LIST OF FIGURES

LIST OF ALGORITHMS

CHAPTER I

INTRODUCTION

Nowadays, the growing demand for spreading and exchanging information in digital form requires ever increasing transmission capacity. However, increasing the data rate in a digital communication system almost unavoidably translates into a higher level of distortion in the received signal introduced by the communication channel. In particular intersymbol interference (ISI), caused by the distortion introduced by the finite bandwidth and the nonideal characteristics of the devices used in the system, becomes more pronounced at high data rates for which the memory of the channel spans more symbol intervals. This calls for more sophisticated signal processing techniques in the receiver in order to compensate for this effect and yield a reliable data link with an acceptably low error rate, especially when no knowledge of the channel parameters is available *a priori*.

The general model of a digital transmission system considered in this thesis is shown in Figure 1. The source is assumed to produce a stationary random sequence $\{a(k)\}$ of complex random variables, which are the data to be transmitted, at a rate $1/T$. This data sequence is sent to a linear modulator which performs pulse shaping and frequency translation so as to produce the continuous-time physical signal to be transmitted. This signal is bandpass filtered to minimize out of band radiation and then sent through the channel.

The received signal (channel output) is again bandpass filtered to reduce thermal noise and adjacent channel interference effects and then demodulated (translated to the baseband) and sampled. The block labeled 'Equalizer' in Figure 1 has the mission of compensating for the channel induced distortion by adequately processing the sampled signal. The equalizer output is then fed to a decision device (usually a nearest-neighbor classifier) in order to produce an estimate $\{\hat{a}(k-d)\}$ of the transmitted symbol sequence, possibly including a transmission delay $d \geq 0$.

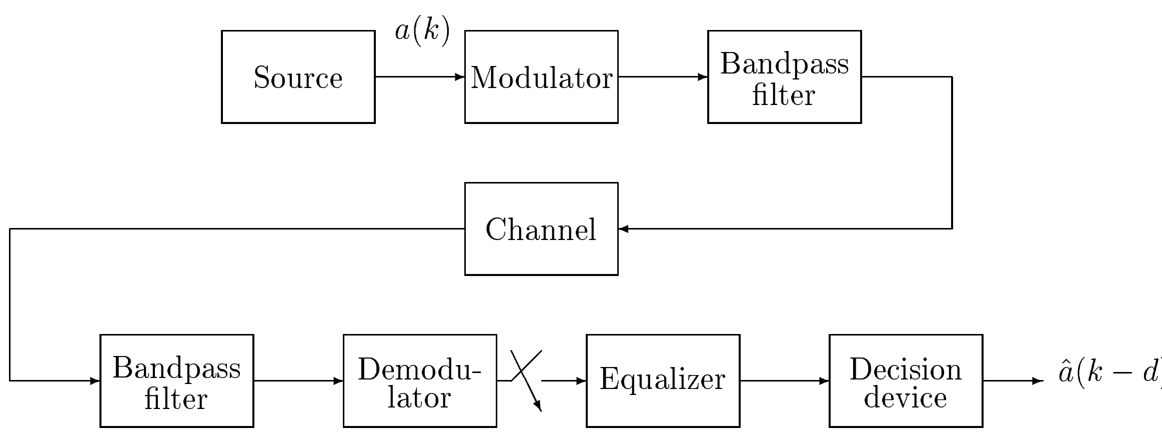

Figure 1: Model for a communications system over a time-dispersive channel.

Although this receiver configuration (equalizer followed by a symbol-by-symbol detector) is known to be suboptimal, it is widely used since it usually provides a good trade-off between computational complexity and performance when compared to the optimal receiver [24].

In this work we are primarily concerned about the effects of ISI in the received signal and the corresponding problem of equalizer design. Hence it will be assumed that the demodulator and sampler are ideal, that is, perfect carrier frequency, carrier phase, and timing recovery are assumed. In addition the channel will be modeled as a time-invariant system with additive noise (assumed statistically independent of the transmitted symbols) at its output. The resulting baseband equivalent system is shown in Figure 2, where now the block labeled 'Time-invariant channel' includes the effects of the physical channel as well as the transmitter and receiver filters.

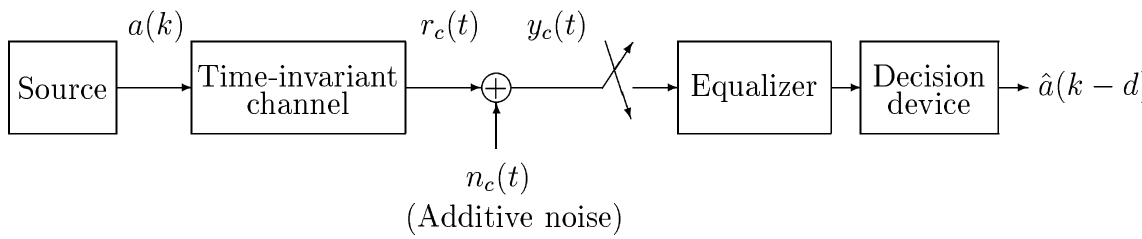

Figure 2: Baseband equivalent model of a communications system.

Traditionally, equalizer design has been based on the knowledge of the channel characteristics, which in most practical situations is not available beforehand. Further in many applications the channel is not exactly time-invariant. One possible approach is to design and use a compromise equalizer which compensates for the average of the range of expected channel characteristics. Sometimes, however, the variation of such characteristics is big enough as to make this approach impractical. In such cases the channel profile can be learned by transmitting a training signal known to the receiver, which uses some kind of adaptation algorithm to identify the channel or directly update the equalizer parameters [25].

In many applications the use of training signals may severely degrade the transmission throughput, particularly for time-varying channels that require frequent retraining. In those cases, blind equalization methods emerge as an attractive alternative. These techniques attempt to obtain the equalizer parameters (either directly or by identifying the channel first) using the received signal and knowledge of the statistics of the transmitted symbols, thus dispensing with the need for training signals. In a general sense, blind equalization approaches can be divided in two categories, depending on the kind of information about the received signal that they exploit: second-order statistics (SOS) methods and higher-order statistics (HOS) methods. HOS methods appeared first as they are the only class of blind techniques applicable to linear single-input single-output (SISO) channels, since the SOS power spectrum of the output of a linear SISO system does not convey information about the channel phase. On the other hand, in recent years there has been considerable interest in SOS methods after the seminal work [29] showed that under certain conditions, linear finite impulse response (FIR) single-input multiple-output (SIMO) channels can be perfectly equalized by means of a bank of FIR filters, whose weights can be computed from knowledge of the SOS of the received signal alone. A SIMO channel can be obtained in practice either by sampling the received continuous-time signal at a rate faster than the symbol rate whenever the continuous-time channel has excess bandwidth, or by deploying multiple sensors at the receiver, or by a combination of both. SOS-based methods are usually preferred since larger sample sets are generally required to form reliable estimates of higher-order statistics.

With a few exceptions [12, 26], the study of SOS-based blind equalization techniques has been devoted to the case of linear channels. Many communication channels, however, are inherently nonlinear. Examples include satellite and microwave links where the amplifiers are operated at or near saturation for power efficiency reasons, magnetic and optical recording channels, physiological systems, etc. Discarding the channel nonlinearities when designing the equalizer may result in significant performance degradation, which is clearly undesirable. On the other hand, nonlinear systems cannot be characterized by transfer functions and hence extensions of equalizer design techniques available for the linear channel case are not straightforward. Most results in nonlinear channel identification apply to SISO channels, based on input-output (i.e. non-blind) methods, and often employing higher-order output statistics; see e.g. [11] and the references therein. However, in view of the advantages that the SIMO channel configuration offers in the linear case, it makes sense to ask whether these features can be exploited as well when the channel becomes nonlinear. In this thesis we consider several problems that arise when one adopts such a framework.

The remainder of this chapter is organized as follows. Section 1.1 reviews the now well-understood problem of equalization of linear SIMO channels, from which the work in this thesis takes off. Section 1.2 presents a review of the characteristics of several nonlinear channels encountered in practical situations. An outline of the thesis is then given in section 1.3.

1.1 Equalization of linear SIMO channels

Suppose that the time-invariant channel in Figure 2 is linear with impulse response $h_c(t)$. Then the received signal $y_c(t)$ is given by

$$y_c(t) = \sum_k a(k) h_c(t - kT) + n_c(t),$$

where T is the symbol interval and $n_c(t)$ is the additive noise. If several sensors (say p) are used, then $h_c(t)$, $n_c(t)$, $y_c(t)$ are $p \times 1$ vectors. In the single sensor case, sampling $y_c(t)$ at a rate p/T also results in a multichannel configuration [29]. In both cases the discrete-time input to the equalizer takes the form

$$y(k) = \sum_i h(i) a(k - i) + n(k)$$

where $y(k)$, $h(k)$, $n(k)$ are $p \times 1$ vectors:

$$y(k) = \begin{bmatrix} y_0(k) \\ \vdots \\ y_{p-1}(k) \end{bmatrix}, \qquad h(k) = \begin{bmatrix} h_0(k) \\ \vdots \\ h_{p-1}(k) \end{bmatrix}, \qquad n(k) = \begin{bmatrix} n_0(k) \\ \vdots \\ n_{p-1}(k) \end{bmatrix}.$$

In this framework the channel is a 1-input, p-output system, while the equalizer is a p-input, 1-output system. If the subchannels are FIR with transfer functions

$$H_i(z) = \sum_{k=0}^{l} h_i(k) z^{-k}, \qquad i = 0, 1, \ldots p-1,$$

then it can be shown that it is possible to find FIR filters $G_i(z) = \sum_{k=0}^{m-1} g_i(k) z^{-k}$, $0 \le i \le p-1$, satisfying

$$H_0(z)G_0(z) + \cdots + H_{p-1}(z)G_{p-1}(z) = z^{-d} \qquad \text{for any } 0 \le d \le l+m-1 \qquad (1.1)$$

provided that (i) the transfer functions $H_i(z)$ do not share any common zero, and (ii) $m \ge \frac{l}{p-1}$. These are known as the *zero and length* conditions [28]; eq. (1.1) is known as a *Bezout equation*. The equalizer is then given by the set of filters $G_0(z)$, $\ldots$, $G_{p-1}(z)$. Note that ISI can be completely eliminated, since in the noiseless case the equalizer output is simply $a(k-d)$ if (1.1) is satisfied. This approach, in which the equalizer is designed so that its output reduces to a delayed version of the symbol sequence when the noise is absent is known as *zero-forcing* (ZF) equalization. Figure 3 illustrates the channel-equalizer configuration.

A useful interpretation of the Bezout equation is as follows: under the zero and

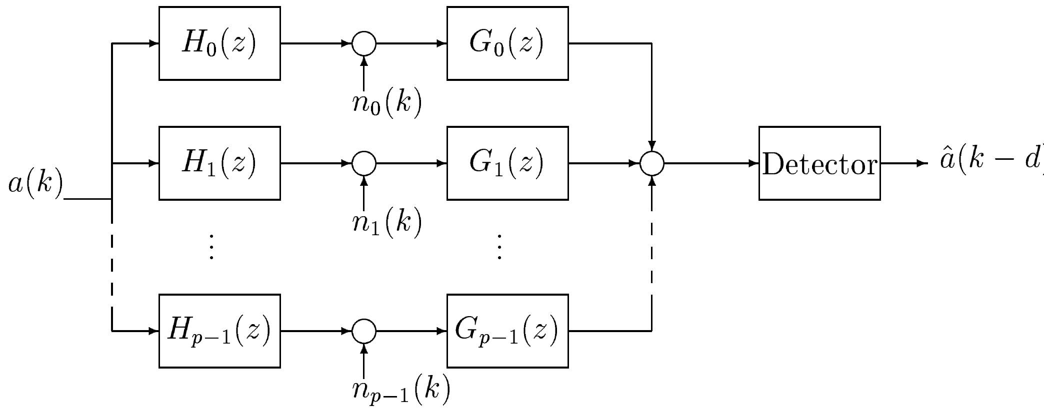

Figure 3: Equalization of a linear SIMO channel.

length condition, the $mp \times (m+l)$ generalized Sylvester matrix

$$\mathcal{H} = \begin{bmatrix} h(0) & h(1) & \cdots & h(l) & 0 & 0 & \cdots & 0 \\ 0 & h(0) & h(1) & \cdots & h(l) & 0 & \cdots & 0 \\ \vdots & \ddots & \ddots & \ddots & \vdots & \ddots & \ddots & \vdots \\ 0 & \cdots & 0 & 0 & h(0) & h(1) & \cdots & h(l) \end{bmatrix}$$

has full column rank [29]. $\mathcal{H}$ is known as the channel convolution matrix, or simply the channel matrix, since upon defining the vectors

$$\begin{aligned} Y(k) &\triangleq [\ y(k) \quad y(k-1) \quad \cdots \quad y(k-m+1)\ ]^T, \\ N(k) &\triangleq [\ n(k) \quad n(k-1) \quad \cdots \quad n(k-m+1)\ ]^T, \\ S(k) &\triangleq [\ a(k) \quad a(k-1) \quad \cdots \quad a(k-l-m+1)\ ]^T, \end{aligned}$$

of sizes $mp \times 1$, $mp \times 1$ and $(m+l) \times 1$ respectively, one has

$$Y(k) = \mathcal{H}S(k) + N(k).$$

If $\mathcal{H}$ has full column rank, then there exist $mp \times 1$ vectors g_d, $0 \leq d \leq m+l-1$, such that $g_d^H \mathcal{H} = e_{d+1}^H$ where e_k is a $(m+l) \times 1$ vector of all zeros except for a 1 in the k-th position. In that case, if the noise is absent ($N(k) = 0$),

$$g_d^H Y(k) = g_d^H \mathcal{H} S(k) = e_{d+1}^H S(k) = a(k-d),$$

showing that the coefficients of the ZF equalizer with associated delay d can be recovered from the vector g_d. Observe that these vectors are just the rows of the Moore-Penrose pseudoinverse matrix $\mathcal{H}^{\#}$, since $\mathcal{H}^{\#}\mathcal{H} = I$ if $\mathcal{H}$ has full column rank. Tong, Xu and Kailath showed in [29] that the matrix $\mathcal{H}$ can be recovered to within a scaling constant from the matrices

$$C_y(0) \triangleq E[Y(k)Y(k)^H], \qquad C_y(1) \triangleq E[Y(k)Y(k-1)^H],$$

provided that the zero and length conditions are satisfied and that both the symbol and noise sequences are white processes. Note that $C_y(0)$, $C_y(1)$ are simply second-order statistics of the received signal, which can be estimated by the receiver without aid from the transmitter (i.e. training signals).

A potential drawback of the ZF approach is that in the presence of noise a ZF equalizer can yield unacceptably high noise enhancement, especially if the channel has deep spectral nulls. A widely used alternate criterion is the minimization of the mean-squared error (MSE) between the equalizer output and the transmitted symbol sequence. This criterion can be seen as the best compromise between ISI reduction and noise amplification. A relation linking the ZF and minimum-MSE (MMSE) equalizers was shown in [22]. Its significance is that of showing how the MMSE equalizers can be obtained from the ZF ones. Hence SOS-based blind methods can be effectively used under the MMSE criterion.

1.2 Nonlinear channel examples

We present now a brief review of the particular characteristics of three kinds of nonlinear channels found in practice: satellite and microwave radio links, magnetic and optical recording channels.

1.2.1 Satellite microwave links

In these systems, operation of the satellite transponder and Earth station amplifiers (usually traveling-wave tubes (TWT)) at or near saturation may be necessary in order to obtain good power efficiency [10]. This results in a nonlinearly distorted signal at the amplifier output. Typically, a radiofrequency (RF) amplifier operated in a nonlinear region exhibits two kinds of nonlinearities. The first one relates the output power to the input power, and is often referred to as AM/AM conversion. The second one relates the output phase shift to the input power, and is usually known as AM/PM conversion. A popular model for these effects was given by Saleh [27]. Let $r(t)\cos[\omega_c t + \psi(t)]$ be the RF input to the amplifier; here ω_c is the carrier frequency, and $r(t)$, $\psi(t)$ are the modulated envelope and phase respectively. The corresponding output is modeled as

$$A[r(t)]\cos\{\omega_c t + \psi(t) + \Phi[r(t)]\}$$

where

$$A(r) = \frac{\alpha_a r}{1+\beta_a r^2}, \qquad \Phi(r) = \frac{\alpha_\phi r^2}{1+\beta_\phi r^2}.$$

Here α_a, β_a, α_ϕ and β_ϕ are parameters depending on the particular amplifier. In a satellite link model, this nonlinearity is preceded and followed by two linear time-invariant systems $h_{up}(t)$, $h_{down}(t)$ modeling respectively the uplink and downlink propagation channels. In [5] it was shown that the sampled baseband equivalent of the overall system can be accurately described by a truncated Volterra series of the form

$$y(k) = \sum_{i=0}^{D} \sum_{j_1=0}^{M_{2i+1}} \cdots \sum_{j_{2i+1}=0}^{M_{2i+1}} h_{2i+1}(j_1, \cdots, j_{2i+1}) \prod_{l=1}^{i} a^*(k-j_l) \prod_{l=i+1}^{2i+1} a(k-j_l), \tag{1.2}$$

where $\{a(k)\}$ is the sequence of transmitted symbols, $y(k)$ is the noiseless component of the received signal, and $h_{2i+1}(k_1, \cdots, k_{2i+1})$ are the baseband equivalent Volterra kernels, which can be determined from $h_{up}(t)$, $h_{down}(t)$ and the coefficients of the Taylor series expansion of the amplifier nonlinearity. Observe that only odd-order kernels appear in (1.2), and that these have one more unconjugated input than conjugated inputs. The absence of even-order distortions is due to the fact that they generate spectral components which lie outside the channel bandwidth (centered at ω_c) and therefore are rejected by the bandpass filter following the amplifier.

1.2.2 Magnetic digital channels

In digital saturation-recording, binary data are stored in the magnetic media by saturating the corresponding bit positions in the media into one of two flux directions, with a change in the direction of the flux representing a '1' and no change representing a '0'. No intermediate flux directions are allowed in saturation-recording because of hysteresis effects in the media; thus the channel is inherently binary ($a(k) \in \{-1, +1\}$). In reading the storage media, a read-head output signal is induced by changes in flux direction as the media passes under the head. This induced signal is amplified and then processed by the detection circuitry to produce a decision. Nominally, the read process is assumed to be linear; however, nonlinear interaction between the stored flux regions on the disk can lead to significant nonlinear ISI in the storage channel, especially in thin-film media and at high linear densities. Volterra models for magnetic recording channels have been proposed in [6, 15]. In these models, data cross-products represent interactions between magnetic transitions in the medium, which do not extend beyond a few bit intervals. Therefore the Volterra kernels characterizing dependences on products involving well separated data tend to have very small magnitudes, i.e. the memory of the nonlinearities is not excessively high (between 5 and 10). Usually third-order Volterra series provide an accurate model of the nonlinear behavior of these systems. For example, for channels based on magnetoresistive (MR) heads, the channel output can be accurately written as a linear combination of the products

$$a(k), \qquad a(k)a(k-1), \qquad a(k)a(k-2), \qquad a(k)a(k-3), \qquad a(k)a(k-1)a(k-2),$$

and their delays, while for channels based on magnetoinductive (MI) heads the generating products are

$$a(k), \qquad a(k)a(k-1)a(k-2), \qquad a(k)a(k-1)a(k-3), \qquad a(k)a(k-2)a(k-3).$$

In particular, the second-order Volterra kernels are absent. This is a consequence of the symmetry between the positive and negative pulses of the impulse response, which is a typical feature of MI heads [6].

1.2.3 Optical recording channels

In these systems the data are recorded in the media using a tightly focused spot of light (the *optical stylus*), produced by means of passing a laser beam through a series of lenses. The stylus is made as small as possible (e.g. 0.8 μm for standard CDs) and is used to produce a series of small dents termed *pits* on the media surface. The write beam is modulated by the binary data to be stored on the disk. The most popular format is non-return to zero inverse (NRZI) modulation, in which the beginning and end of a pit mark the positions of '1' bits in the data. The write signal that modulates the laser can be written as

$$w(t) = A + A\sum_i (-1)^i \mathrm{step}(t - j_i T),$$

where step(t) is the unit step function, T is the bit interval, $2A$ is the peak amplitude of $w(t)$ and the '1' bits occur at times $j_1, j_2, \ldots$ in the data stream.

Readout from the media is accomplished with the laser operating in a low-power mode. The reflected beam, collected by the objective lens used to focus the incident beam on to the medium, is modulated as a result of the interaction with the physical structure of the encoded information. Elements in the optical head convert this modulation into an intensity variation, sensed by a combination of photodetectors, to produce the electrical readout signal $r(t)$. In [16] the scalar theory of diffraction was used in order to obtain a model of the readout process. The media reflectivity was modeled making use of the Fourier series analysis of periodic structures, so that the reflected light equals the incident field times the phase profile of the media. Thus the model consists of four blocks: propagation from the laser to the disc, reflection, propagation to the photodetector, and optoelectric conversion.

It was noted in [2] that the dominant source of nonlinearity in the process arises from the photodetector, which responds to the incident intensity (i.e. the squared magnitude of the incident field). Consequently a second-order Volterra series model for the optical recording channel was suggested. It turned out that such linear-quadratic model provides an accurate representation of Hopkins' model for the readout process. The sampled readout signal is then modeled as

$$y(k) = \sum_{i=0}^{l_1} h_1(i)a(k-i) + \sum_{i=0}^{l_2}\sum_{j=0}^{l_2} h_2(i,j)a(k-i)a(k-j) + n(k)$$

where $a(k) \in \{-1, +1\}$ is the data sequence to be recovered, h_1 and h_2 are the linear and quadratic kernels respectively, and $n(k)$ is additive noise. Although at moderate recording densities nonlinear distortion in the readout signal is not too high (i.e. $|h_2| \ll |h_1|$), its effect increases drastically as the data are packed more tightly in the media [2].

1.3 Thesis outline

The goal of this thesis is to extend the SOS-based techniques available for blind equalization of linear channels to the case of nonlinear channels. In order to do so, a series of problems that arise in that framework will have to be considered.

When the received signal is sampled at a rate faster than the symbol rate, the overall system can be cast in a multirate framework. Although the area of multirate linear systems is a well established field [31], a comparable theory of nonlinear multirate systems is unavailable. In Chapter II the basic elements of such a theory are developed. Although our main motivation stems from the channel equalization problem, other applications such as subband nonlinear filtering could also benefit from this theory.

As advanced in the previous sections, ZF and MMSE equalizers for linear SIMO channels can be obtained from the received signal SOS under certain conditions. In Chapter III we investigate possible extensions of this fact to include nonlinear SIMO channels. As a result, conditions are derived which allow one to assess whether a given type of nonlinear channel can be blindly equalized from SOS.

For nonlinear channels satisfying those conditions, the next logical step is to derive a means to obtain the corresponding equalizers. In Chapter IV equalization algorithms are developed for the important particular case in which the transmitted symbols $\{a(k)\}$ are independent and identically distributed (iid).

The equalizability conditions developed in Chapter III include the requirement that a certain channel matrix be full column rank. In Chapter V we investigate the possibility of relaxing this requirement, and then we develop equalization algorithms for channels not satisfying this full rank condition.

Finally, Chapter VI presents a novel SOS-based blind equalization technique for linear channels with correlated input symbols $\{a(k)\}$, which constitutes a natural extension of the original algorithm for white symbols of Tong, Xu and Kailath [29].

The proofs of all results in this thesis are presented in the appendix.

CHAPTER II

MULTIRATE NONLINEAR SYSTEMS

Since the decision device at the receiver end operates at the symbol rate $1/T$ to produce one decision every T seconds, traditionally the received continuous-time signal $y_c(t)$ was sampled at this same rate $1/T$ and then these samples fed to the equalizer. This configuration is known as *baud-spaced equalization* (BSE). The drawback of this approach is that the sampling process may introduce severe distortion due to aliasing unless the spectral components of $y_c(t)$ beyond $1/(2T)$ Hz are removed. However, passing this signal through a receive filter with high attenuation beyond $1/(2T)$ Hz increases the overall ISI.

An alternative is to sample $y_c(t)$ every $T' < T$ seconds. In particular, if α denotes the excess bandwidth, that is if the received signal $y_c(t)$ is confined to the frequency band $[-\frac{1+\alpha}{2T}, \frac{1+\alpha}{2T}]$, one can choose $T' \leq \frac{T}{1+\alpha}$ so that the sampling rate $1/T'$ is greater than twice the highest frequency component of $y_c(t)$ and the problem of aliasing disappears. An equalizer operating on this principle is called a *fractionally spaced equalizer* (FSE) [4]. An additional advantage of FSE over BSE is the high degree of robustness with respect to variations in the sampling instant [25].

The fractionally spaced equalization setting can be cast in a multirate framework. A multirate system is marked by the presence of two multirate elements, the upsampler (or expander) and the downsampler (or decimator), shown in figure 4. An M-fold downsampler operates on a sequence $u(k)$ to produce the output sequence $x_d(k) = u(kM)$, effectively discarding $M - 1$ out of M consecutive samples. An

L-fold upsampler operates on a sequence $u(k)$ to produce the output sequence

$$x_u(k) = \begin{cases} u(k/L) & \text{if } k \bmod L = 0, \\ 0 & \text{else,} \end{cases}$$

effectively introducing $L - 1$ zero samples between two consecutive samples of the input sequence.

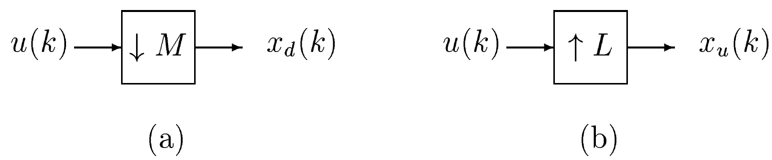

Figure 4: Multirate blocks. (a) M-fold downsampler, (b) L-fold upsampler.

In order to present the multirate setting of a fractionally spaced equalization configuration in which the channel and/or the equalizer are nonlinear, we shall model the input-output relation of the continuous-time channel as

$$r_c(t) = \sum_j h_c(t - jT;\ a(j), a(j-1), \cdots), \tag{2.1}$$

where the waveforms $h_c(t; \cdot, \cdot, \cdots)$, which are termed *chips*, are zero outside the interval $(0, T)$. Thus $h_c(t - jT;\ a(j), a(j-1), \cdots)$ is the waveform generated in the j-th symbol interval, and it depends on the symbols transmitted up to that point in time since the channel is assumed causal. This description of the nonlinear channel does not convey any loss of generality [4]. Further, we shall assume that the channel response to a zero input signal is zero. Quantitatively,

$$h_c(t - jT;\ a(j), a(j-1), \cdots) = 0 \qquad \text{for } jT \le t \le (j+1)T \qquad \text{if } a(j) = 0, \tag{2.2}$$

that is, if the current symbol is zero then the corresponding chip is identically zero during that symbol interval.

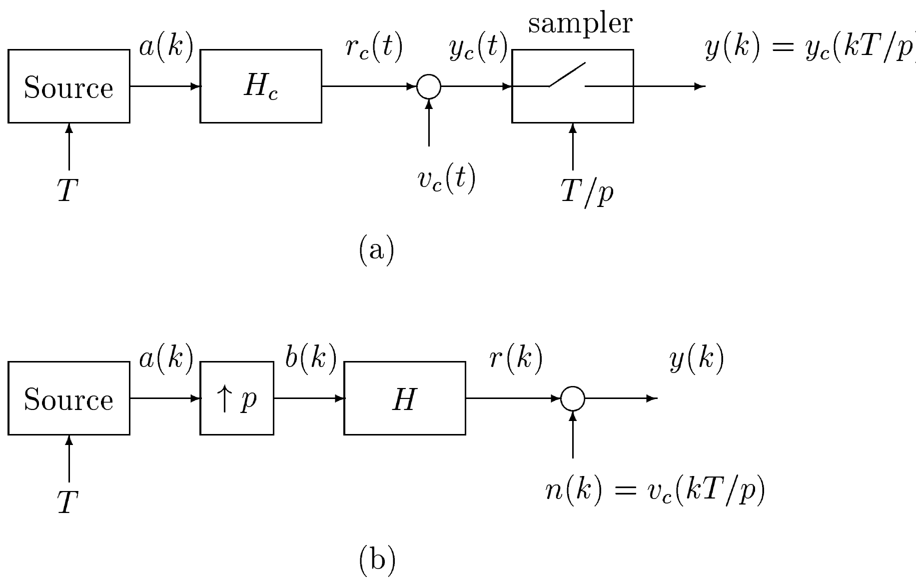

Figure 5: Two equivalent channels. (a) Continuous-time, (b) discrete-time.

Consider now the continuous-time representation of figure 5(a), in which the channel H_c is given by the input-output relation (2.1) and its output is sampled at a rate p/T. Let $b(k)$ the sequence obtained after upsampling the sequence $a(k)$ by a factor of p; observe that downsampling $b(k)$ by p recovers $a(k)$, so that $a(k) = b(kp)$. This allows us to write

$$
\begin{aligned}
r_c(kT/p) &= \sum_j h_c(kT/p - jT;\ a(j), a(j-1), \cdots) && (2.3)\\
&= \sum_j h_c(kT/p - jT;\ b(jp), b((j-1)p), b((j-2)p), \cdots) && (2.4)\\
&= \sum_{j'} h_c(kT/p - j'T/p;\ b(j'), b(j'-p), b(j'-2p), \cdots) && (2.5)\\
&= \sum_{j=-\infty}^{k} h(k-j;\ b(j), b(j-1), b(j-2), \cdots). && (2.6)
\end{aligned}
$$

In passing from (2.4) to (2.5) we have made $j' = jp$ and used (2.2) since $b(j) = 0$ unless $j \bmod p = 0$. In passing from (2.5) to (2.6) we have introduced the discrete-time chips

$$h(k-j;\ b(j), b(j-1), b(j-2), \cdots) \triangleq h_c((k-j)T/p;\ b(j), b(j-p), b(j-2p), \cdots). \quad (2.7)$$

Therefore we have shown that the two systems shown in figure 5 are equivalent, where H is the discrete-time channel defined by the input/output relation

$$r(k) = \sum_{j=-\infty}^{k} h(k-j;\ b(j), b(j-1), \cdots). \quad (2.8)$$

Similarly the FSE can be thought of as a SISO system G (possibly nonlinear) whose output is decimated by a factor of p. The overall channel-equalizer configuration is depicted in figure 6.

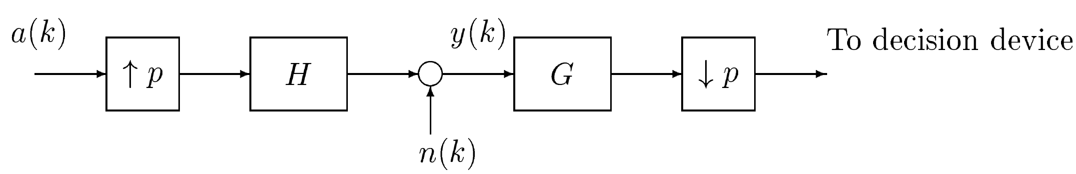

Figure 6: Multirate representation of a fractionally spaced equalizer.

Therefore the FSE setting with nonlinear channels and/or equalizers can be viewed as a multirate system design problem in which some of the blocks are nonlinear. Although a theory of linear multirate systems has achieved considerable maturity over the past decades, a comparable theory for nonlinear multirate systems is unavailable. In the remainder of this chapter the basic elements of such a theory are developed. To do so, the use of transfer functions, a common tool in the analysis of multirate linear systems, is replaced by operator techniques. Although our main motivation stems from the context of channel equalization, other applications could also benefit from this theory, for example subband nonlinear filtering of digital images.

2.1 Review of the basic building blocks

We shall denote the M-fold downsampler and L-fold upsampler of figure 4 as D_M and U_L respectively, so that when their input is $u(k)$ their outputs become $D_M u(k)$ and $U_L u(k)$. As an example of this operator notation, the output of the FSE configuration in figure 6 becomes

$$D_p G[n(k) + HU_p a(k)].$$

The operators D_M, U_L are linear but not time invariant. An operator H is time invariant if $Hz^{-1} = z^{-1}H$, where z^{-1} is the unit delay operator, i. e. $z^{-1}u(k) = u(k-1)$. If we define

$$Z_p = \begin{bmatrix} 1 & z^{-1} & \cdots & z^{-p+1} \end{bmatrix}^T \tag{2.9}$$

we can list several useful properties of the operators D_p, U_p, [31]:

$$z^{-1}D_p = D_p z^{-p} \tag{2.10}$$

$$U_p z^{-1} = z^{-p} U_p \tag{2.11}$$

$$D_p U_p = I \quad \text{(identity operator)} \tag{2.12}$$

$$\sum_{j=0}^{p-1} z^{-j} U_p D_p z^j = I \tag{2.13}$$

$$D_p Z_p Z_p^T U_p = \begin{bmatrix} 1 & 0 & \cdots & 0 \\ 0 & 0 & \cdots & z^{-1} \\ \vdots & \vdots & \ddots & \vdots \\ 0 & z^{-1} & \cdots & 0 \end{bmatrix} \tag{2.14}$$

Identities (2.10) and (2.11) are known as the *noble identities* [31]. Identities (2.13) and (2.14) are illustrated in fig. 7.

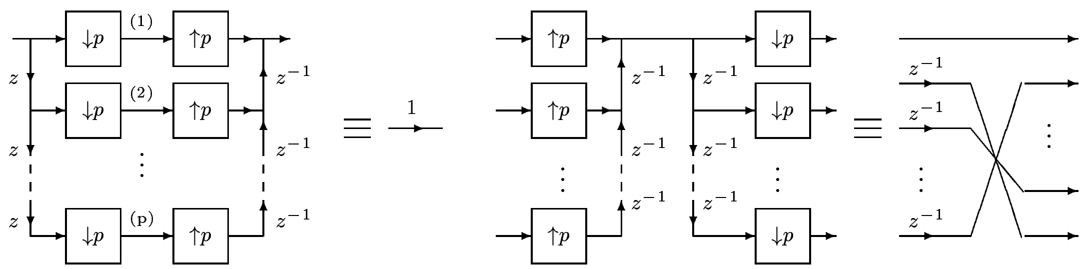

(a) (b)

Figure 7: Illustrating (a) identity (2.13), (b) identity (2.14).

A major feature of nonlinear operator theory is that with A, B, C nonlinear operators, while $(A+B)C = AC + BC$, in general $C(A+B) \neq CA + CB$; and $AB \neq BA$. Observe also that a $m \times l$ nonlinear operator H does not necessarily separate in to a $m \times l$ matrix operator $[H_{ij}]$ such that for a $l \times 1$ vector input $u(k) = [u_1(k), \cdots, u_l(k)]^T$, the i-th element of the output vector satisfies

$$[Hu(k)]_i = \sum_{j=1}^{l} H_{ij} u_j(k). \tag{2.15}$$

Operators H that obey (2.15) will henceforth be referred to as *matrix operators.*

2.2 Polyphase representation

The polyphase representation plays a pivotal role in the study of multirate linear systems. A general discrete-time linear filter

$$H(z) = \sum_{k=-\infty}^{\infty} h_k z^{-k}$$

can be written, for a given integer p, as

$$H(z) = \sum_{l=0}^{p-1} z^{-l} H_l(z^p), \tag{2.16}$$

where $H_0(z)$, ..., $H_{p-1}(z)$ are the so-called (type I) polyphase components, given by

$$H_l(z) = \sum_{k=-\infty}^{\infty} h_{kp+l} z^{-k}, \qquad 0 \leq l \leq p-1. \tag{2.17}$$

In this section we develop an appropriate definition of the polyphase components of a nonlinear operator H. First, we need to introduce the following result.

Lemma 2.1 *If H is time invariant, then $D_p H U_p$ is time invariant as well.*

Lemma 2.1 allows us to introduce the polyphase components of H.

Definition 2.1 (Polyphase components) *The p-fold polyphase components of an operator H are defined as $H_i \triangleq D_p z^i H U_p$, for $0 \le i \le p-1$.*

Several observations are in order:

1. From lemma 2.1, it follows that the polyphase components of a time invariant operator are time invariant.

2. If H is linear time invariant, the polyphase components as defined above reduce to the standard type I polyphase components [31]. That is, if H has transfer function $H(z) = \sum_{i=0}^{p-1} z^{-i} H_i(z^p)$, then H_i has transfer function $H_i(z)$.

3. In general, the polyphase components do not completely determine a nonlinear time invariant operator. This is in contrast with the linear case. For example, let $Hu(k) = u(k)u(k-1)$. Then for all $p > 1$, *all* the p-fold polyphase components of H are zero. This is so because the product of successive samples may be zero due to the upsampling process implicit in the definition of H_i.

Of particular interest are those operators which are completely described by their polyphase components; we shall refer to the class of such operators as *separable*. It is also of help to introduce the *dilation* of an operator, as follows:

Definition 2.2 (Dilation) *Let H be a time invariant operator, defined by*

$$Hu(k) = f\Big(\cdots, \;\; u(k+2), \;\; u(k+1), \;\; u(k), \;\; u(k-1), \;\; \cdots \Big),$$

*for some (nonlinear) function f. The p-*fold dilation *of H, $H^{[p]}$, is defined as*

$$H^{[p]}u(k) = f\Big(\ \cdots,\ \ u(k+2p),\ \ u(k+p),\ \ u(k),\ \ u(k-p),\ \ \cdots\ \Big). \tag{2.18}$$

For example, if the operator H is defined as $Hu(k) = u(k-1) + u^2(k)u(k-2)$, then its dilation becomes $H^{[p]}u(k) = u(k-p) + u^2(k)u(k-2p)$. The following two fundamental properties of the dilation $H^{[p]}$ are readily checked:

1. The p-fold dilation of a time invariant operator is time invariant.

2. If H is linear time invariant with transfer function $H(z)$, then the dilation $H^{[p]}$ is linear time invariant with transfer function $H(z^p)$.

Less obvious is the following property:

Lemma 2.2 *If $H = FG$ with F and G time invariant, then $H^{[p]} = F^{[p]}G^{[p]}$.*

Using this dilation operator, it is possible to reformulate the noble identities in the nonlinear operator framework.

Lemma 2.3 (Noble identities) *Let H be any time invariant operator such that $H\mathbf{0} = \mathbf{0}$ where $\mathbf{0}$ denotes the zero sequence. Then*

$$HD_p = D_pH^{[p]}, \qquad U_pH = H^{[p]}U_p. \tag{2.19}$$

For linear H, these identities reduce to the familiar form depicted in figure 8, which are a direct consequence of the linearity of D_p, U_p and properties (2.10) and (2.11).

As mentioned above, in general a nonlinear operator H is not uniquely determined by its polyphase components H_i. In order to characterize the class of operators for which an expression in terms of their polyphase components exists, the concept of *separability* is introduced next.

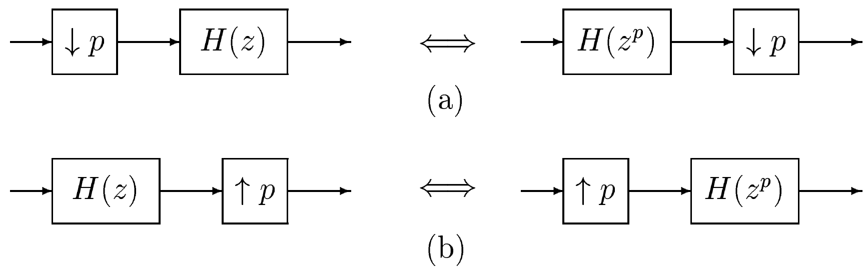

Figure 8: The noble identities in the linear case, for (a) decimators and (b) expanders.

Definition 2.3 (Separability) *A single-input single-output time invariant operator H is said to be p-*separable *if there exists a p-input 1-output operator T such that*

$$H = T \begin{bmatrix} H_0^{[p]} \\ H_1^{[p]} \\ \vdots \\ H_{p-1}^{[p]} \end{bmatrix}, \tag{2.20}$$

where H_0, ..., H_{p-1} are the p-fold polyphase components of H. If in addition T is linear, then H is said to be linearly p-separable.

Every linear operator is clearly linearly p-separable for all p, since in view of (2.16) one can take $T = Z_p^T$. Also note that it is not enough for H to be of the form

$$H = T \begin{bmatrix} (F^{(0)})^{[p]} \\ (F^{(1)})^{[p]} \\ \vdots \\ (F^{(p-1)})^{[p]} \end{bmatrix} \qquad \text{for some } T,\ F^{(0)},\ \dots,\ F^{(p-1)},$$

in order to be p-separable; the operators $F^{(0)}$, ..., $F^{(p-1)}$ must also be the polyphase components of H. This suggests that if H is p-separable as in (2.20), then the operator T must satisfy some additional constraints. In particular the following result holds.

Lemma 2.4 *If the time invariant operator H is linearly p-separable, i.e. if (2.20) holds with T $1 \times p$ linear, then one can assume without loss of generality that $T = Z_p^T$.*

Lemma 2.4 shows that any linearly p-separable time invariant operator H can be written as

$$H = \sum_{j=0}^{p-1} z^{-j} H_j^{[p]} = \sum_{j=0}^{p-1} H_j^{[p]} z^{-j},$$

which is similar to the familiar polyphase decomposition (2.16) for linear systems. As an example, let H be the nonlinear operator defined by

$$Hu(k) = u(k)u(k-2) + u^2(k-1)u(k-5).$$

Then H is linearly separable for $p = 2$, since

$$H_0 u(k) = u(k)u(k-1), \qquad H_1 u(k) = u^2(k)u(k-2),$$

and H satisfies

$$Hu(k) = \left(H_0^{[2]} + z^{-1} H_1^{[2]}\right) u(k).$$

In principle, one could similarly consider as separable those operators H satisfying

$$H = \begin{bmatrix} H_0^{[p]} & H_1^{[p]} & \cdots & H_{p-1}^{[p]} \end{bmatrix} T \tag{2.21}$$

for some 1-input, p-output operator T. However, the analog of lemma 2.4 (i.e whether linearity of T in (2.21) allows one to take $T = Z_p$) is not true for such operators. The following example for $p = 2$ illustrates this point. Consider the nonlinear time invariant operator F defined via

$$Fu(k) = \begin{cases} \frac{u^2(k)}{u(k-1)} & \text{if } u(k-1) \neq 0, \\ 0 & \text{otherwise,} \end{cases}$$

and let $H = F^{[2]}(1+z^{-1})$. One can check that the 2-fold polyphase components of H are just $H_0 = H_1 = F$. However, one has

$$\begin{bmatrix} H_0^{[2]} & H_1^{[2]} \end{bmatrix} Z_2 = \begin{bmatrix} F^{[2]} & F^{[2]} \end{bmatrix} \begin{bmatrix} 1 \\ z^{-1} \end{bmatrix} = F^{[2]} + F^{[2]} z^{-1} = F^{[2]} + z^{-1} F^{[2]},$$

which is *not* the same as $F^{[2]}(1+z^{-1})$, due to the nonlinearity of $F^{[2]}$.

2.3 Nonlinear filter banks

A configuration commonly found in signal processing is the maximally decimated filter bank, shown in figure 9 for the linear filter case. This system is widely used in the area of subband coding of speech and image signals, whose energy is not evenly distributed in the frequency domain. First, the analysis filters $H_i(z)$ split the input $u(k)$ into p frequency subbands; the subband signals are decimated by a factor of p, appropriately coded, and stored/transmitted. The full band signal can be reconstructed using the expanders, which restore the original sampling rate, and the synthesis filters $F_i(z)$ which smooth out the upsampled signals. The outputs of the synthesis filters are added up to produce the reconstructed signal $\hat{u}(k)$. Several con-

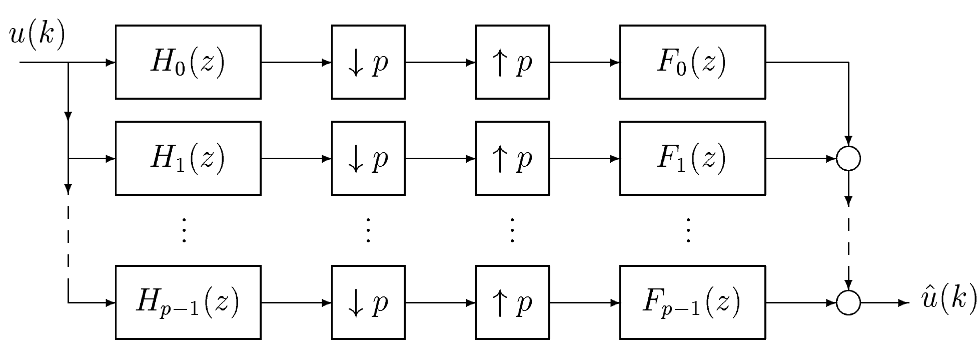

Figure 9: Linear p-channel maximally decimated filter bank.

siderations must be taken into account in filterbank design. Ideally, the reconstructed signal $\hat{u}(k)$ should be as accurate a replica of $u(k)$ as possible. However, because of the presence of decimators and expanders, the filter bank is in general a time-varying system. Careful design of the analysis and synthesis filters can provided the desired time invariance.

Once time invariance of the filter bank is achieved, it is possible to obtain *perfect reconstruction*, which means that $\hat{u}(k) = cu(k-d)$ for some $c \neq 0$ and integer d. Necessary and sufficient conditions for time invariance and perfect reconstruction are known for linear filter banks [31]. In this section similar conditions for architectures with nonlinear analysis and/or synthesis filters are developed. The utility of incorporating nonlinear filters in subband coding banks for digital images has been discussed in [9, 13], where simple perfect reconstruction architectures were considered.

Figure 10(a) shows the general structure of a p-channel maximally decimated nonlinear filter bank. If we denote the input-output relation of the filter bank as $y(k) = Gu(k)$, then we can write G explicitly as

$$G = FU_pD_p \left[\begin{array}{cccc} H^{(0)} & H^{(1)} & \ldots & H^{(p-1)} \end{array} \right]^T, \tag{2.22}$$

where $H^{(0)}, \ldots, H^{(p-1)}$ are the time-invariant single-input single-output analysis filters, and the p-input, 1-output operator F represents the time invariant analysis bank. Observe that in general F need not be a matrix operator of the form

$$\left[\begin{array}{cccc} F^{(0)} & F^{(1)} & \ldots & F^{(p-1)} \end{array} \right], \tag{2.23}$$

since nonlinear interactions between different subband signals are in principle possible (If F is linear, though, it *must* be of the form 2.23)). Let X_p be the $p \times p$ exchange matrix with ones in the antidiagonal and zeros elsewhere. Let us introduce

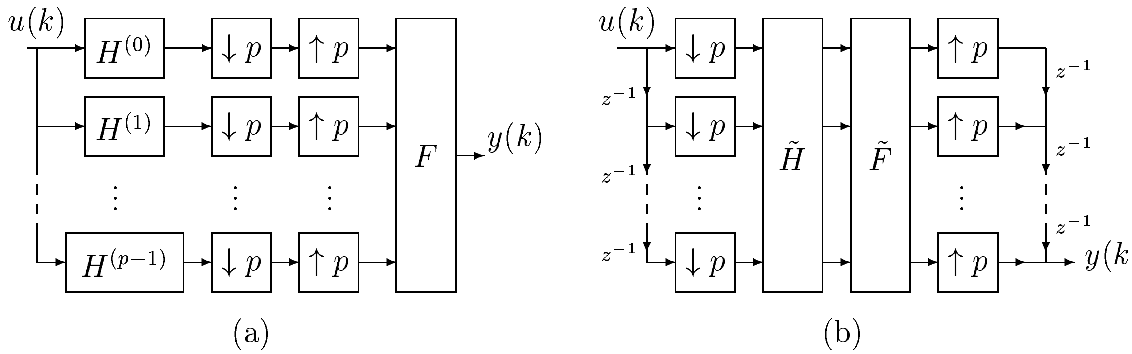

Figure 10: A p-channel maximally decimated filterbank. (a) General form, (b) equivalent system.

the operators

$$L_p \triangleq \begin{bmatrix} z^{-p+1} & \cdots & z^{-1} & 1 \end{bmatrix} U_p = Z_p^T U_p X_p, \tag{2.24}$$

$$B_p \triangleq D_p \begin{bmatrix} 1 & z^{-1} & \cdots & z^{-p+1} \end{bmatrix}^T = D_p Z_p, \tag{2.25}$$

$$R_p \triangleq \begin{bmatrix} 0 & I_{p-1} \\ z^{-1} & 0 \end{bmatrix}. \tag{2.26}$$

Then one has the following result:

Lemma 2.5 *The filter bank (2.22) can be equivalently expressed as*

$$G = L_p \tilde{F} \tilde{H} B_p, \tag{2.27}$$

where

$$\tilde{F} = \begin{bmatrix} F_{p-1} & \cdots & F_1 & F_0 \end{bmatrix}^T, \qquad \tilde{H} = D_p \begin{bmatrix} H^{(0)} & H^{(1)} & \cdots & H^{(p-1)} \end{bmatrix}^T L_p z R_p. \tag{2.28}$$

If in addition the analysis filters are linearly p-separable, then

$$\tilde{H} = \begin{bmatrix} H_0^{(0)} & H_1^{(0)} & \cdots & H_{p-1}^{(0)} \\ H_0^{(1)} & H_1^{(1)} & \cdots & H_{p-1}^{(1)} \\ \vdots & \vdots & \ddots & \vdots \\ H_0^{(p-1)} & H_1^{(p-1)} & \cdots & H_{p-1}^{(p-1)} \end{bmatrix}. \tag{2.29}$$

Note that $\tilde{F}$, $\tilde{H}$ are time-invariant operators. This equivalent description of the filter bank is depicted in figure 10(b). The formulation (2.27) is analog to the familiar representation of linear filter banks in terms of the polyphase matrices [31]. If the analysis filters are linear with polyphase decompositions

$$H^{(i)}(z) = \sum_{j=0}^{p-1} z^{-j} H_j^{(i)}(z^p)$$

then $\tilde{H}$ in (2.29) reduces to the standard polyphase matrix with elements $[\tilde{H}(z)]_{i,j} = H_j^{(i)}(z)$. Similarly, if the synthesis bank F assumes the particular matrix structure of (2.23), then $\tilde{F}$ can be written as

$$\tilde{F} = \begin{bmatrix} F_{p-1}^{(0)} & F_{p-1}^{(1)} & \cdots & F_{p-1}^{(p-1)} \\ F_{p-2}^{(0)} & F_{p-2}^{(1)} & \cdots & F_{p-2}^{(p-1)} \\ \vdots & \vdots & \ddots & \vdots \\ F_0^{(0)} & F_0^{(1)} & \cdots & F_0^{(p-1)} \end{bmatrix},$$

and if these synthesis filters are linear with transfer functions

$$F^{(i)}(z) = \sum_{j=0}^{p-1} z^{-j} F_j^{(i)}(z^p)$$

then $\tilde{F}$ is the polyphase matrix with elements $[\tilde{F}(z)]_{i,j} = F_{p-i-1}^{(j)}(z)$.

With the representation (2.27) for the filter bank, one can obtain conditions for time invariance ($Gz^{-1} = z^{-1}G$) and perfect reconstruction ($G = cz^{-d}$ for some $c \neq 0$ and integer d) properties of the overall system.

Lemma 2.6 (Filterbank time invariance) *The filter bank $G = L_p\tilde{F}\tilde{H}B_p$ is time invariant if and only if $\tilde{F}\tilde{H}$ commutes with the $p \times p$ operator R_p given in (2.26).*

Lemma 2.7 (Perfect reconstruction) *The filter bank $G = L_p\tilde{F}\tilde{H}B_p$ has the perfect reconstruction property if and only if*

$$\tilde{F}\tilde{H} = cz^{-m}\begin{bmatrix} 0 & I_{p-r} \\ z^{-1}I_r & 0 \end{bmatrix}$$

for some $c \neq 0$ and integers m, $0 \leq r \leq p-1$.

2.4 Nonlinear fractionally spaced equalizers

The multirate equivalent of a fractionally spaced equalization setting was shown in figure 6. Referring to this figure, and ignoring the additive noise $n(k)$ at the channel output, the mapping from the transmitted symbols $\{a(k)\}$ to the equalizer output $\{y(k)\}$ can be written as

$$y(k) = D_pGHU_pa(k).$$

Therefore the ZF equalization problem is: given the channel H, find an equalizer G such that $D_pGHU_p = z^{-d}$ for some integer d which represents the associated equalization delay. In view of our definition of the polyphase components of a nonlinear operator (cf. definition 2.1), the overall system D_pGHU_p is just the 0-th p-fold polyphase component of the operator GH; therefore if G, H are time invariant, so is $(GH)_0 = D_pGHU_p$. The next result shows an alternative representation of this setting.

Lemma 2.8 *The operator $(GH)_0 = D_pGHU_p$ can be equivalently expressed as*

$$(GH)_0 = \tilde{G}\begin{bmatrix} H_0 & H_1 & \cdots & H_{p-1} \end{bmatrix}^T, \tag{2.30}$$

where the p-input, 1-output operator $\tilde{G}$ is given by

$$\tilde{G} = D_pGZ_p^TU_p$$

and $H_0, \ldots, H_{p-1}$ *are the* p*-fold polyphase components of the channel* H*.*

Lemma 2.8 is illustrated in figure 11. The overall operator can be explicitly written in terms of the polyphase components of the channel, *even if the channel* H *is not separable.* This representation is similar to the linear multichannel framework of figure 3. Observe that if the noise $n(k)$ is taken into account, the configuration of figure 6 is not equivalent to just the setting of figure 3 with the noise corrupting the equalizer input unless the equalizer G is linear, since in general $G[n(k) + HU_p a(k)] \neq Gn(k) + GHU_p a(k)$.

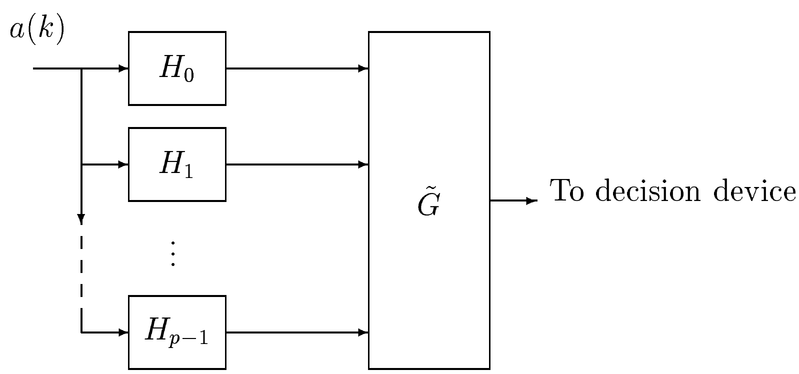

Figure 11: Equivalent fractionally spaced equalization setting (noiseless case).

In general, the overall system is not completely specified by the polyphase components of the equalizer G. However, in the particular case of a linearly p-separable G, one has $G = [\; G^{[p]}{}_0 \;\; \cdots \;\; G^{[p]}{}_{p-1} \;] Z_p$, so that

$$\begin{aligned}
\tilde{G} &= D_p G Z_p^T U_p \\
&= D_p \begin{bmatrix} G^{[p]}{}_0 & \cdots & G^{[p]}{}_{p-1} \end{bmatrix} Z_p Z_p^T U_p \\
&= \begin{bmatrix} G_0 & \cdots & G_{p-1} \end{bmatrix} D_p Z_p Z_p^T U_p. \qquad (2.31)
\end{aligned}$$

In passing from the second to the third line we have used (2.19). Using (2.31) together with (2.14) the following expression for the overall noiseless system is obtained:

$$\begin{aligned}(GH)_0 &= \tilde{G}\begin{bmatrix} H_0 & H_1 & \cdots & H_{p-1}\end{bmatrix}^T \\ &= \begin{bmatrix} G_0 & \cdots & G_{p-1}\end{bmatrix} D_p Z_p Z_p^T U_p \begin{bmatrix} H_0 & \cdots & H_{p-1}\end{bmatrix}^T \\ &= \begin{bmatrix} G_0 & \cdots & G_{p-1}\end{bmatrix}\begin{bmatrix} 1 & 0 \\ 0 & z^{-1}X_{p-1}\end{bmatrix}\begin{bmatrix} H_0 \\ \vdots \\ H_{p-1}\end{bmatrix} \\ &= G_0 H_0 + z^{-1}\sum_{i=1}^{p-1} G_i H_{p-i}. \end{aligned} \tag{2.32}$$

This is the expression found in the linear case; the difference is that now the polyphase components G_i, H_i may be nonlinear.

The zero-forcing equalizer design problem is seen to be equivalent to solving for the G_i in the nonlinear Bezout equation that is obtained by equating the right-hand side of (2.32) to z^{-d}. In this general framework, unless some assumptions are adopted about the operators H_i, even determining the *existence* of solutions G_i (which for practical purposes should be constrained to be stable and causal operators) to this generalized Bezout equation appears to be a very difficult problem.

Due to this fact, in the remainder of this thesis we shall limit ourselves to nonlinear channels that admit a certain parametric description, as shown in the next chapter. This class of channels includes as a particular case polynomial approximations of nonlinear systems (i.e. truncated Volterra series), which as saw in chapter I constitute a popular description of nonlinear communication channels.

CHAPTER III

SOS-BASED BLIND EQUALIZABILITY OF NONLINEAR CHANNELS

As seen in the previous chapter, it is often convenient to describe the input-output relation of the nonlinear channel in parametric form. We shall assume that this relation can be accurately described by the following 1-input p-output model:

$$y(k) = \sum_{i=1}^{q} \sum_{j=0}^{l_i} h_{ij} s_i(k-j) + n(k), \tag{3.1}$$

where $s_1(k) \triangleq a(k)$ is the scalar stationary channel input sequence, the terms $s_i(k) = \phi_i(a(k), a(k-1), \cdots)$ for $i = 2, \ldots, q$ are scalar nonlinear causal functions of $\{a(k)\}$; h_{ij} are $p \times 1$ coefficient vectors, and $n(k)$, $y(k)$ are $p \times 1$ signal vectors representing an additive disturbance and the observed channel output, respectively. The noise $\{n(k)\}$ and the symbols $\{a(k)\}$ are assumed to be independent. This model accommodates, for example, polynomial approximations of nonlinear channels (Volterra models), for which the generating terms $s_i(\cdot)$ are monomial functions of $a(k)$ and its delays [12]. It is assumed that the functions $\phi_i(\cdot, \cdot, \cdots)$ generating the nonlinearities are known, so that all the uncertainty about the channel is in the coefficients h_{ij}.

The advantage of using the model (3.1) resides in the fact that, while describing a nonlinear input-output relation, it is linear in the channel parameters h_{ij}. This feature allows one to obtain a matrix-vector representation of the channel, which can be exploited in order to extend SOS-based blind linear channel equalization techniques to the case of interest.

In this chapter we ask the following question: What information can be obtained about the channel (3.1) from the SOS of its output? As stated in Chapter I, in the linear channel case, under the 'zero and length' conditions the channel coefficients can be estimated from SOS up to a multiplicative constant [28]. We shall show that this is not true in general for the nonlinear model (3.1), but that nevertheless under certain conditions the output SOS still contain enough information for the design of ZF linear equalizers.

The channel input-output relation can be expressed in matrix-vector form as follows. By collecting m successive observations in the vector

$$Y(k) \triangleq [\ y(k)^T \quad y(k-1)^T \quad \cdots \quad y(k-m+1)^T\ ]^T, \tag{3.2}$$

one can write

$$Y(k) = \mathcal{H}S(k) + N(k), \tag{3.3}$$

where $N(k)$ and $S(k)$ are the noise and signal vectors respectively, given by

$$N(k) \triangleq [\ n(k)^T \quad n(k-1)^T \quad \cdots \quad n(k-m+1)^T\ ]^T, \tag{3.4}$$

and $S(k) \triangleq [\ S_1^T(k) \quad S_2^T(k)\ ]^T$ with

$$S_1^T(k) \triangleq [\ a(k) \quad a(k-1) \quad \cdots \quad a(k-l_1-m+1)\ ], \tag{3.5}$$

$$\begin{aligned} S_2^T(k) \triangleq [\ & s_2(k) \quad s_2(k-1) \quad \cdots \quad s_2(k-l_2-m+1) \quad | \quad \cdots \\ & \cdots \quad | \quad s_q(k) \quad s_q(k-1) \quad \cdots \quad s_q(k-l_q-m+1)\ ], \end{aligned} \tag{3.6}$$

which represent the linear and nonlinear parts of $S(k)$. The channel matrix $\mathcal{H}$ is

$$\mathcal{H} \triangleq [\ \mathcal{H}_1 \quad \mathcal{H}_2 \quad \cdots \quad \mathcal{H}_q\ ],$$

with every $\mathcal{H}_i$ block Toeplitz:

$$\mathcal{H}_i \triangleq \begin{bmatrix} h_{i0} & h_{i1} & \cdots & h_{il_i} & & & \\ & h_{i0} & h_{i1} & \cdots & h_{il_i} & & \\ & & \ddots & \ddots & & \ddots & \\ & & & h_{i0} & h_{i1} & \cdots & h_{il_i} \end{bmatrix} \qquad pm \times (m + l_i). \tag{3.7}$$

$\mathcal{H}$ has size $pm \times (qm + \sum_{i=1}^{q} l_i)$. For convenience, let $d_1 \triangleq m + l_1$, which is the size of $S_1(k)$, and $d_2 \triangleq (q-1)m + l_2 + \cdots + l_q$, which is the size of $S_2(k)$. Thus $S(k)$ has size $d_1 + d_2$.

Giannakis and Serpedin considered in [12] the problem of equalizing Volterra channels of the form (3.1). They pointed out that, even though the channel is nonlinear, under certain conditions perfect zero-forcing equalization can still be achieved by using a bank of linear finite impulse response (FIR) filters, which is a very appealing result. They also presented a blind, deterministic approach for equalizer design. Although this algorithm is elegant and relatively simple, it has several drawbacks. First it assumes that the channel matrix $\mathcal{H}$ is full-rank and square, claiming that squareness can always be achieved, if necessary, by decreasing the number of channels p and increasing the equalizer length m. However, a longer equalizer would increase the computational complexity; further if some channels are to be dropped it is not possible to ensure *a priori* that the surviving channels satisfy the corresponding full-rank condition, even if the original set did. Thus the selection of the channels to drop is a difficult problem. One issue addressed in this chapter is whether this squareness assumption can be relaxed.

Secondly, in the event the linear kernel has the same length as another kernel, i.e. $l_i = l_1$ for some $i \geq 2$, [12] has to resort to higher order methods to equalize the channel. In this chapter it is shown that this restriction on the linear kernel length is not necessary for SOS methods to apply.

Third, when a kernel other than the linear one has the largest memory ($\max\{l_i\} \neq l_1$), then the techniques of [12] only recover the input term $s_i(k)$ corresponding to this largest kernel. In our case, we show that under the right conditions even the linear kernel input $a(k)$ is recoverable despite the violation of this particular length requirement.

Observe that the model (3.1) could be seen as a linear multiple-input multiple-output (MIMO) system by viewing the signals $\{s_i(k)\}$, $2 \leq i \leq q$ as additional inputs. Although SOS-based techniques exist for equalization within such a framework [28], they usually assume that the different inputs are independent (which is no longer true in our setting, since for $i \geq 2$, $\{s_i(k)\}$ is a function of $\{s_1(k)\}$), and they only resolve $\mathcal{H}$ to within a mixing matrix. In the current context, this would mean that only a linear mixture of $a(k)$, $s_2(k)$, $\ldots$, $s_q(k)$ could be obtained. The results of this chapter show that under right conditions the structure of the mixing matrix permits obtaining linear ZF equalizers. These conditions are on the statistical properties of the symbols $a(\cdot)$ and the remaining generating terms $s_i(\cdot)$. Therefore they can be checked *a priori* in order to determine whether a given channel structure can be equalized from SOS.

The following notation is adopted. $E[\cdot]$ denotes statistical expectation; $(\cdot)^*$, $(\cdot)^T$, $(\cdot)^H$ and $(\cdot)^\#$ denote conjugate, transpose, conjugate transpose and pseudoinverse respectively. J_k denotes the $k \times k$ shift matrix with ones in the first subdiagonal and zeros elsewhere; X_k is the $k \times k$ exchange matrix with ones in the antidiagonal and zeros elsewhere; and e_k denotes a vector of all zeros except for a 1 in the k-th position. We use the direct sum notation $A \oplus B$ for block diagonal matrices:

$$A \oplus B \triangleq \begin{bmatrix} A & 0 \\ 0 & B \end{bmatrix}.$$

3.1 Problem formulation

The second order statistical information about the channel output $\{y(k)\}$ is contained in the covariance sequence

$$\begin{aligned} C_y(l) &\triangleq \text{cov}[Y(k), Y(k-l)] \\ &= E[Y(k)Y(k-l)^H] - E[Y(k)]E[Y(k-l)^H] \\ &= \mathcal{H}C_s(l)\mathcal{H}^H + C_n(l), \end{aligned} \tag{3.8}$$

where $C_s(l)$, $C_n(l)$ are the source and noise covariance sequences given by

$$C_s(l) \triangleq \text{cov}[S(k), S(k-l)], \qquad C_n(l) \triangleq \text{cov}[N(k), N(k-l)]. \tag{3.9}$$

We consider covariance matrices rather than autocorrelation matrices, since the channel nonlinearities may induce nonzero mean $\{s_i(k)\}$ terms even if $\{a(k)\}$ is zero mean. Our goal is to extract as much information about the channel matrix $\mathcal{H}$ from the sequence $\{C_y(l)\}$ as possible. The following standard assumptions are adopted throughout this chapter:

A1: The channel matrix $\mathcal{H}$ is tall and has full column rank.

A2: The noise $\{n(k)\}$ is zero-mean white with covariance $\sigma_n^2 I_p$.

A3: The covariance matrix $C_s(0)$ is positive definite.

Assumption **A1** is a 'coprimeness' requirement on the subchannels. Since $\mathcal{H}$ is $pm \times (qm + \sum_{i=1}^{q} l_i)$, a necessary condition for **A1** to hold is

$$pm > qm + \sum_{i=1}^{q} l_i \qquad \Rightarrow \qquad (p-q)m > \sum_{i=1}^{q} l_i > 0,$$

for which $p > q$ must hold. This condition parallels the 'more outputs than inputs' requirement in blind identification of MIMO channels [28]. Observe that **A1** ensures the existence of vectors g_d such that $g_d^H \mathcal{H} = e_{d+1}^H$. Thus in the noiseless case, for

$0 \leq d \leq d_1 - 1$ one has $g_d^H Y(k) = a(k-d)$ so that these $pm \times 1$ vectors provide ZF linear equalizers with associated delay d. Whether **A1** can be relaxed will be investigated in Chapter V.

Under **A2**, one has $C_n(l) = \sigma_n^2 J_{pm}^{pl}$. In particular,

$$C_y(0) = \mathcal{H} C_s(0) \mathcal{H}^H + \sigma_n^2 I_{pm}.$$

Since $\mathcal{H} C_s(0) \mathcal{H}^H$ is necessarily singular (because $\mathcal{H}$ is tall by assumption **A1**), it is seen that σ_n^2 is the smallest eigenvalue of $C_y(0)$ and therefore it can be readily obtained. Therefore the effect of noise can be removed from $C_y(l)$ by subtracting the matrix $\sigma_n^2 J_{pm}^{pl}$. Henceforth we shall assume that this has been already done, so that $C_y(l) = \mathcal{H} C_s(l) \mathcal{H}^H$.

Assumption **A3** constitutes a 'persistent excitation' condition on the process $\{a(k)\}$. It allows one to write

$$C_s(0) = QQ^H \qquad \text{with } Q \text{ invertible.} \tag{3.10}$$

In order to state the blind equalizability problem, let us first introduce the concept of *compatibility.*

Definition 3.1 (Compatibility) *A $pm \times (qm + \sum_{i=1}^{q} l_i)$ matrix $\tilde{\mathcal{H}}$ is said to be* compatible *with the second order statistics of $\{Y(k)\}$ up to lag $\bar{l}$ if it satisfies*

$$\tilde{\mathcal{H}} C_s(l) \tilde{\mathcal{H}}^H = \mathcal{H} C_s(l) \mathcal{H}^H, \qquad l = 0, 1, \ldots \bar{l}. \tag{3.11}$$

In view of this definition, it is clear that the best we can hope to extract from the output channel SOS is a compatible matrix, which may or may not coincide with the true channel matrix $\mathcal{H}$. The problem then becomes determining whether this is good enough for our purposes:

Blind Equalizability Problem: *Let $\tilde{\mathcal{H}}$ be compatible with the SOS of $\{Y(k)\}$ up to lag $\bar{l}$. Determine conditions under which a ZF equalizer g_d for any compatible $\tilde{\mathcal{H}}$ is also a ZF equalizer for $\mathcal{H}$:*

$$g_d^H \tilde{\mathcal{H}} = e_{d+1}^H \qquad \Longrightarrow \qquad g_d^H \mathcal{H} = c e_{d+1}^H, \qquad \text{for some } 0 \le d \le d_1 - 1 \text{ and } c \neq 0. \tag{3.12}$$

As said in Chapter I, this was solved in [29] for the particular case of linear channels ($q = 1$) with white inputs, for which if $\tilde{\mathcal{H}}$ is compatible up to lag $\bar{l} = 1$, then $\tilde{\mathcal{H}} = \mathrm{e}^{j\theta}\mathcal{H}$ for some real θ so that (3.12) holds. This is not necessarily true in our case, as shown by the following example. Suppose that the different terms $\{s_i(k)\}$ are uncorrelated: $\mathrm{cov}[s_i(k_1), s_j(k_2)] = 0$ if $i \neq j$. Then $C_s(l)$ is block diagonal (with q blocks in its diagonal) for all l, so that any matrix of the form

$$\tilde{\mathcal{H}} = [\ \mathrm{e}^{j\theta_1}\mathcal{H}_1 \quad \mathrm{e}^{j\theta_2}\mathcal{H}_2 \quad \cdots \quad \mathrm{e}^{j\theta_q}\mathcal{H}_q\ ]$$

is compatible up to any lag. Thus *in general $\mathcal{H}$ cannot be identified to within a single scaling constant.* However, this may not be necessary in order for (3.12) to hold, i.e. a higher level of indeterminacy in the channel parameters could still allow equalization. We explore this issue in the next section.

3.2 A test for blind equalizability

Let Q be a square root of $C_s(0)$ as in (3.10). Define the *normalized* channel and source covariance matrices respectively as

$$H \triangleq \mathcal{H}Q, \qquad \bar{C}_s(l) \triangleq Q^{-1}C_s(l)Q^{-H}. \tag{3.13}$$

Note that in view of **A1** and **A3**, H has full column rank. Using (3.13), the matrices $C_y(l)$ become

$$C_y(l) = H\bar{C}_s(l)H^H, \qquad \text{with } \bar{C}_s(0) = I_{d_1+d_2}. \tag{3.14}$$

Similarly, if $\tilde{\mathcal{H}}$ is compatible up to lag $\bar{l}$, let $\tilde{H} = \tilde{\mathcal{H}}Q$, so that $\tilde{H}$ satisfies

$$\tilde{H}\bar{C}_s(l)\tilde{H}^H = H\bar{C}_s(l)H^H, \qquad 0 \leq l \leq \bar{l}. \tag{3.15}$$

For $l = 0$, (3.15) gives $\tilde{H}\tilde{H}^H = HH^H$. Since H has full column rank, this implies $\tilde{H} = HP$ for some unitary matrix P ($PP^H = I_{d_1+d_2}$). Thus the corresponding (unnormalized) compatible channel matrix must satisfy

$$\tilde{\mathcal{H}} = \tilde{H}Q^{-1} = \mathcal{H}(QPQ^{-1}), \tag{3.16}$$

which shows that any compatible channel matrix is related to the true channel via a *mixing matrix* of the form $\tilde{P} = QPQ^{-1}$. Observe that although P is unitary, in general $\tilde{P}$ is not. Let us introduce now the concept of admissibility.

Definition 3.2 (Admissibility) *A (d_1+d_2)-square matrix T is said to be* admissible *if it is of the form*

$$T = \begin{bmatrix} \Lambda & 0 \\ \times & \times \end{bmatrix}, \quad \textit{with } \Lambda \ d_1 \times d_1 \textit{ diagonal invertible}, \tag{3.17}$$

where '$\times$' indicates irrelevant values. Note that if T is admissible and invertible, so is T^{-1}; and that any function of an admissible matrix is admissible.

Observe that if $\tilde{\mathcal{H}} = \mathcal{H}\tilde{P}$ is compatible with $\tilde{P} = QPQ^{-1}$ admissible, then (3.12) is satisfied. Thus resolution of the channel matrix to within this ambiguity suffices for equalization purposes. Our goal is to determine conditions under which this mixing matrix $\tilde{P}$ is ensured to be admissible. To address this issue, we must explore the constraints that the conditions (3.15) impose on the unitary matrix P. Substituting $\tilde{H} = HP$ into (3.15) and using the fact that H has full rank, these constraints can be written as

$$P\bar{C}_s(l) = \bar{C}_s(l)P, \qquad 1 \leq l \leq \bar{l}. \tag{3.18}$$

That is, P must commute with the normalized source covariance matrices $\bar{C}_s(1), \ldots, \bar{C}_s(\bar{l})$. Determining the general form of all unitary matrices P that satisfy (3.18) requires solving $\bar{l}$ linear sets of equations with quadratic constraints given by $PP^H = I_{d_1+d_2}$. Fortunately, this problem can be replaced by one of solving $\bar{l}$ linear sets of equations with *linear* constraints. First recall that any unitary matrix P can be written as $P = \mathrm{e}^{jW}$ where W is a Hermitian matrix ($W = W^H$) with all its eigenvalues in $[0, 2\pi)$ [19]. Then one has the following result:

Theorem 3.1 *Let W be (d_1+d_2)-square Hermitian and $P = \mathrm{e}^{jW}$. Then P and $\bar{C}_s(l)$ commute if and only if W and $\bar{C}_s(l)$ commute.*

In view of theorem 3.1, the problem of determining the set of unitary matrices that commute with $\bar{C}_s(l)$ is equivalent to finding the set of Hermitian matrices that commute with $\bar{C}_s(l)$. Hence the blind equalizability problem can be broken into these three steps:

1. Select a square root Q of $C_s(0)$.

2. Find all Hermitian matrices W commuting with $\bar{C}_s(l) = Q^{-1}C_s(l)Q^{-H}$ for $1 \leq l \leq \bar{l}$.

3. Check whether for these matrices W, QWQ^{-1} is admissible. If so, the channel can be equalized using second-order statistics, as QWQ^{-1} admissible implies $\mathrm{e}^{jQWQ^{-1}} = Q\mathrm{e}^{jW}Q^{-1} = QPQ^{-1}$ admissible.

The utility of theorem 3.1 is revealed in that steps 2 and 3 above are much easier to solve for Hermitian matrices than for unitary matrices.

Note that the matrix Q such that $C_s(0) = QQ^H$ is not unique. Although it is true that an adequate choice of Q can considerably simplify the test for SOS-based equalizability, as will be discussed in section 3.3, it must be pointed out that the result of the test is independent of the particular Q. This is because all square roots can be parameterized as $Q = Q_0 U$, where Q_0 is a particular solution and U is any unitary matrix. Hence P_0 unitary commutes with $Q_0^{-1} C_s(l) Q_0^{-H}$ if and only if $P = U^H P_0 U$, which is unitary, commutes with $Q^{-1} C_s(l) Q^{-H}$. In addition, one has $QPQ^{-1} = Q_0 P_0 Q_0^{-1}$, so that admissibility of QPQ^{-1} is equivalent to that of $Q_0 P_0 Q_0^{-1}$.

We proceed now to determine sufficient conditions on the source statistics and the channel nonlinearities in order to ensure success of the above SOS-based equalizability test *a priori*.

3.3 Main results

It is useful to consider block lower triangular square roots Q (with block partition corresponding to linear and nonlinear parts of $S(n)$, as in (3.17)), for the following reason. Suppose that any Hermitian W solving step 2 of our test is block diagonal. Then $P = \mathrm{e}^{jW}$ is block diagonal, so that if Q was block lower triangular, then so is $\tilde{P} = QPQ^{-1}$. Having $\tilde{P}$ block lower triangular (i.e. as in (3.17) but with Λ not necessarily diagonal) can be seen as the first step towards admissibility; its significance is that if a vector g_d satisfies $g_d^H \tilde{\mathcal{H}} = e_{d+1}^H$ for some $0 \le d \le d_1 - 1$, and $\tilde{P}$ is block lower triangular, then this vector removes all the nonlinear ISI since $g_d^H \mathcal{H} = e_{d+1}^H \tilde{P}^{-1}$ and P^{-1} is block lower triangular. Once this has been achieved, additional conditions for the removal of the residual linear ISI can be sought.

3.3.1 A preliminary result

The following result gives sufficient conditions under which any Hermitian W commuting with $\bar{C}_s(1)$ is block diagonal.

Theorem 3.2 *Assume that there exists a matrix Q such that $C_s(0) = QQ^H$ and*

$$\bar{C}_s(1) = Q^{-1}C_s(1)Q^{-H} = \begin{bmatrix} C_{11} & 0 \\ C_{21} & C_{22} \end{bmatrix}, \tag{3.19}$$

with C_{ij} having size $d_i \times d_j$, $i, j \in \{1, 2\}$. Suppose that either (i) C_{11}, C_{22} do not share any eigenvalues; or (ii) $C_{21} = 0$, and C_{11}, C_{22} do not share any elementary Jordan block in their Jordan decompositions, i.e Jordan blocks belonging to the same eigenvalues have different sizes. Then any Hermitian W commuting with $\bar{C}_s(1)$ must have the following block diagonal form:

$$W = W_{11} \oplus W_{22}, \tag{3.20}$$

with W_{ii} Hermitian of size $d_i \times d_i$, $i = 1, 2$.

Most of the results in the next sections hinge on theorem 3.2.

3.3.2 A useful square root Q

With the result from theorem 3.2 in mind, we shall focus on block triangular square roots Q and look for conditions under which (3.19) is satisfied. To this end, let us define the $d_i \times d_j$ matrices

$$A_{ij} \triangleq \operatorname{cov}[S_i(n), S_j(n)], \qquad B_{ij} \triangleq \operatorname{cov}[S_i(n), S_j(n-1)], \qquad i, j \in \{1, 2\}, \tag{3.21}$$

so that the covariance matrices $C_s(0)$, $C_s(1)$ can be written as

$$C_s(0) = \begin{bmatrix} A_{11} & A_{12} \\ A_{12}^H & A_{22} \end{bmatrix}, \qquad C_s(1) = \begin{bmatrix} B_{11} & B_{12} \\ B_{21} & B_{22} \end{bmatrix}. \tag{3.22}$$

With the vectors w_{11}, w_{12} and w_{21} defined as

$$w_{1i} \triangleq \operatorname{cov}[S_i(n-1), a(n)] \quad \text{for } i \in \{1, 2\}, \qquad w_{21} \triangleq \operatorname{cov}[S_2(n), a(n-d_1)], \tag{3.23}$$

the shift structure of the signal vector $S_1(n)$ yields the following relations:

$$B_{11} = J_{d_1} A_{11} + e_1 w_{11}^H \tag{3.24}$$

$$= A_{11} J_{d_1} + X_{d_1} w_{11}^* e_{d_1}^H, \tag{3.25}$$

$$B_{12} = J_{d_1} A_{12} + e_1 w_{12}^H, \tag{3.26}$$

$$B_{21} = A_{12}^H J_{d_1} + w_{21} e_{d_1}^H. \tag{3.27}$$

Define the Schur complement of $C_s(0)$ with respect to A_{11}^{-1}

$$A_0 \triangleq A_{22} - A_{12}^H A_{11}^{-1} A_{12}, \tag{3.28}$$

which is positive definite. The following choice of Q will prove particularly useful:

$$Q = \begin{bmatrix} A_{11}^{1/2} & 0 \\ A_{12}^H A_{11}^{-H/2} & A_0^{1/2} \end{bmatrix} \quad \Rightarrow \quad Q^{-1} = \begin{bmatrix} A_{11}^{-1/2} & 0 \\ -A_0^{-1/2} A_{12}^H A_{11}^{-1} & A_0^{-1/2} \end{bmatrix}, \tag{3.29}$$

with $A_{11}^{1/2}$, $A_0^{1/2}$ square roots of A_{11}, A_0 respectively:

$$A_{11} = A_{11}^{1/2} A_{11}^{H/2}, \qquad A_0 = A_0^{1/2} A_0^{H/2}.$$

Using (3.29), the matrix $\bar{C}_s(1) = Q^{-1} C_s(1) Q^{-H}$ becomes

$$\bar{C}_s(1) = (A_{11}^{-1/2} \oplus A_0^{-1/2}) \begin{bmatrix} B_{11} & B_{12} - B_{11} A_{11}^{-1} A_{12} \\ B_{21} - A_{12}^H A_{11}^{-1} B_{11} & B_0 - A_{12}^H A_{11}^{-1} B_{12} - B_{21} A_{11}^{-1} A_{12} \end{bmatrix} \times (A_{11}^{-H/2} \oplus A_0^{-H/2}) \tag{3.30}$$

where B_0 is defined as

$$B_0 \triangleq B_{22} - A_{12}^H A_{11}^{-1} B_{11} A_{11}^{-1} A_{12}. \tag{3.31}$$

3.3.3 Block triangular $\bar{C}_s(1)$

By using (3.24)-(3.27), the off-diagonal terms of the middle matrix in (3.30) can be rewritten as

$$B_{12} - B_{11}A_{11}^{-1}A_{12} = e_1(w_{12} - A_{12}^H A_{11}^{-1} w_{11})^H, \tag{3.32}$$

$$B_{21} - A_{12}^H A_{11}^{-1} B_{11} = (w_{21} - A_{12}^H A_{11}^{-1} X_{d_1} w_{11}^*) e_{d_1}^H. \tag{3.33}$$

Introduce the vectors

$$\alpha \triangleq -A_{11}^{-1} w_{11}, \qquad \bar{\alpha} \triangleq -A_{11}^{-1} X_{d_1} w_{11}^* \tag{3.34}$$

which comprise the coefficients of the optimum forward prediction error filter (FPEF) and optimum backward prediction error filter (BPEF), respectively, of order d_1 associated to the process $\{a(k)\}$ [15]. These prediction errors are given by

$$f(k) = a(k) + \alpha^H S_1(k-1) \qquad \text{(forward prediction error)} \tag{3.35}$$

$$b(k) = a(k-d_1) + \bar{\alpha}^H S_1(k) \qquad \text{(backward prediction error)} \tag{3.36}$$

One can readily check that

$$\mathrm{cov}[S_2(k-1), f(k)] = w_{12} + A_{12}^H \alpha = w_{12} - A_{12}^H A_{11}^{-1} w_{11}, \tag{3.37}$$

$$\mathrm{cov}[S_2(k), b(k)] = w_{21} + A_{12}^H \bar{\alpha} = w_{21} - A_{12}^H A_{11}^{-1} X_{d_1} w_{11}^*. \tag{3.38}$$

Substituting (3.37)-(3.38) into (3.32)-(3.33), one obtains

$$B_{12} - B_{11}A_{11}^{-1}A_{12} = e_1\, \mathrm{cov}[S_2(k-1), f(k)]^H, \tag{3.39}$$

$$B_{21} - A_{12}^H A_{11}^{-1} B_{11} = \mathrm{cov}[S_2(k), b(k)] e_{d_1}^H. \tag{3.40}$$

Thus for Q as in (3.29), $\bar{C}_s(1)$ is block lower triangular iff $\mathrm{cov}[S_2(k-1), f(k)] = 0$; in that case, upon defining the vector

$$v \triangleq \mathrm{cov}[S_2(n), b(n)], \tag{3.41}$$

the matrix $\bar{C}_s(1)$ takes the form

$$\bar{C}_s(1) = \begin{bmatrix} A_{11}^{-1/2}(J_{d_1} - e_1\alpha^H)A_{11}^{1/2} & 0 \\ A_0^{-1/2} v e_{d_1}^H A_{11}^{-H/2} & A_0^{-1/2}(B_0 - v e_{d_1}^H A_{11}^{-1} A_{12}) A_0^{-H/2} \end{bmatrix} \quad (3.42)$$

The following result gives sufficient conditions on the symbol statistics for having $\bar{C}_s(1)$ block lower triangular:

Theorem 3.3 *Suppose that the symbol sequence $\{a(k)\}$ is an autoregressive (AR) process of order not exceeding d_1 with independent, identically distributed (iid) innovations, i.e. it is generated by means of stable all-pole filtering of an iid process $\{w(k)\}$ as follows:*

$$a(k) = w(k) - \sum_{i=1}^{d_1} \gamma_i a(k-i). \quad (3.43)$$

Assume that **A1**-**A3** *hold, that*

$$\Upsilon \triangleq \operatorname{cov}\left(\begin{bmatrix} S_1(k) \\ a(k-d_1) \end{bmatrix}, \begin{bmatrix} S_1(k) \\ a(k-d_1) \end{bmatrix} \right) > 0 \quad (3.44)$$

and that the matrices $J_{d_1} - e_1\alpha^H$ and $A_0^{-1}(B_0 - v e_{d_1}^H A_{11}^{-1} A_{12})$ do not have any common eigenvalues. Then $\bar{C}_s(1)$ is block lower triangular, and any matrix compatible with the SOS of the channel output up to the lag $\bar{l} = 1$ is related to the true channel matrix via an admissible matrix.

The following remarks are in order about theorem 3.3:

1. Condition (3.44) merely requires that the sequence $\{a(k)\}$ do not contain deterministic components, which is satisfied in any practical communication system.

2. The AR condition on the symbols $\{a(k)\}$ is sufficient for having $\bar{C}_s(1)$ block lower triangular, but it is by no means necessary. If even for non-AR symbols $\operatorname{cov}[S_2(k-1), f(k)] = 0$ holds, one can use theorem 3.2 in order to reduce the

blind equalizability problem to an eigenvalue check on the matrices $J_{d_1} - e_1\alpha^H$ and $A_0^{-1}(B_0 - ve_{d_1}^H A_{11}^{-1}A_{12})$.

3. The matrix $A_0^{-1}(B_0 - ve_{d_1}^H A_{11}^{-1}A_{12})$ has a linear prediction interpretation. Let $\tilde{S}_2(k)$ be the prediction error obtained when approximating $S_2(k)$ by a linear function of $S_1(k)$:

$$\tilde{S}_2(k) = S_2(k) - \Gamma^H S_1(k).$$

The value of Γ that minimizes trace$\{\text{cov}[\tilde{S}_2(k), \tilde{S}_2(k)]\}$ is $\Gamma = A_{11}^{-1}A_{12}$, for which one has $\text{cov}[\tilde{S}_2(k), \tilde{S}_2(k)] = A_0$, and $\text{cov}[\tilde{S}_2(k), \tilde{S}_2(k-1)] = B_0 - ve_{d_1}^H A_{11}^{-1}A_{12}$ provided that $\text{cov}[S_2(k-1), f(k)] = 0$ holds. Therefore

$$A_0^{-1}(B_0 - ve_{d_1}^H A_{11}^{-1}A_{12}) = \text{cov}[\tilde{S}_2(k), \tilde{S}_2(k)]^{-1}\,\text{cov}[\tilde{S}_2(k), \tilde{S}_2(k-1)].$$

The problem of isolating conditions under which this matrix and $J_{d_1} - e_1\alpha^H$ do not have common eigenvalues remains open.

4. Theorem 3.3 covers the important case of iid symbols $\{a(k)\}$ (by having $\gamma_1 = \cdots = \gamma_{d_1} = 0$), for which $\alpha = \bar{\alpha} = 0$, $f(k) = a(k)$, $b(k) = a(k-d_1)$ and $A_{11} = \sigma_a^2 I_{d_1}$. More will be said about the iid input case in Theorem 3.4 and section 3.3.5.

3.3.4 Block diagonal $\bar{C}_s(1)$

It is clear from (3.39)-(3.40) that for our choice of Q, $\bar{C}_s(1)$ is block diagonal if and only if in addition to $\text{cov}[S_2(n-1), f(n)] = 0$ one also has $v = \text{cov}[S_2(n), b(n)] = 0$, in which case the resulting value is

$$\bar{C}_s(1) = [A_{11}^{-1/2}(J_{d_1} - e_1\alpha^H)A_{11}^{1/2}] \oplus [A_0^{-1/2}B_0A_0^{-H/2}]. \tag{3.45}$$

The theorems below provide sufficient conditions for (3.45) to hold. The first one makes the following additional assumptions:

A4: The transmitted symbol sequence $\{a(k)\}$ is iid with $E[|a(k)|^2] = \sigma_a^2$.

A5: $\mathrm{cov}[S_2(k), a(k-d_1)] = 0$.

Observe that under assumptions **A1**-**A5**, and taking Q as in (3.29) with $A_{11}^{1/2} = \sigma_a I_{d_1}$, in addition to being block diagonal the matrix $\bar{C}_s(1) = Q^{-1} C_s(1) Q^{-H}$ takes the form

$$\bar{C}_s(1) = J_{d_1} \oplus [A_0^{-1/2} B_0 A_0^{-H/2}], \tag{3.46}$$

since $\alpha = 0$ for iid $\{a(k)\}$.

Theorem 3.4 *Under assumptions* **A1**-**A5**, *if the Jordan decomposition of the matrix $A_0^{-1} B_0$ has no Jordan block of size d_1 associated to the zero eigenvalue, then any matrix compatible with the channel output SOS up to lag 1 is related to the true channel matrix by an admissible matrix.*

A sufficient, though not necessary condition for **A5** to hold is that **A4** hold and the linear kernel memory be no less than that of the nonlinear part. In that case, $S_2(k)$ is a function of $a(k)$, $a(k-1)$, $\ldots$, $a(k-d_1+1)$ so that if $\{a(k)\}$ is iid then the random variables $S_2(k)$ and $a(k-d_1)$ are independent and **A5** follows.

The next result applies for channels in which the linear and nonlinear parts are uncorrelated.

Theorem 3.5 *Assume that Υ defined in (3.44) is positive definite and that for $i > 1$ and for all n,*

$$\mathrm{cov}[a(k), s_i(k-n)] = 0.$$

Then with Q as in (3.29), the matrix $\bar{C}_s(1)$ is block diagonal. If $A_{11}^{-1} B_{11}$ and $A_{22}^{-1} B_{22}$ do not share any elementary Jordan block in their Jordan decompositions, then for any Hermitian W commuting with $\bar{C}_s(1)$ the matrix QWQ^{-1} is admissible.

Thus when the linear and nonlinear parts are uncorrelated, the 'no common Jordan blocks' condition is sufficient for blind equalizability from $\bar{C}_s(0)$, $\bar{C}_s(1)$.

The next result is as follows:

Theorem 3.6 *Suppose assumptions* **A1**-**A3** *hold, the symbols* $\{a(k)\}$ *are Gaussian, and the memory of the nonlinear part of the channel does not exceed that of the linear part, i.e.* $S_2(k) = \phi(S_1(k))$ *where* $\phi(\cdot)$ *is a memoryless mapping. Also assume that the Jordan decompositions of the matrices* $J_{d_1} - e_1\alpha^H$ *and* $A_0^{-1}B_0$ *do not have any common elementary Jordan block, and that* Υ*, defined in (3.44), is positive definite. Then any matrix compatible with the SOS of the channel output up to the lag* $\bar{l} = 1$ *is related to the true channel matrix via an admissible matrix.*

The following remarks are in order about theorem 3.3:

1. Gaussianity of the symbols $\{a(k)\}$ is sufficient for having $\bar{C}_s(1)$ block diagonal, but it is not necessary. In general, as long as $\text{cov}[S_2(k-1), f(k)] = \text{cov}[S_2(k), b(k)] = 0$ is satisfied, theorem 3.2 allows one to reduce the blind equalizability problem to a check on the Jordan structures of $J_{d_1} - e_1\alpha^H$ and $A_0^{-1}B_0$.

2. If the conditions of theorem 3.6 are satisfied, the color of the symbols $\{a(k)\}$ does not affect blind equalizability. It is conceivable, however, that for Gaussian symbols a particular choice of the symbol autocorrelation could result in the two diagonal blocks of $\bar{C}_s(1)$ sharing a Jordan block.

3. An example of a communications system in which the symbols are approximately Gaussian is the Orthogonal Frequency Division Multiplexing (OFDM) scheme [7], in which the original symbol stream is divided in blocks that undergo an Inverse Discrete Fourier Transform (IDFT) operation prior to transmission. If the original symbols were zero-mean iid then the IDFT output is asymptotically (i.e. as the block size tends to infinity) white Gaussian [8]. Constellation

shaping is another technique that produces a Gaussian-like symbol sequence [33].

3.3.5 A result for iid symbols

So far we have considered the problem of equalizability from $C_y(0)$ and $C_y(1)$, that is, we have taken $\bar{l} = 1$ in (3.1). Although it is desirable to keep $\bar{l}$ small in order to reduce complexity, other choices are clearly possible and may lead to different equalizability conditions, as the next result shows.

Theorem 3.7 *Under Assumptions* **A1**-**A3***, suppose that the symbols* $\{a(k)\}$ *are iid and that the memory of the linear part of the channel is* strictly greater *than that of the nonlinear part, i.e.*

$$S_2(k) = \phi(\ a(k), \ \ldots \ , a(k - d_1 + 2)\ ) \qquad \text{with } \phi(\cdot, \ldots, \cdot) \text{ a memoryless mapping.} \tag{3.47}$$

Then the ZF equalizers of delays 0 *and* $d_1 - 1$ *obtained for any channel matrix compatible with the second-order statistics of the received signal up to lag* $\bar{l} = d_1 - 1$ *are also ZF equalizers for the true channel. That is, (3.12) holds with* $d = 0$ *and* $d = d_1 - 1$.

Observe that although this result places more stringent requirements on the source statistics and the channel memory than theorems 3.3- 3.6, it has the advantage of completely disposing of the eigenvalue condition on $\bar{C}_s(1)$ that those results required for equalizability (via theorem 3.2). We must also note that once the zero-delay ZF equalizer is available, the ZF equalizers for other delays can be readily computed:

Lemma 3.1 *Let* g_0 *be a zero-delay ZF equalizer for* $\mathcal{H}$*, i.e.* $g_0^H \mathcal{H} = e_1^H$*. Under assumptions* **A1** *and* **A3***, the ZF equalizer of delay* d*,* g_d*, is given by*

$$g_d = C_y(0)^{\#} C_y(d) g_0, \tag{3.48}$$

where $C_y(0)$ and $C_y(d)$ are de-noised output covariance matrices, i.e.

$$C_y(0) = \mathcal{H}C_s(0)\mathcal{H}^H, \qquad C_y(d) = \mathcal{H}C_s(d)\mathcal{H}^H.$$

3.4 Some examples

We give now some examples of application of the results developed in the previous sections.

3.4.1 Linear-quadratic channels

Suppose that the only nonlinearities in the channel are of quadratic type:

$$s_i(k) = a(k)a(k-n_i) \qquad \text{for some } n_i \geq 0 \text{ and } i > 1.$$

It is assumed without loss of generality that $n_i \neq n_j$ if $i \neq j$. Suppose also that the symbols $\{a(k)\}$ are real, iid, and symmetrically distributed about the origin; in that case, $E[a^n(k)] = 0$ for n odd. Under these conditions, one has

$$\text{cov}[s_i(k), s_j(k-n)] = \sigma_i^2 \delta(i-j)\delta(n),$$

where $\delta(\cdot)$ is the Kronecker delta and

$$\sigma_i^2 \triangleq \text{cov}[s_i(k), s_i(k)] = \begin{cases} E[a^2(k)] & \text{if } i = 1, \\ E[a^2(k)]^2 & \text{if } i > 1 \text{ and } n_i \neq 0, \\ E[a^4(k)] - E^2[a^2(k)] & \text{if } i > 1 \text{ and } n_i = 0. \end{cases}$$

In these conditions, assumptions **A4**-**A5** are satisfied, and the source covariance matrices are given by

$$C_s(l) = \sigma_1^2 J^l_{m+l_1} \oplus \sigma_2^2 J^l_{m+l_2} \oplus \cdots \oplus \sigma_q^2 J^l_{m+l_q}.$$

Thus by choosing $Q = \sigma_1 I_{m+l_1} \oplus \cdots \oplus \sigma_q I_{m+l_q}$, the corresponding normalized source covariance sequence becomes simply

$$\bar{C}_s(l) = J^l_{m+l_1} \oplus J^l_{m+l_2} \oplus \cdots \oplus J^l_{m+l_q}.$$

Observe that $\bar{C}_s(1)$ is already a Jordan form, whose only eigenvalue is zero, and which has q elementary Jordan blocks of sizes $m+l_1$, $m+l_2$, ..., $m+l_q$. Hence if $l_i \neq l_1$ for $i \neq 1$, we can invoke Theorem 3.4 to conclude that the channel is blindly equalizable from $C_y(0)$, $C_y(1)$.

In addition, this 'length disparity condition' is also necessary for blind equalizability from the channel output SOS. For if $l_2 = l_1$, then any matrix of the form

$$\tilde{\mathcal{H}} = \mathcal{H}(T \oplus I_{m+l_3} \oplus \cdots \oplus I_{m+l_q})$$

with T of the form

$$T = \begin{bmatrix} \cos\alpha \cdot I_{m+l_1} & \frac{\sigma_1}{\sigma_2}\mathrm{e}^{j\beta}\sin\alpha \cdot I_{m+l_1} \\ \frac{\sigma_2}{\sigma_1}\mathrm{e}^{j\gamma}\sin\alpha \cdot I_{m+l_1} & -\mathrm{e}^{j(\beta+\gamma)}\cos\alpha \cdot I_{m+l_1} \end{bmatrix} \tag{3.49}$$

is compatible with the channel output SOS up to any lag $\bar{l}$. Therefore the ambiguity represented by the parameters α, β, γ in (3.49) cannot be resolved using SOS. And if g_d satisfies $g_d^H\tilde{\mathcal{H}} = e_{d+1}^H$ for some $0 \leq d \leq m+l_1-1$, when applied to the actual channel g_d does not totally remove ISI: in the noiseless case, one has

$$g_d^H Y(k) = \cos\alpha \cdot a(k-d) + \frac{\sigma_2}{\sigma_1}\mathrm{e}^{-j\beta}\sin\alpha \cdot s_2(k-d),$$

so that a certain amount of nonlinear ISI remains at the equalizer output.

3.4.2 Satellite links with PSK modulation

Here we consider the baseband equivalent nonlinear model for a satellite link. As discussed in section 1.2.1, due to the bandpass nature of the channel these systems can be modeled by the truncated Volterra series given in (1.2), which can be readily reformulated to fit the model 3.1. The generating terms $\{s_i(k)\}$ are monomials that can be written as

$$s_i(k) = \prod_{j=1}^{m_i} a^*(k-t_{ij}) \prod_{j=m_i+1}^{2m_i+1} a(k-t_{ij}), \tag{3.50}$$

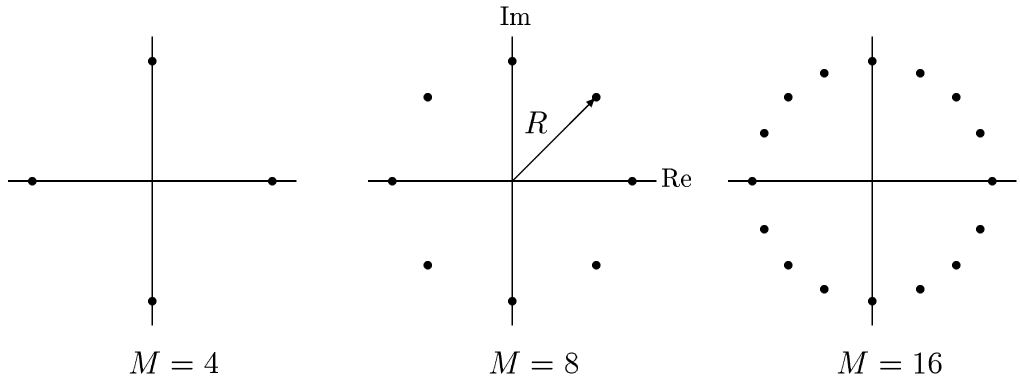

Figure 12: The PSK constellation for three values of M.

i.e. there is an odd number of terms in the monomial, with one more unconjugated than conjugated terms.

We shall assume that the communication system uses phase-shift keying (PSK) modulation, as this is a popular format for satellite links [4]. In that case the symbols $\{a(k)\}$ are independent, equally likely, and drawn from a constellation of the form

$$a(k) \in \{R \cdot \mathrm{e}^{j2\pi n/M}, \quad n = 0, 1, \ldots, M-1\}$$

where M is the alphabet size, which is usually a power of 2. The PSK constellation is illustrated in figure 12.

The channel structure (3.50) leads to the following result:

Lemma 3.2 *Consider the generating terms $\{s_i(k)\}$ of the baseband equivalent Volterra channel, given by (3.50). If the symbols $\{a(k)\}$ are independent and drawn from an M-ary PSK constellation, then each $\{s_i(k)\}$ is a white process, and for $i \neq j$ one has* $\mathrm{cov}[s_i(n), s_j(k)] = 0$ *for all n, k.*

In these conditions, assumptions **A4**-**A5** are satisfied, and the source covariance matrices are given by

$$C_s(l) = \sigma_1^2 J_{m+l_1}^l \oplus \sigma_2^2 J_{m+l_2}^l \oplus \cdots \oplus \sigma_q^2 J_{m+l_q}^l,$$

where $\sigma_i^2 \triangleq E[|s_i(k)|^2]$, which is the same structure we found in the previous section for linear-quadratic channels with real symbols. Thus by choosing again $Q = \sigma_1 I_{m+l_1} \oplus \cdots \oplus \sigma_q I_{m+l_q}$, the normalized source covariance matrices become again

$$\bar{C}_s(l) = J_{m+l_1}^l \oplus J_{m+l_2}^l \oplus \cdots \oplus J_{m+l_q}^l.$$

As in section 3.4.1, we conclude that if $l_i \neq l_1$ for $i \neq 1$, the channel is blindly equalizable from $C_y(0)$, $C_y(1)$; and that this 'length disparity condition' is also necessary for blind equalizability from the channel output SOS.

3.4.3 Colored sources

So far we have considered cases for which the symbols $\{a(k)\}$ are uncorrelated. In this section we give an example in which the source symbol sequence is colored.

Offset Quadrature Phase-Shift Keying (OQPSK) is a modulation technique obtained by delaying the quadrature digits by T_b seconds relative to the in-phase digits in a 4-PSK modulator, where T_b is the bit interval [4]. This fact constraints the maximum phase shift between two consecutive symbols to $\pm 90°$ in contrast with standard QPSK in which $180°$ phase transitions are possible. Usually the transmitted QPSK signal is bandpass filtered so as to reduce out-of-band radiation and hence co-channel interference. The envelope of the filtered QPSK signal approaches zero at the time instants when the $180°$ phase jumps occur, an effect that is highly undesirable when the signal undergoes nonlinear amplification. This is because the out-of-band spectral sidelobes are enhanced by the nonlinear amplifier, therefore destroying the filtering action at the transmitter. By eliminating the possibility of $180°$ phase jumps OQPSK reduces the envelope fluctuations after filtering, thus allowing for more efficient amplification [23].

OQPSK modulation produces a sequence of symbols that is correlated. Suppose the constellation $\{1+j, 1-j, -1+j, -1-j\}$ is employed, and let $\{b_k\}$ be the stream of independent, equiprobable 'bipolar bits' ($b_k \in \{-1, +1\}$). Assuming that the basic signaling pulse is rectangular in shape, then due to the offset between the in-phase and quadrature components the OQPSK symbols can be seen as generated according to the following rule:

$$a(k) = \begin{cases} b_{k-1} + jb_k & \text{for } k \text{ even,} \\ b_k + jb_{k-1} & \text{for } k \text{ odd.} \end{cases}$$

From this one finds that the covariance of the symbols is given by

$$\operatorname{cov}[a(k), a(k-n)] = \begin{cases} 2, & n = 0, \\ 1, & n = \pm 1, \\ 0, & \text{else.} \end{cases}$$

Now consider a nonlinear channel of the form (3.1) with $q = 2$, $s_1(k) = a(k)$ and

$$s_2(k) = a(k)a^*(k-1).$$

One can check that $\operatorname{cov}[s_1(k), s_2(k-n)] = 0$ for all n, so that we are in the conditions of theorem 3.5. In addition,

$$\operatorname{cov}[s_2(k), s_2(k-n)] = \begin{cases} 3, & n = 0, \\ 1, & n = \pm 1, \\ 0, & \text{else.} \end{cases}$$

Therefore $\{s_1(k)\}$, $\{s_2(k)\}$ are first-order Moving Average (MA(1)) processes, with autocovariance coefficients

$$\rho_1 \triangleq \frac{\operatorname{cov}[s_1(k), s_1(k-1)]}{\operatorname{cov}[s_1(k), s_1(k)]} = \frac{1}{2}, \qquad \rho_2 \triangleq \frac{\operatorname{cov}[s_2(k), s_2(k-1)]}{\operatorname{cov}[s_2(k), s_2(k)]} = \frac{1}{3}.$$

According to theorem 3.5, a sufficient condition for blind equalizability from $C_y(0)$, $C_y(1)$ is that the matrices

$$C_{11} \triangleq A_{11}^{-1/2} B_{11} A_{11}^{-H/2}, \qquad C_{22} \triangleq A_{22}^{-1/2} B_{22} A_{22}^{-H/2}$$

do not share any elementary Jordan block in their Jordan decompositions. Now these matrices are similar respectively to the matrices

$$A_{11}^{-1} B_{11}, \qquad A_{22}^{-1} B_{22}.$$

These are companion matrices associated to the FPEFs of orders d_1 and d_2, respectively, for the processes $\{s_1(k)\}$ and $\{s_2(k)\}$. It turns out that the transfer functions of the FPEFs of MA(1) processes with covariance coefficients $\rho_1 = 1/2$ and $\rho_2 = 1/3$ are coprime for all values of d_1 and d_2. Therefore the matrices C_{11} and C_{22} do not share eigenvalues, and blind equalizability from $C_y(0)$, $C_y(1)$ follows.

CHAPTER IV

EQUALIZATION ALGORITHMS FOR NONLINEAR CHANNELS WITH INDEPENDENT SOURCES

In Chapter III we have presented sufficient conditions on the source statistics and the channel nonlinearities in order to guarantee that the channel output SOS contain sufficient information about the ZF equalizers. The next logical step is the development of algorithms to extract these equalizers. In this chapter we consider this problem focusing on the particular but important case in which the symbols $\{a(k)\}$ are independent and identically distributed (iid). In particular we will consider the cases covered by theorems 3.4 and 3.7. The development in the next section is valid for both settings; after that, the two particular cases are treated separately.

Once the ZF equalizers have been obtained, their MMSE counterparts can be computed as shown in section 4.4. Simulation results are presented in section 4.5.

4.1 General considerations

For convenience, the assumptions corresponding to the settings of theorems 3.4 and 3.7 are repeated here. For both settings, it is assumed that **A1**-**A4** hold:

A1: The channel matrix $\mathcal{H}$ is tall and has full column rank.

A2: The noise $\{n(k)\}$ is zero-mean white with covariance $\sigma_n^2 I_p$.

A3: The covariance matrix $C_s(0)$ is positive definite.

A4: The transmitted symbol sequence $\{a(k)\}$ is iid with $E[|a(k)|^2] = \sigma_a^2$.

In addition, the setting of theorem 3.4 also requires **A5**:

A5: $\text{cov}[S_2(k), a(k-d_1)] = 0$.

On the other hand, the setting of theorem 3.7 requires $\mathbf{A5}'$ instead of $\mathbf{A5}$:

$\mathbf{A5}'$**:** The vector $S_2(k)$ can be written as $S_2(k) = \phi(\ a(k),\ \ \ldots\ \ , a(k-d_1+2)\ )$, with $\phi(\cdot,\ldots,\cdot)$ a memoryless mapping.

Observe that $\mathbf{A5}'$ implies $\mathbf{A5}$, but that the converse is not true in general. Therefore in any of these settings the normalized lag 1 source covariance matrix $\bar{C}_s(1)$ takes the form shown in (3.46), repeated here for convenience:

$$\bar{C}_s(1) = J_{d_1} \oplus [A_0^{-1/2} B_0 A_0^{-H/2}] = J_{d_1} \oplus C,$$

where C is defined as

$$C \triangleq A_0^{-1/2} B_0 A_0^{-H/2}. \tag{4.1}$$

Our development consists of two conceptual steps:

1. The (normalized) channel matrix H can be determined from $C_y(0)$ to within a unitary mixing matrix.

2. The information contained in $C_y(l)$ with $l \geq 1$ is then used to resolve the indeterminacy represented by this mixing matrix.

The first step is achieved as follows. As in [29], perform a singular value decomposition (SVD) of $C_y(0)$:

$$C_y(0) = [\ U_1 \quad U_2\ ] \begin{bmatrix} \Sigma^2 & 0 \\ 0 & 0 \end{bmatrix} \begin{bmatrix} U_1^H \\ U_2^H \end{bmatrix}, \tag{4.2}$$

where $\Sigma^2 > 0$ is a $(d_1+d_2) \times (d_1+d_2)$ diagonal matrix of singular values and U_1 has d_1+d_2 columns. Recall that, with H the normalized channel matrix defined in (3.13), one has $C_y(0) = HH^H$. Since H has full column rank, it follows that $H = U_1 \Sigma V$ for some unitary $(d_1+d_2) \times (d_1+d_2)$ matrix V. Thus in order to identify the channel, it remains to obtain this matrix V.

However, for equalization purposes it is not necessary to obtain the whole matrix V. To see this, let us partition V as $V = [\ V_1 \quad V_2\ ]$ where each V_i has d_i columns, $i = 1, 2$. Let us collect the ZF equalizers g_i in the $pm \times d_1$ matrix

$$\mathcal{G}_{\text{ZF}} \triangleq [\ g_0 \quad g_1 \quad \cdots \quad g_{d_1-1}\ ].$$

Observe that

$$\begin{aligned}
\mathcal{G}_{\text{ZF}}^H &= [\ I_{d_1} \quad 0\ ]\mathcal{H}^{\#} \\
&= [\ I_{d_1} \quad 0\ ]QH^{\#} \\
&= [\ I_{d_1} \quad 0\ ]Q(U_1 \Sigma V)^{\#} \\
&= \sigma_a [\ I_{d_1} \quad 0\ ]V^H \Sigma^{-1} U_1^H \\
&= \sigma_a V_1^H \Sigma^{-1} U_1^H,
\end{aligned} \tag{4.3}$$

where we have used the fact that

$$[\ I_{d_1} \quad 0\ ]Q = [\ I_{d_1} \quad 0\ ] \begin{bmatrix} \sigma_a I_{d_1} & 0 \\ \frac{1}{\sigma_a} A_{12}^H & A_0^{1/2} \end{bmatrix} = \sigma_a [\ I_{d_1} \quad 0\ ].$$

Since Σ, U_1 are available from the SVD of $C_y(0)$, it follows that for equalization purposes we just need to estimate V_1. The remaining columns of V are of no interest to us.

We show now that if either the first or last column of V_1 were available, then the remaining columns could be recovered by making use of the lag 1 covariance matrix $C_y(1)$. To do so, define the matrix

$$R \triangleq \Sigma^{-1} U_1^H C_y(1) U_1 \Sigma^{-1}. \tag{4.4}$$

Substituting $C_y(1) = \mathcal{H} C_s(1) \mathcal{H}^H = H \bar{C}_s(1) H^H$ in (4.4), and using the fact that

$U_1^H U_1 = I_{d_1+d_2}$, one finds

$$\begin{aligned} R &= \Sigma^{-1} U_1^H H \bar{C}_s(1) H^H U_1 \Sigma^{-1} \\ &= \Sigma^{-1} U_1^H (U_1 \Sigma V) \bar{C}_s(1) (V^H \Sigma U_1^H) U_1 \Sigma^{-1} \\ &= V \bar{C}_s(1) V^H \\ &= \begin{bmatrix} V_1 & V_2 \end{bmatrix} \begin{bmatrix} J_{d_1} & 0 \\ 0 & C \end{bmatrix} \begin{bmatrix} V_1^H \\ V_2^H \end{bmatrix} \\ &= V_1 J_{d_1} V_1^H + V_2 C V_2^H. \end{aligned} \tag{4.5}$$

Note that since V is unitary, one has

$$V_1^H V_1 = I_{d_1}, \qquad V_2^H V_2 = I_{d_2}, \qquad V_1^H V_2 = 0. \tag{4.6}$$

Therefore (4.5) yields

$$R V_1 = V_1 J_{d_1}, \qquad R^H V_1 = V_1 J_{d_1}^H. \tag{4.7}$$

If we partition V_1 columnwise as $V_1 = [\, v_{1,1} \quad \cdots \quad v_{1,d_1} \,]$, then eqs. (4.7) read as

$$R v_{1,d_1} = 0, \qquad R v_{1,i-1} = v_{1,i} \quad i = d_1, \ldots, 3, 2, \tag{4.8}$$

$$R^H v_{1,1} = 0, \qquad R^H v_{1,j} = v_{1,j-1} \quad j = 2, 3, \ldots, d_1. \tag{4.9}$$

Thus once an estimate of either $v_{1,1}$ or v_{1,d_1} is available, the remaining columns $v_{1,i}$ can be recovered via (4.8)-(4.9).

Therefore the problem reduces to finding $v_{1,1}$ or v_{1,d_1} from the channel output SOS. In the original algorithm of [29] for linear channels, one had $\bar{C}_s(1) = J_{d_1}$, i.e. the block C in (4.5) was absent. This allowed for $v_{1,1}$, v_{1,d_1} to be taken as the left and right singular vectors of the matrix R associated to the smallest singular value. This approach would work in our case provided that C in (4.5) is nonsingular. However we would like to allow for singular C as well since this is usually the case in practice.

We shall present first the solution for the setting of theorem 3.7, as the resulting algorithm is considerably simpler than that obtained in the framework of theorem 3.4.

4.2 The setting of theorem 3.7

Consider the matrix

$$\tilde{R} \triangleq \Sigma^{-1} U_1^H C_y(d_1 - 1) U_1 \Sigma^{-1}. \tag{4.10}$$

Substituting $C_y(d_1 - 1) = \mathcal{H} C_s(d_1 - 1)\mathcal{H}^H = H\bar{C}_s(d_1 - 1)H^H$ in (4.10), and using again $U_1^H U_1 = I_{d_1+d_2}$, one has

$$\begin{aligned}
\tilde{R} &= \Sigma^{-1} U_1^H H \bar{C}_s(d_1 - 1) H^H U_1 \Sigma^{-1} \\
&= \Sigma^{-1} U_1^H (U_1 \Sigma V) \bar{C}_s(d_1 - 1)(V^H \Sigma U_1^H) U_1 \Sigma^{-1} \\
&= V \bar{C}_s(d_1 - 1) V^H.
\end{aligned}$$

It is shown in the proof of theorem 3.7 that under the conditions of this setting (i.e. assumptions **A1**-**A4** and **A5′**) the matrix $\bar{C}_s(d_1 - 1)$ satisfies

$$\bar{C}_s(d_1 - 1) = (e_{d_1} e_1^H) \oplus 0_{d_2 \times d_2}. \tag{4.11}$$

Therefore

$$\begin{aligned}
\tilde{R} &= V \bar{C}_s(d_1 - 1) V^H \\
&= \begin{bmatrix} V_1 & V_2 \end{bmatrix} \begin{bmatrix} e_{d_1} e_1^H & 0 \\ 0 & 0 \end{bmatrix} \begin{bmatrix} V_1^H \\ V_2^H \end{bmatrix} \\
&= V_1 e_{d_1} e_1^H V_1^H \\
&= v_{1,d_1} v_{1,1}^H.
\end{aligned} \tag{4.12}$$

The relation (4.12) shows that $\tilde{R}$ is a rank one matrix, and that its only nonzero singular value equals 1. The vectors v_{1,d_1}, $v_{1,1}$ can be obtained up to a constant of the form $e^{j\theta}$ as the left and right singular vectors, respectively, associated to the largest singular value of $\tilde{R}$. An alternative and computationally cheaper way is to directly extract v_{1,d_1} as a normalized column of $\tilde{R}$ and $v_{1,1}$ as a normalized row:

$$\hat{v}_{1,d_1} = \frac{\tilde{R}e_{i_{\max}}}{||\tilde{R}e_{i_{\max}}||}, \quad \text{with } i_{\max} = \arg\max\{||\tilde{R}e_i||,\ 1 \leq i \leq d_1 + d_2\}, \tag{4.13}$$

$$\hat{v}_{1,1}^H = \frac{e_{j_{\max}}^H \tilde{R}}{||e_{j_{\max}}^H \tilde{R}||}, \quad \text{with } j_{\max} = \arg\max\{||e_j^H \tilde{R}||,\ 1 \leq j \leq d_1 + d_2\}. \tag{4.14}$$

In this way these estimates $\hat{v}_{1,d_1}$, $\hat{v}_{1,1}$ are related to the true quantities v_{1,d_1}, $v_{1,1}$ by some complex constants with unit modulus. From these, the remaining columns of V_1 can be estimated via either of the Jordan chains (4.8)-(4.9), thus obtaining an estimate $\hat{V}_1$ satisfying $\hat{V}_1 = \mathrm{e}^{j\theta} V_1$ for some real θ. In view of (4.3), the matrix $\hat{\mathcal{G}}_{\mathrm{ZF}} = \sigma_a U_1 \Sigma^{-1} \hat{V}_1$ satisfies $\hat{\mathcal{G}}_{\mathrm{ZF}} \mathcal{H} = \mathrm{e}^{j\theta} I_{d_1}$, providing equalization up to an unknown phase rotation. This is acceptable since the need for a phase reference can be sidestepped by differentially encoding the data. The algorithm is summarized next.

Algorithm 4.1: Blind equalization under the conditions of theorem 3.7

---

1. Perform an SVD of $C_y(0)$ as in (4.2) to obtain U_1, Σ.
2. Construct the matrix R as in (4.4).
3. Construct the matrix $\tilde{R}$ as in (4.10).
4. Form the estimates $\hat{v}_{1,d_1}$, $\hat{v}_{1,1}$ via (4.13)-(4.14).
5. For $i = 2, 3, \ldots, d_1$, let $\hat{v}_{1,i} = R\hat{v}_{1,i-1}$. Alternatively, for $j = d_1, d_1 - 1, \ldots, 2$, let $\hat{v}_{1,j-1} = R^H \hat{v}_{1,j}$.
6. Construct the ZF equalizers as $\hat{\mathcal{G}}_{\mathrm{ZF}} = \sigma_a U_1 \Sigma^{-1} [\ \hat{v}_{1,1} \ \cdots \ \hat{v}_{1,d_1}\ ]$.

4.3 The setting of theorem 3.4

In this framework, conditions **A1**-**A5** are assumed to hold, and in addition it is assumed that the Jordan decomposition of the matrix C defined in (4.1) does not have any elementary Jordan block of size d_1 associated to the zero eigenvalue.

Observe that assumption **A5** is weaker than assumption **A5**$'$ and as a consequence it does not guarantee that $\bar{C}_s(d_1 - 1)$ be of the form (4.11). Nevertheless, we show in this section how V_1 can be estimated from the powers of the matrix R. Note that due to (4.6), one has for all n,

$$R^n = V_1 J_{d_1}^n V_1^H + V_2 C^n V_2^H. \tag{4.15}$$

Also observe that the powers of the shift matrix J_{d_1} satisfy

$$J_{d_1}^{d_1 - 1} = e_{d_1} e_1^H, \qquad J_{d_1}^n = 0 \quad \text{for } n \geq d_1.$$

Suppose for the moment that $V_2 C^{d_1-1} V_2^H$ has been found. Then we could construct the matrix $R^{d_1-1} - V_2 C^{d_1-1} V_2^H$, which in view of (4.15) satisfies

$$R^{d_1-1} - V_2 C^{d_1-1} V_2^H = V_1 e_{d_1} e_1^H V_1^H = v_{1,d_1} v_{1,1}^H.$$

Hence $(v_{1,1}, v_{1,d_1})$ could then readily be estimated from this matrix, up to a constant of the form $e^{j\theta}$. Therefore our goal shall be to determine $V_2 C^{d_1-1} V_2^H$.

Consider a Jordan decomposition of the matrix C:

$$C = T(\hat{Y} \oplus Y \oplus Z)T^{-1} \tag{4.16}$$

where $\hat{Y}$ is a direct sum of shift matrices J_i with $i < d_1$, Y is a direct sum of shift matrices J_i with $i > d_1$, and Z is square nonsingular. Observe that there is no block J_{d_1} in the Jordan form in (4.16), as this was required by theorem 3.4 for blind equalizability. Now let us partition the matrix T in (4.16) as

$$T = [\ \hat{T}_1 \quad T_1 \quad T_2\ ]$$

with $\hat{T}_1$, T_1 and T_2 having the same number of columns as $\hat{Y}$, Y and Z respectively. Then the matrix T^{-1} is given by

$$T^{-1} = \begin{bmatrix} \hat{T}_1^{\#} \\ T_1^{\#} \\ T_2^{\#} \end{bmatrix},$$

so that

$$T^{-1}T = \begin{bmatrix} \hat{T}_1^{\#} \\ T_1^{\#} \\ T_2^{\#} \end{bmatrix} [\ \hat{T}_1 \quad T_1 \quad T_2\ ] = \begin{bmatrix} \hat{T}_1^{\#}\hat{T}_1 & \hat{T}_1^{\#}T_1 & \hat{T}_1^{\#}T_2 \\ T_1^{\#}\hat{T}_1 & T_1^{\#}T_1 & T_1^{\#}T_2 \\ T_2^{\#}\hat{T}_1 & T_2^{\#}T_1 & T_2^{\#}T_2 \end{bmatrix} = \begin{bmatrix} I & 0 & 0 \\ 0 & I & 0 \\ 0 & 0 & I \end{bmatrix}.$$

Therefore one can express

$$V_2 C V_2^H = \hat{\Gamma} + \Gamma + \Delta, \tag{4.17}$$

where

$$\hat{\Gamma} \triangleq V_2 \hat{T}_1 \hat{Y} \hat{T}_1^{\#} V_2^H, \qquad \Gamma \triangleq V_2 T_1 Y T_1^{\#} V_2^H, \qquad \Delta \triangleq V_2 T_2 Z T_2^{\#} V_2^H. \tag{4.18}$$

Moreover one has for all n

$$\begin{aligned} V_2 C^n V_2^H &= V_2 \hat{T}_1 \hat{Y}^n \hat{T}_1^{\#} V_2^H + V_2 T_1 Y^n T_1^{\#} V_2^H + V_2 T_2 Z^n T_2^{\#} V_2^H \\ &= \hat{\Gamma}^n + \Gamma^n + \Delta^n. \end{aligned}$$

Since $\hat{Y}$ is a direct sum of shift matrices of size smaller than d_1, $\hat{\Gamma}^{d_1-1} = 0$ so that the matrix of interest reduces to

$$V_2 C^{d_1-1} V_2^H = \Gamma^{d_1-1} + \Delta^{d_1-1}. \tag{4.19}$$

Denote $\mathcal{J}_{rn}$ as the r-fold direct sum of J_n:

$$\mathcal{J}_{rn} \triangleq J_n \oplus \overset{(r \text{ times})}{\cdots} \oplus J_n.$$

Letting $n_1 > n_2 > \cdots > n_u > d_1$, the matrix Y can be written without loss of generality as

$$Y = \mathcal{J}_{r_1 n_1} \oplus \mathcal{J}_{r_2 n_2} \oplus \cdots \oplus \mathcal{J}_{r_u n_u}, \tag{4.20}$$

for some r_i, n_i, u. Likewise partition $T_1 = [\ T_{11} \quad T_{12} \quad \cdots \quad T_{1u}\ ]$, with T_{1i} having the same number of columns as $\mathcal{J}_{r_i n_i}$. Note that the matrices

$$\Gamma_i \triangleq V_2 T_{1i} \mathcal{J}_{r_i n_i} T_{1i}^{\#} V_2^H$$

satisfy $\Gamma^k = \sum_{i=1}^{u} \Gamma_i^k$ for all k, and also

$$\Gamma_i^k = V_2 T_{1i} \mathcal{J}_{r_i n_i}^k T_{1i}^{\#} V_2^H = \begin{cases} 0 & \text{if } k > n_i - 1 \\ V_2 T_{1i} \left(\bigoplus_{j=1}^{r_i} e_{n_i} e_1^H \right) T_{1i}^{\#} V_2^H & \text{if } k = n_i - 1 \end{cases} \tag{4.21}$$

In view of this and (4.19), it suffices to find the matrices $\Gamma_1, \ldots, \Gamma_u$ and $\Delta^{d_1 - 1}$. We propose the following 'peeling' algorithm for this purpose.

For $i = 1$ to u do:

Step 1: Find $\Delta^{n_i - 1} = V_2 T_2 Z^{n_i - 1} T_2^{\#} V_2^H$.

Step 2: Find $\Gamma_i = V_2 T_{1i} \mathcal{J}_{r_i n_i} T_{1i}^{\#} V_2^H$.

end for;

Step 3: Find $\Delta^{d_1 - 1} = V_2 T_2 Z^{d_1 - 1} T_2^{\#} V_2^H$.

At the end one obtains the matrix of interest as $V_2 C^{d_1 - 1} V_2^H = \sum_{i=1}^{u} \Gamma_i^{d_1 - 1} + \Delta^{d_1 - 1}$. We now show how these steps can be accomplished.

Steps 1 and 3: Define the matrix $\bar{R} \triangleq V_1 J_{d_1} V_1^H$. In the ith iteration of Step 1, the matrix

$$R_i \triangleq R - \sum_{j=1}^{i-1} \Gamma_j = \bar{R} + \hat{\Gamma} + \sum_{j=i}^{u} \Gamma_j + \Delta \tag{4.22}$$

is available ($R_1 \triangleq R$). Similarly, at Step 3 the matrix $R_{u+1} = R - \Gamma = \bar{R} + \hat{\Gamma} + \Delta$ is available. One has

$$k \geq n_i \qquad \Longrightarrow \qquad R_i^k = \underbrace{\bar{R}^k}_{=0} + \underbrace{\hat{\Gamma}^k}_{=0} + \sum_{j=i}^{u} \underbrace{\Gamma_j^k}_{=0} + \Delta^k = \Delta^k. \tag{4.23}$$

Now let t be the size of the matrix Z, and let $\rho(\lambda)$ be the characteristic polynomial of Z:

$$\rho(\lambda) \triangleq \det[\lambda I_t - Z] = \lambda^t + \rho_1 \lambda^{t-1} + \cdots + \rho_t. \tag{4.24}$$

Note that $\rho(\lambda)$ is known to us and that since Z is nonsingular, $\rho_t \neq 0$ must hold. By the Cayley-Hamilton theorem [19], $\rho(Z) = 0$ and therefore $Z^{n_i-1}\rho(Z) = 0$:

$$Z^{n_i+t-1} + \rho_1 Z^{n_i+t-2} + \cdots + \rho_t Z^{n_i-1} = 0,$$

which gives

$$Z^{n_i-1} = -\frac{1}{\rho_t}(Z^{n_i+t-1} + \rho_1 Z^{n_i+t-2} + \cdots + \rho_{t-1} Z^{n_i}).$$

In view of (4.23), this implies

$$\begin{aligned} \Delta^{n_i-1} &= -\frac{1}{\rho_t}(\Delta^{n_i+t-1} + \rho_1 \Delta^{n_i+t-2} + \cdots + \rho_{t-1} \Delta^{n_i}) \\ &= -\frac{1}{\rho_t}(R_i^{n_i+t-1} + \rho_1 R_i^{n_i+t-2} + \cdots + \rho_{t-1} R_i^{n_i}), \end{aligned} \tag{4.25}$$

which shows how to obtain Δ^{n_i-1} at iteration i of Step 1. Similarly, at Step 3 one computes Δ^{d_1-1} as per

$$\Delta^{d_1-1} = -\frac{1}{\rho_t}(R_{u+1}^{d_1+t-1} + \rho_1 R_{u+1}^{d_1+t-2} + \cdots + \rho_{t-1} R_{u+1}^{d_1}).$$

Step 2: Observe that $R_i^{n_i-1} = \Gamma_i^{n_i-1} + \Delta^{n_i-1}$. Therefore at the ith iteration, $\Gamma_i^{n_i-1} = R_i^{n_i-1} - \Delta^{n_i-1}$ is available. For notational convenience, let

$$\Phi \triangleq V_2 T_{1i}, \qquad \Psi^H \triangleq T_{1i}^{\#} V_2^H$$

so that

$$\Gamma_i = \Phi \mathcal{J}_{r_i n_i} \Psi^H.$$

Note that $\Psi^H \Phi = I$, that is, $\Psi^H = \Phi^{\#}$. We shall also make use of the pseudoinverse of the matrix R. Since in view of (4.5) R satisfies $R = V(J_{d_1} \oplus C)V^H$, with V unitary, it follows that $R^{\#}$ is given by $R^{\#} = V(J_{d_1}^H \oplus C^{\#})V^H$, that is,

$$\begin{aligned} R^{\#} &= V \begin{bmatrix} I_{d_1} & \\ & T \end{bmatrix} \begin{bmatrix} J_{d_1}^H & & & \\ & \hat{Y}^H & & \\ & & Y^H & \\ & & & Z^{-1} \end{bmatrix} \begin{bmatrix} I_{d_1} & \\ & T^{-1} \end{bmatrix} V^H \\ &= V_1 J_{d_1}^H V_1^H + (V_2 \hat{T}_1) \hat{Y}^H (\hat{T}_1^{\#} V_2^H) \\ &\quad + (V_2 T_1) Y^H (T_1^{\#} V_2^H) + (V_2 T_2) Z^{-1} (T_2^{\#} V_2^H). \end{aligned} \tag{4.26}$$

Note that $R^{\#}$ is available to us, since R is. Also note that

$$V_1^H \Phi = 0, \qquad (T_2^{\#} V_2^H)\Phi = 0, \qquad (T_{1i}^{\#} V_2^H)\Phi = I, \qquad (T_{1j}^{\#} V_2^H)\Phi = 0 \quad \text{for } j \neq i. \tag{4.27}$$

Therefore from (4.26) and (4.27),

$$R^{\#}\Phi = \Phi \mathcal{J}_{r_i n_i}^H. \tag{4.28}$$

In the same way one finds that

$$(R^{\#})^H \Psi = \Psi \mathcal{J}_{r_i n_i}. \tag{4.29}$$

For convenience let $r = r_i$ and $n = n_i$. Partition

$$\Phi = [\ \Phi_1 \ \cdots \ \Phi_r\ ] = [\ \phi_{11} \ \cdots \ \phi_{1n} \mid \cdots \mid \phi_{r1} \ \cdots \ \phi_{rn}\ ], \quad (4.30)$$

$$\Psi = [\ \Psi_1 \ \cdots \ \Psi_r\ ] = [\ \psi_{11} \ \cdots \ \psi_{1n} \mid \cdots \mid \psi_{r1} \ \cdots \ \psi_{rn}\ ], \quad (4.31)$$

and note from (4.28)-(4.29) the following Jordan chain relations for each $j = 1, \ldots, r$:

$$R^{\#}\phi_{jl} = \phi_{j,l-1}, \qquad (R^{\#})^H \psi_{j,l-1} = \psi_{jl}, \qquad l = 2, \ldots, s. \quad (4.32)$$

In view of (4.32), the matrix $\Gamma_i = \Phi \mathcal{J}_{r_i n_i} \Psi^H$ can be written as

$$\begin{aligned}
\Gamma_i &= \sum_{j=1}^{r} \Phi_j J_n \Psi_j^H \\
&= \sum_{j=1}^{r} [\ \phi_{j2} \ \cdots \ \phi_{jn}\ ][\ \psi_{j1} \ \cdots \ \psi_{j,n-1}\ ]^H \\
&= \sum_{j=1}^{r} \sum_{k=1}^{s-1} (R^{\#})^{s-k-1} \phi_{jn} \psi_{j1}^H (R^{\#})^{k-1} \\
&= \sum_{k=1}^{n-1} (R^{\#})^{n-k-1} \left(\sum_{j=1}^{r} \phi_{jn} \psi_{j1}^H \right) (R^{\#})^{k-1} \\
&= \sum_{k=1}^{n-1} (R^{\#})^{n-k-1} \Gamma_i^{n-1} (R^{\#})^{k-1}. \qquad (4.33)
\end{aligned}$$

The last line follows because in view of (4.21), one has

$$\Gamma_i^{n-1} = \sum_{j=1}^{r} \phi_{jn} \psi_{j1}^H.$$

Eq. (4.33) shows how to find Γ_i from Γ_i^{n-1} and $R^{\#}$.

The algorithm is summarized next. The quantities ρ_i and the integer t are defined in (4.24), while the integers n_i, u are defined in (4.20).

Algorithm 4.2: Blind equalization under the conditions of theorem 3.4

---

1. Perform an SVD of $C_y(0)$ as in (4.2) to obtain U_1, Σ.

2. Construct the matrix R as in (4.4).

3. Set $R_1 = R$.

4. For $i = 1, 2, \ldots, u$:

    - Let $\Delta^{n_i-1} = -\frac{1}{\rho_t}\sum_{k=0}^{t-1}\rho_k R_i^{n_i+t-k-1}$ with $\rho_0 \triangleq 1$.
    - Let $\Gamma_i^{n_i-1} = R_i^{n_i-1} - \Delta^{n_i-1}$.
    - Let $\Gamma_i = \sum_{k=1}^{n_i-1}(R^{\#})^{n_i-k-1}\Gamma_i^{n_i-1}(R^{\#})^{k-1}$.
    - Let $R_{i+1} = R_i - \Gamma_i$.

    End for.

5. Let $\Delta^{d_1-1} = -\frac{1}{\rho_t}\sum_{k=0}^{t-1}\rho_k R_i^{d_1+t-k-1}$.

6. Let $\tilde{R} = R^{d_1-1} - \sum_{i=1}^{u}\Gamma_i^{d_1-1} - \Delta^{d_1-1}$.

7. Form the estimates $\hat{v}_{1,d_1}$, $\hat{v}_{1,1}$ via (4.13)-(4.14).

8. For $i = 2, 3, \ldots, d_1$, let $\hat{v}_{1,i} = R\hat{v}_{1,i-1}$. Alternatively, for $j = d_1, d_1 - 1, \ldots, 2$, let $\hat{v}_{1,j-1} = R^H\hat{v}_{1,j}$.

9. Construct the ZF equalizers as $\hat{\mathcal{G}}_{\text{ZF}} = \sigma_a U_1 \Sigma^{-1}[\ \hat{v}_{1,1}\ \ \cdots\ \ \hat{v}_{1,d_1}\ ]$.

4.4 Computing the MMSE equalizers

The algorithms of the previous sections determine the ZF equalizers under the right conditions. In this section it is shown how the MMSE equalizers can be obtained from the ZF ones. The approach is similar to that in [22] where the linear channel case was considered.

As before we denote by g_d the ZF equalizer vector with associated delay d. The MMSE equalizer vector for the delay d, denoted by f_d, is defined as

$$f_d \triangleq \arg\min_f E[|f^H Y(k) - a(k-d)|^2]. \tag{4.34}$$

The following lemma establishes the desired connection.

Lemma 4.1 *Assume that $\mathcal{H}$ is full column rank and that $C_s(0)$, $C_y(0) = \mathcal{H}C_s(0)\mathcal{H}^H + C_n(0)$ are positive definite. Then the delay-d MMSE equalizer f_d is related to the delay-d ZF equalizer g_d by*

$$f_d = [I - C_y^{-1}(0)C_n(0)]g_d. \tag{4.35}$$

Observe that in general the noise covariance matrix $C_n(0)$ is positive definite and therefore so is the undenoised matrix $C_y(0)$. If the noise is white, then (4.35) reduces to

$$f_d = [I - \sigma_n^2 C_y^{-1}(0)]g_d. \tag{4.36}$$

If the matrix $\mathcal{H}$ is tall, then the noise variance σ_n^2 can be estimated as the smallest eigenvalue of $C_y(0) = \mathcal{H}C_s(0)\mathcal{H}^H + \sigma_n^2 I_{pm}$. In that case, all the information needed in order to obtain f_d from g_d is available in the channel output SOS.

4.5 Simulation results

In this section we present the results obtained by the proposed algorithms with several numerical examples. For illustration purposes, the phase ambiguity inherent to the method was removed before computing the error rates. Averages were computed based on 100 independent runs. The Signal to Noise Ratio (SNR) is defined as

$$\mathrm{SNR} = 10\log_{10}\frac{\mathrm{trace}\,\mathrm{cov}[\mathcal{H}_1 S_1(k), \mathcal{H}_1 S_1(k)]}{\mathrm{trace}\,\mathrm{cov}[N(k), N(k)]},$$

which in the case of iid symbols $\{a(k)\}$ and white noise $\{n(k)\}$ equals

$$\mathrm{SNR} = 10\log_{10}\frac{\sigma_a^2 \sum_{j=0}^{l_1} ||h_{1j}||^2}{p\sigma_n^2}.$$

The Linear to Nonlinear Distortion Ratio (LNDR) is defined as

$$\mathrm{LNDR} = 10\log_{10}\frac{\mathrm{trace}\,\mathrm{cov}[\mathcal{H}_1 S_1(k), \mathcal{H}_1 S_1(k)]}{\mathrm{trace}\,\mathrm{cov}[\mathcal{H}_{\mathrm{nl}} S_2(k), \mathcal{H}_{\mathrm{nl}} S_2(k)]}$$

where $\mathcal{H}_{\mathrm{nl}} \triangleq [\ \mathcal{H}_2 \ \ \cdots \ \ \mathcal{H}_q\ ]$.

4.5.1 Example 1

First we consider the real nonlinear channel from Example 1 in [12], whose expression is

$$y(k) = \sum_{j=0}^{2} h_{1j} a(k-j) + \sum_{j=0}^{1} h_{2j} s_2(k-j) + n(k),$$

where $s_2(k) \triangleq a(k)a(k-1)$. Thus $q = 2$, $l_1 = 2$, $l_2 = 1$. The input $\{a(k)\}$ is iid taking the values ± 1 with equal probabilities. The number of subchannels is $p = 3$. The noise $\{n(k)\}$ is zero-mean white Gaussian with variance σ_n^2. The channel coefficients are

$$h_{10} = [\ 1 \ \ 0.5 \ \ 2\ ]^T, \qquad h_{11} = [\ -2.5 \ \ 3 \ \ 0\ ]^T, \qquad h_{12} = [\ 1 \ \ 5 \ \ 2\ ]^T,$$

$$h_{20} = [\ 2 \ \ 0.3 \ \ -0.7\ ]^T, \qquad h_{21} = [\ 0.7 \ \ 1.2 \ \ 3\ ]^T,$$

resulting in an LNDR of 5.13 dB. Observe that the memory of the linear part of this channel is not strictly larger than that of the nonlinear part, and consequently the conditions of theorem 3.7 do not hold. However, the requirements of theorem 3.4 are satisfied since $\text{cov}[S_2(k), a(k-m-l_1)] = 0$ for all equalizer lengths m. In addition, the normalized lag-1 source covariance matrix for this channel is $\bar{C}_s(1) = J_{d_1} \oplus J_{d_2}$, with $d_1 = m+2$, $d_2 = m+1$. This is already in Jordan form, and it is seen from theorem 3.4 that the channel is blindly equalizable from $C_y(0$, $C_y(1)$.

In the first experiment we considered an equalizer length $m = 4$, which yields a channel matrix $\mathcal{H}$ of size 12×11. The procedure is as follows:

1. Collect K samples of the received signal $\{y(k)\}$ and from these, estimate the matrices $C_y(0)$, $C_y(1)$.

2. Use Algorithm 4.1 to estimate the ZF equalizers.

3. Use (4.35) to obtain the MMSE equalizers.

Figure 13(a) shows the Symbol Error Rate (SER) versus SNR obtained with the MMSE equalizers with associated delay d, $0 \leq d \leq m + l_1 - 1 = 5$. It is seen that the zero delay yields the poorest performance. The best results are obtained for intermediate values of the delays ($d = 2, 3, 4$). Also shown in figure 13(b) is the SER as a function of the number of snapshots K used to estimate the covariance matrices for SNR = 0, 5 and 10 dB, for the MMSE equalizer with associated delay $d = 3$. As could be expected, the performance improves as K is increased until eventually the curves flatten out due to the noise floor effect.

In the second experiment for this channel we compared the performance of our proposed algorithm with that of Giannakis and Serpedin [12]. Since the deterministic algorithm of [12] requires a square channel matrix, we set the equalizer length $m = 3$; in this way, $\mathcal{H}$ has size 9×9. With a full-rank square $\mathcal{H}$ the matrix $\mathcal{H}C_s(0)\mathcal{H}^H$ becomes nonsingular; thus it is not feasible to estimate the noise variance σ_n^2 as the smallest eigenvalue of $C_y(0)$. Because of this, the effect of noise was ignored in the algorithm

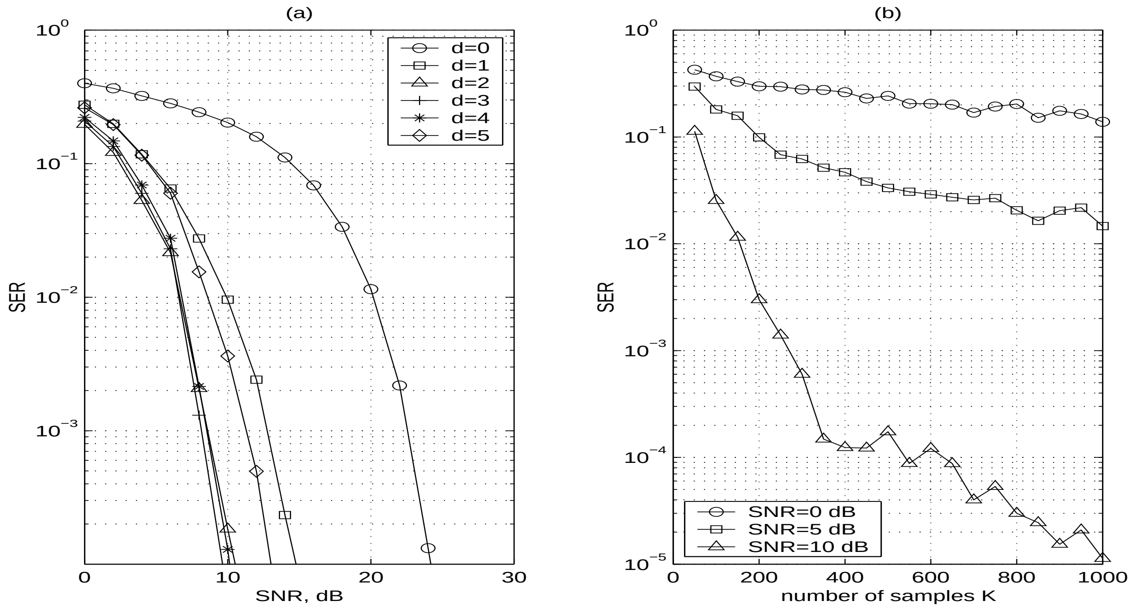

Figure 13: Performance of the new algorithm for the nonlinear channel in Example 1, equalizer order $m = 4$. (a) SER vs. SNR, $K = 500$ symbols. (b) SER vs. sample size K, equalization delay $d = 3$.

and the ZF equalizers were used instead of the MMSE ones. The algorithm of [12] also neglects the effect of noise, and it also presents the additional drawback of providing only ZF equalizers with minimal and maximal delays (i.e. $d = 0$ and $d = d_1 - 1$). However, in general the best performance is attained for some intermediate delay.

Figure 14 shows the SER as a function of the SNR using $K = 500$ snapshots. It is seen that the performance of the two algorithms is very close for $d = 0$. For $d = 4$, however, the new algorithm clearly outperforms the method from [12]. We must also keep in mind that, although for comparison purposes only the performance of the ZF equalizers with minimal and maximal delay is shown in figure 14, the new algorithm provides the equalizers with intermediate delay as well.

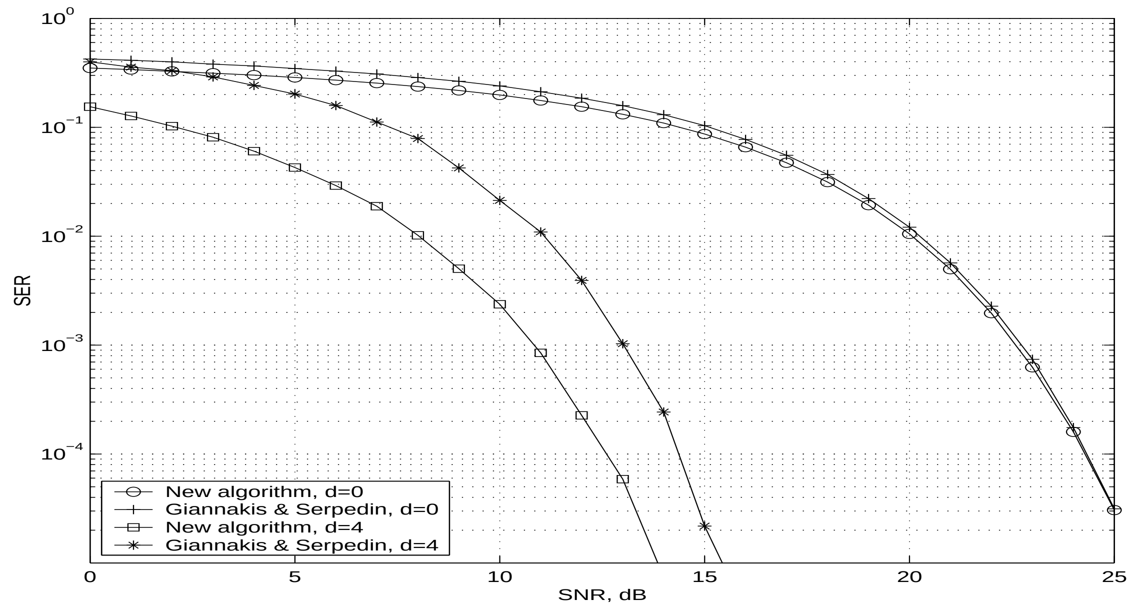

Figure 14: Performance of the ZF equalizers for the nonlinear channel in Example 1. $K = 500$ symbols, equalizer order $m = 3$.

4.5.2 Example 2

The second channel that we consider is the complex channel from Example 3 in [12], whose expression is

$$y(k) = \sum_{j=0}^{3} h_{1j} a(k-j) + \sum_{j=0}^{1} h_{2j} s_2(k-j) + n(k),$$

where now the nonlinear term is given by $s_2(k) \triangleq a(k)a(k-1)a^*(k-2)$. Thus $q = 2$, $l_1 = 3$, $l_2 = 1$. The symbols $\{a(k)\}$ are i.i.d., drawn from the Quadrature Phase Shift Keying (QPSK) constellation $\{1+j, 1-j, -1+j, -1-j\}$ with equal probabilities, so that $\sigma_a^2 = 2$. The number of subchannels is $p = 3$, and the coefficients are given by

$$h_{10} = [\ 1+j \quad 0.5+0.4j \quad -1+j\ ]^T, \quad h_{11} = [\ -2.5+2j \quad 3+2j \quad 1-2j\ ]^T,$$

$$h_{12} = [\ 1+j \quad -1+j \quad 2+1.3j\ ]^T, \quad h_{13} = [\ 4+0.3j \quad 5+j \quad -3+1.3j\ ]^T,$$

$$h_{20} = [\ 2 \quad 0.3 + 0.2j \quad -0.7 + 0.7j\ ]^T, \quad h_{21} = [\ 0.7 - 0.8j \quad 1.2 + j \quad 3 + 0.1j\ ]^T,$$

resulting in an LNDR of 1.3 dB. Again, the memory of the linear part of this channel is not strictly larger than that of the nonlinear part, so that the conditions of theorem 3.7 do not hold. However, those of theorem 3.4 do hold since $\text{cov}[S_2(k), a(k-m-l_1)] = 0$ for any m. For this channel, one has $\bar{C}_s(1) = J_{d_1} \oplus J_{d_2}$, with $d_1 = m+3$, $d_2 = m+1$, which again is already in Jordan form. Using theorem 3.4, the channel is blindly equalizable from $C_y(0$, $C_y(1)$.

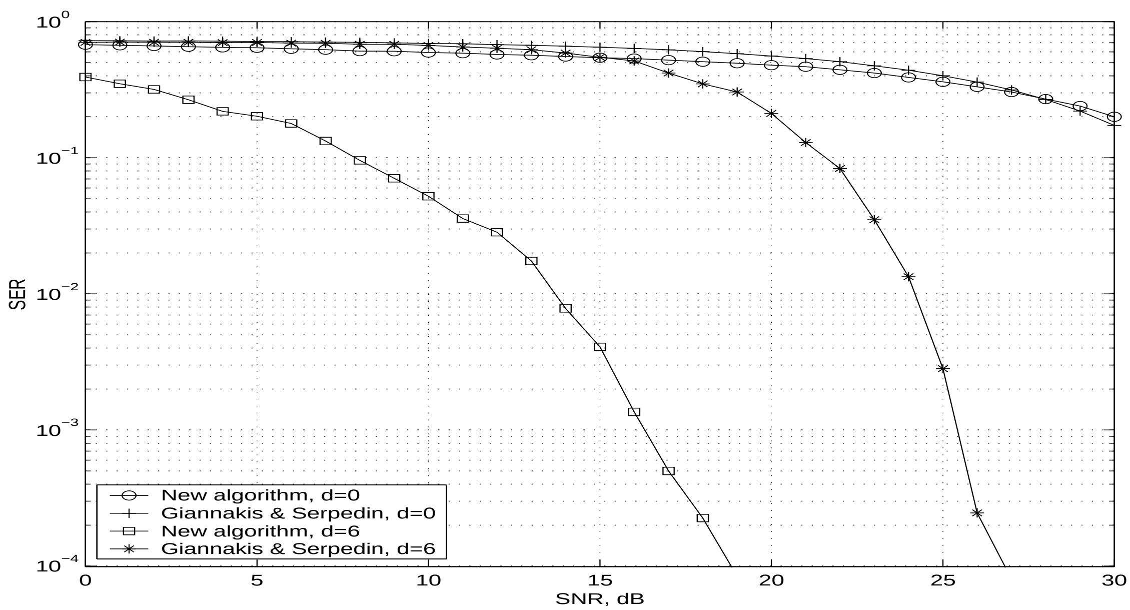

Figure 15: Performance of the ZF equalizers for the nonlinear channel in Example 2. $K = 500$ symbols, equalizer length $m = 4$.

We compared again the new algorithm and the deterministic method of Giannakis and Serpedin [12]. In order to obtain a square channel matrix, an equalizer length $m = 4$ was chosen. Figure 15 shows the performance of the ZF equalizers

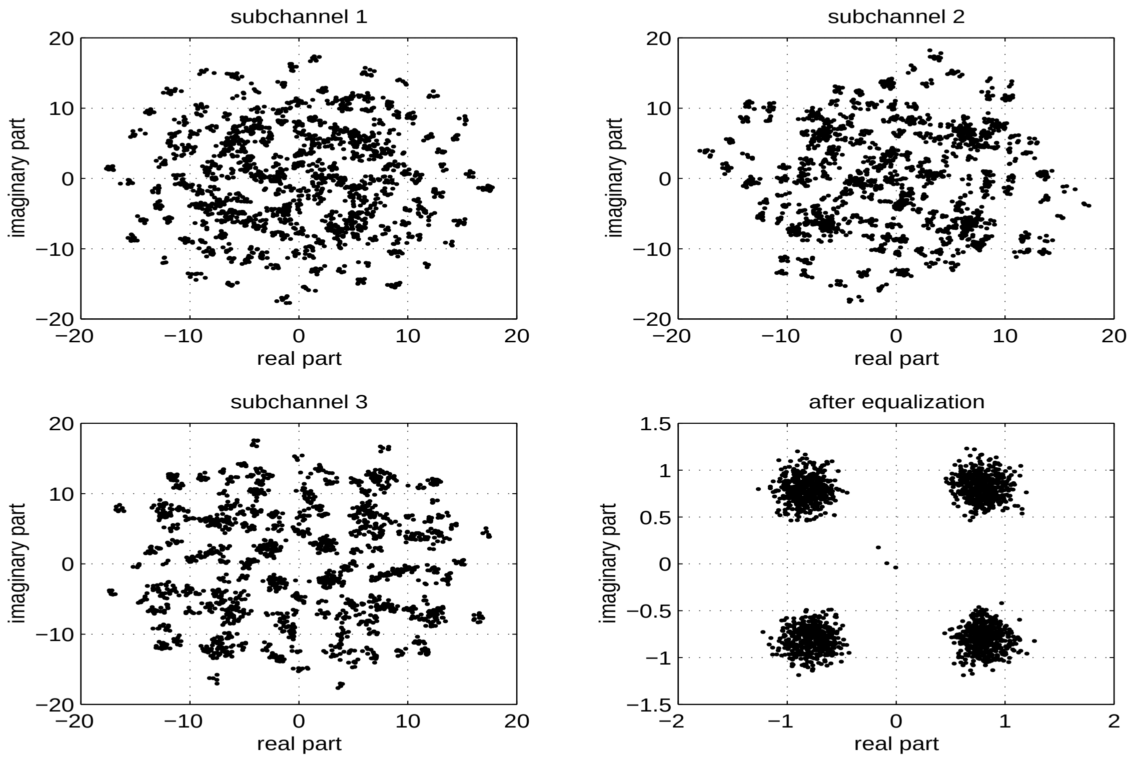

Figure 16: Scatter plots for the nonlinear channel in Example 2. 500 symbols, equalizer length $m = 4$, delay $d = 6$, SNR = 25 dB.

of minimal and maximal delays obtained with both methods using $K = 500$ data samples for covariance estimation. As was the case for the channel in Example 1, for $d = 0$ both algorithms show similar performance, while for the maximum delay $d = 6$ the proposed method presents a clear advantage.

Figure 16 shows typical scatter plots of the subchannel outputs and the output of the length $m = 4$ ZF equalizer of delay $d = 6$ obtained with the proposed algorithm, using $K = 500$ data samples and with SNR = 25 dB.

4.5.3 Example 3

The third channel that we consider is given by

$$y(n) = \sum_{j=0}^{1} h_{1j} a(n-j) + \sum_{j=0}^{1} h_{2j} s_2(n-j) + z(n),$$

where the nonlinear term is $s_2(n) \triangleq a^2(n)a^2(n-1)$. There are $p = 3$ subchannels, given by

$$h_{10} = \begin{bmatrix} 1 \\ 0.2 \\ 0.4 \end{bmatrix}, h_{11} = \begin{bmatrix} -0.5 \\ -0.3 \\ 1 \end{bmatrix}, h_{20} = \begin{bmatrix} 0.15 \\ 0.15 \\ 0.5 \end{bmatrix}, h_{21} = \begin{bmatrix} -0.2 \\ -0.4 \\ 0.2 \end{bmatrix}.$$

Thus $q = 2$, $l_1 = 1$, $l_2 = 1$. The input symbols are i.i.d., drawn from a four-level pulse amplitude modulation (4-PAM) constellation $\{-1, -\frac{1}{3}, \frac{1}{3}, 1\}$ with probabilities

$$P[a(n) = -\frac{1}{3}] = P[a(n) = \frac{1}{3}] = 0.1, \qquad P[a(n) = -1] = P[a(n) = 1] = 0.4.$$

The value of the LNDR for this channel is 13.1 dB. We considered an equalizer length $m = 2$, for which the normalized source covariance matrix $\bar{C}_s(1)$ turns out to be similar to $J_3 \oplus C$ with C given by

$$C = \begin{bmatrix} 0 & 0 & 0.1643 \\ 1 & 0 & -0.3593 \\ 0 & 1 & 0.6216 \end{bmatrix}.$$

Observe that in this case the linear and nonlinear kernels have the same length ($l_0 = l_1 = 1$). This fact makes the deterministic algorithm of Giannakis and Serpedin [12] unable to find the equalizers. However, since all the eigenvalues of C are nonzero, the conditions of theorem 3.7 still hold and the proposed algorithm can still be used to compute the equalizers. Figure 17(a) shows the SER obtained with the ZF equalizers vs. SNR using $K = 5000$ symbols for covariance estimation; while figure 17(a) shows the SER as a function of K for SNR = 25 dB. In this case the best performance is obtained by the equalizer with zero delay.

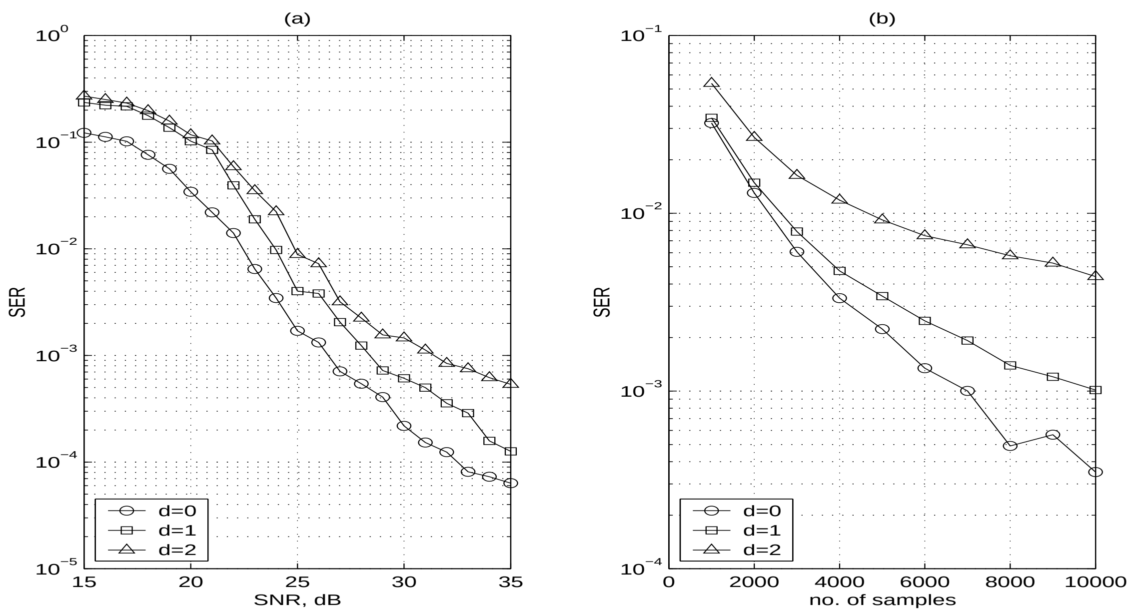

Figure 17: Performance of the new algorithm for the nonlinear channel in Example 3. Equalizer order $m = 2$. (a) SER vs. SNR, $K = 5000$ symbols. (b) SER vs. sample size, SNR = 25 dB.

It can be observed that in order to obtain acceptable performance, the algorithm requires considerably more symbols for covariance estimation and higher SNR than in the previous examples. The reason for this is as follows. The singular values of the matrix $\bar{C}_s(1)$ are $\{1, 1, 1, 1, 0.1643, 0\}$; since the blocks associated to the linear and nonlinear kernels have the same size ($d_1 = d_2 = 3$), the algorithm relies in the separation between the two smallest singular values of $\bar{C}_s(1)$, namely zero (the 'linear' singular value) and 0.1643 (the 'nonlinear' singular value). The closer these two numbers are, the more sensitive the algorithm becomes to the effects of noise and finite sample size, as observed in the simulation results.

4.5.4 Example 4

To close this section we present an example of a complex baseband equivalent channel with PSK modulation that fits the description presented in section 3.4.2. There are 2 nonlinear terms (i.e.$q = 3$) given by

$$s_2(k) \triangleq a^*(k)a(k-1)a(k-2), \qquad s_3(k) \triangleq a(k)a^*(k-1)a(k-2).$$

The lengths of the kernels are $l_1 = 2$, $l_2 = 1$,$l_3 = 3$ and the number of subchannels is $p = 4$. The symbols $\{a(k)\}$ are iid, drawn from an 8-PSK constellation with $\sigma_a^2 = 1$ and equal probabilities. Since $l_i \neq l_1$ for $i \neq 1$, the blind equalizability conditions are satisfied and therefore Algorithm 4.1 can be employed to obtain the equalizers. The channel coefficients are as follows:

$$\begin{aligned}
h_{10} &= [\ 0.4+0.6j \quad 0.5+0.4j \quad -0.5+0.0j \quad -0.2+0.5j\ ]^T,\\
h_{11} &= [\ -0.5+0.2j \quad 0.6+0.8j \quad 0.4-0.9j \quad 0.8-0.3j\ ]^T,\\
h_{12} &= [\ 1.0+0.5j \quad -1.0+0.8j \quad 0.6+0.3j \quad 0.1-0.7j\ ]^T,\\
h_{20} &= [\ 0.1+0.0j \quad 0.3+0.2j \quad -0.1+0.1j \quad 0.1+0.1j\ ]^T,\\
h_{21} &= [\ 0.2-0.2j \quad -0.1+0.1j \quad 0.1+0.1j \quad -0.1+0.0j\ ]^T,\\
h_{30} &= [\ -0.1+0.0j \quad 0.1-0.1j \quad 0.3+0.1j \quad -0.1+0.1j\ ]^T,\\
h_{31} &= [\ -0.1-0.1j \quad 0.3+0.1j \quad -0.1+0.1j \quad -0.2+0.1j\ ]^T,\\
h_{32} &= [\ 0.1+0.2j \quad 0.0+0.0j \quad 0.2-0.2j \quad -0.1+0.2j\ ]^T,\\
h_{33} &= [\ -0.1+0.2j \quad 0.1+0.5j \quad 0.1-0.4j \quad 0.2+0.1j\ ]^T,
\end{aligned}$$

yielding an LNDR of 8.35 dB. An equalizer length $m = 7$ was chosen.

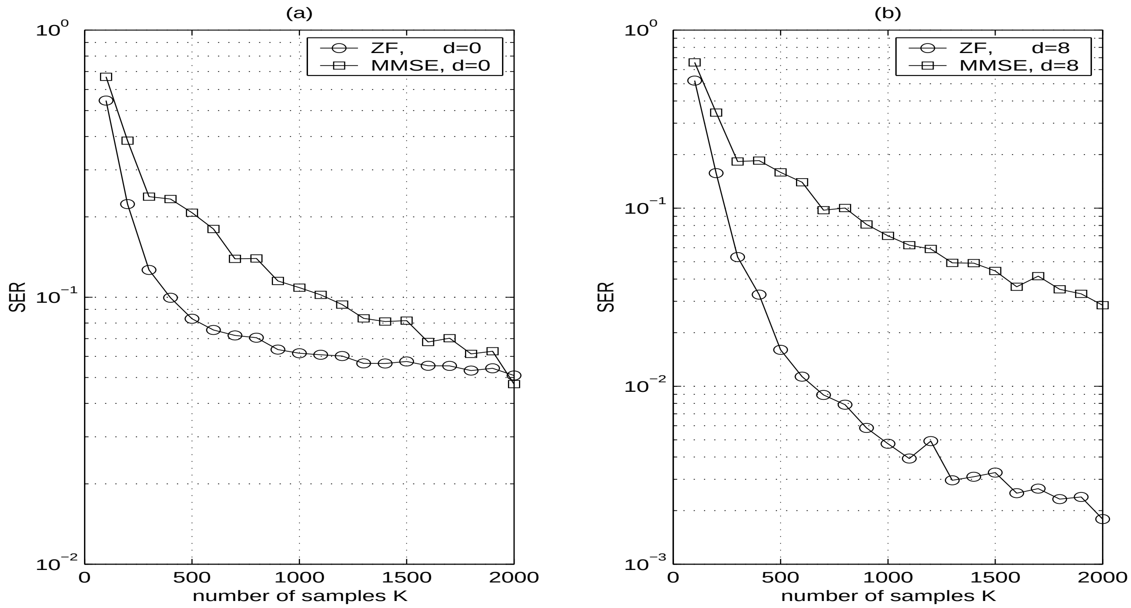

Figure 18: Performance of the new algorithm for the nonlinear channel in Example 4. Equalizer order $m = 7$, SNR = 24 dB. (a) SER vs. sample size, delay $d = 0$. (b) SER vs. sample size, delay $d = 8$.

We compared the performance of both the ZF equalizers obtained by Algorithm 4.1 without denoising the covariance matrices, and the MMSE equalizers obtained with denoising via (4.35). It turned out that the best performance was obtained by the equalizers with maximal delay ($d = 8$) and the worst by those of zero delay. Figure 18 shows the SER as a function of the number of snapshots K for an SNR of 24 dB, while figure 19 shows the SER as a function of the SNR with $K = 1000$ samples. Quite surprisingly, the MMSE equalizers perform worse than the ZF ones for low SNR. This is due to the fact that in noisy environments accurate estimation of the noise variance requires a larger sample size K .

Figure 20 shows typical scatter plots of the output of one of the subchannels

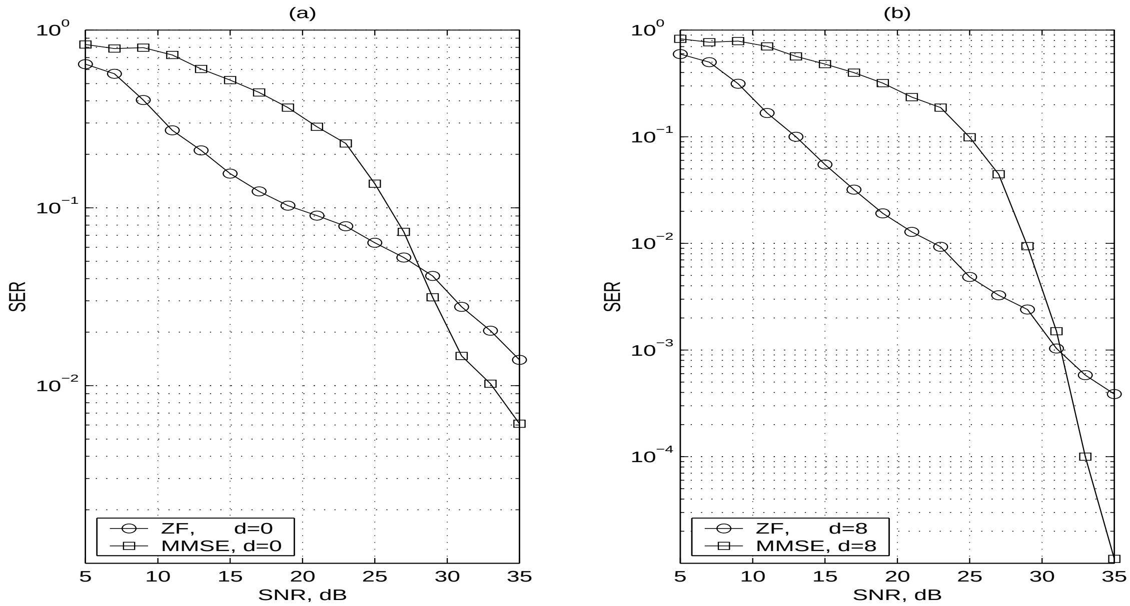

Figure 19: Performance of the new algorithm for the nonlinear channel in Example 4. Equalizer order $m = 7$, $K = 1000$ samples. (a) SER vs. SNR, delay $d = 0$. (b) SER vs. SNR, delay $d = 8$.

and the output of the length $m = 7$ ZF equalizer of delay $d = 8$ obtained with the proposed algorithm, using $K = 1000$ data samples and with SNR = 25 dB.

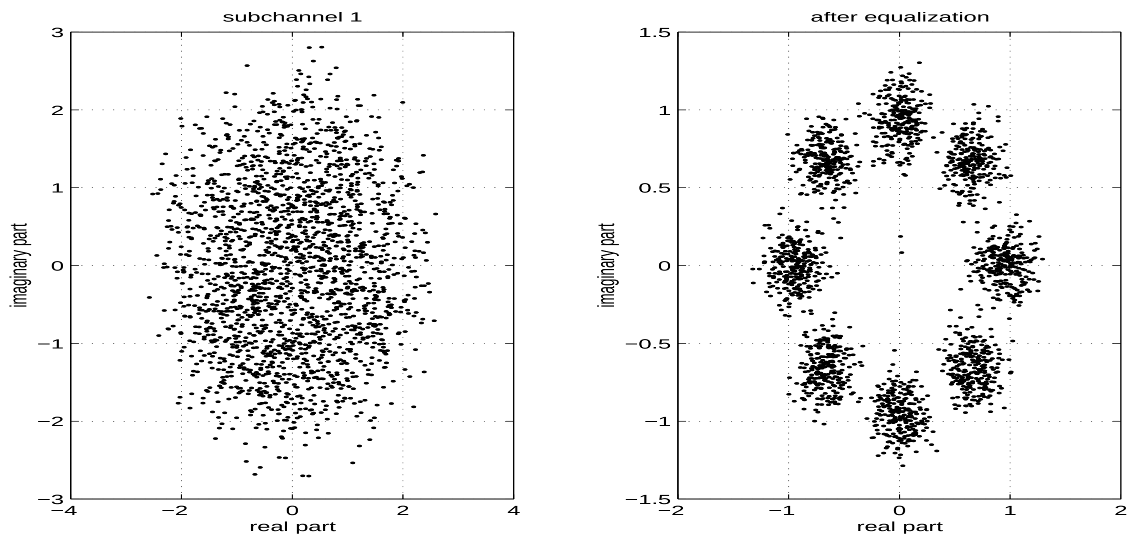

Figure 20: Scatter plots for the nonlinear channel in Example 4. $K = 1000$ symbols, equalizer order $m = 7$, delay $d = 8$, SNR = 25 dB.

CHAPTER V

EQUALIZATION OF NONLINEAR CHANNELS UNDER A RELAXED RANK CONDITION

In Chapters III and IV the blind equalizability problem was investigated under the assumption that the channel matrix $\mathcal{H}$ has full column rank. Under that condition, $\mathcal{H}^{\#}\mathcal{H} = Id_1 + d_2$ so that the first d_1 rows of the pseudoinverse $\mathcal{H}^{\#}$ provide the ZF equalizers. However, this also shows the existence of vectors (the last d_2 rows of $\mathcal{H}^{\#}$) that recover all the nonlinear terms $s_i(k)$ and their delays. This is clearly not necessary since these terms are of no interest to the receiver.

In this chapter we investigate the possibility of relaxing this full rank requirement. Specifically, a necessary and sufficient condition on the matrix $\mathcal{H}$ for the existence of ZF equalizers is given. Then the feasibility of extracting these equalizers from the received signal SOS is analyzed.

5.1 A necessary and sufficient condition

It is convenient to introduce the following partition of the channel matrix:

$$\mathcal{H} = [\ \mathcal{H}_1 \quad \mathcal{H}_{\text{nl}}\ ] \qquad \text{with} \qquad \mathcal{H}_{\text{nl}} \triangleq [\ \mathcal{H}_2 \quad \cdots \quad \mathcal{H}_q\ ]. \tag{5.1}$$

That is, $\mathcal{H}_{\text{nl}}$ comprises the 'nonlinear part' of the channel matrix. Recall that $\mathcal{H}_1$ and $\mathcal{H}_{\text{nl}}$ have sizes $pm \times d_1$ and $pm \times d_2$ respectively.

In this chapter, Assumption **A1** (cf. $\mathcal{H}$ is tall and full column rank) will be replaced by the following:

Assumption A1′: The matrix $\mathcal{H}_1$ has full column rank, and with $r_1 \triangleq \text{rank}(\mathcal{H}_1)$, $r_2 \triangleq \text{rank}(\mathcal{H}_{\text{nl}})$, the channel matrix $\mathcal{H}$ satisfies $\text{rank}(\mathcal{H}) = r_1 + r_2 \leq pm$.

Observe that if $\mathcal{H}$ has full column rank, then Assumption $\mathbf{A1'}$ is satisfied but not conversely. The significance of this condition is reflected in the following result.

Theorem 5.1 *There exists a $pm \times d_1$ matrix $\mathcal{G}$ such that*

$$\mathcal{G}^H \mathcal{H} = [\ I_{d_1} \quad 0_{d_1 \times d_2}\ ] \tag{5.2}$$

if and only if Assumption $\mathbf{A1'}$ holds.

We shall refer to Assumption $\mathbf{A1'}$ as the 'relaxed rank condition'. Its geometrical interpretation is as follows.

Lemma 5.1 *The condition* $\mathrm{rank}([\ \mathcal{H}_1 \quad \mathcal{H}_{\mathrm{nl}}\ ]) = \mathrm{rank}(\mathcal{H}_1) + \mathrm{rank}(\mathcal{H}_{\mathrm{nl}})$ *is equivalent to*

$$\mathrm{range}(\mathcal{H}_1) \bigcap \mathrm{range}(\mathcal{H}_{\mathrm{nl}}) = \{0\},$$

where $\mathrm{range}(A)$ *denotes the subspace spanned by the columns of the matrix A.*

Recall that the normalized channel matrix H was defined as $H = \mathcal{H}Q$ where Q is a square root of the zero lag source covariance matrix $C_s(0)$. Assuming Q nonsingular, $\mathcal{H}$ full column rank implies H full column rank. Similarly, the next result shows the effect of the relaxed rank condition $\mathbf{A1'}$ on H.

Lemma 5.2 *Assume that $\mathcal{H} = [\ \mathcal{H}_1 \quad \mathcal{H}_{\mathrm{nl}}\ ]$ satisfies the relaxed rank condition $\mathbf{A1'}$. Let*

$$Q = \begin{bmatrix} Q_{11} & 0 \\ Q_{21} & Q_{22} \end{bmatrix}$$

be nonsingular, with Q_{ij} of size $d_i \times d_j$, and let

$$H = \mathcal{H}Q = [\ H_1 \quad H_2\ ]$$

where $H_1 = \mathcal{H}_1 Q_{11} + \mathcal{H}_{\mathrm{nl}} Q_{21}$ and $H_2 = \mathcal{H}_{\mathrm{nl}} Q_{22}$. Then H_1 has full column rank and $\mathrm{rank}(H) = \mathrm{rank}(H_1) + \mathrm{rank}(H_2)$.

5.2 Obtaining the equalizers

The previous section has given a necessary and sufficient condition on the channel matrix for the existence of the ZF equalizers. We turn our attention now to the problem of extracting these equalizers form the SOS of the received signal. The following result relates them to the normalized channel matrix $H = \mathcal{H}Q$.

Lemma 5.3 *Assume that $\mathcal{H}$ satisfies the relaxed rank condition* $\mathbf{A1}'$ *and that Q is nonsingular and block lower triangular:*

$$Q = \begin{bmatrix} Q_{11} & 0 \\ Q_{21} & Q_{22} \end{bmatrix}, \qquad Q_{ij} \quad d_i \times d_j. \tag{5.3}$$

Then the matrix $\mathcal{G}$ such that $\mathcal{G}^H\mathcal{H} = [\ I_{d_1} \quad 0_{d_1 \times d_2}\ ]$ (ZF equalizers) is given by

$$\mathcal{G}^H = Q_{11}[\ I_{d_1} \quad 0_{d_1 \times d_2}\ ]H^{\#} \tag{5.4}$$

where $H = \mathcal{H}Q$.

Thus if $H = U_1 \Sigma V$ is an SVD of H, with

$$U_1 : \quad pm \times (r_1 + r_2), \qquad \Sigma : \quad (r_1 + r_2) \times (r_1 + r_2), \qquad V : \quad (r_1 + r_2) \times (d_1 + d_2),$$

then the equalizers are given by

$$\mathcal{G}^H = Q_{11}[\ I_{d_1} \quad 0\ ]V^H \Sigma^{-1} U_1^H.$$

Alternatively, if we partition V as

$$V = [\ V_1 \quad V_2\ ], \qquad V_i \text{ of size } (r_1 + r_2) \times d_i, \tag{5.5}$$

then one has

$$\mathcal{G}^H = Q_{11} V_1^H \Sigma^{-1} U_1^H. \tag{5.6}$$

Observe that Q_{11} is known to us from the source statistics, and that Σ, U_1 can be obtained from an SVD of $C_y(0)$ since

$$C_y(0) = \mathcal{H}C_s(0)\mathcal{H}^H = HH^H = U_1\Sigma^2 U_1^H.$$

Therefore if V_1 could be somehow estimated, the ZF equalizers could be computed. Observe that the rows of V are orthonormal, i.e.

$$VV^H = V_1V_1^H + V_2V_2^H = I_{r_1+r_2}.$$

An additional property is shown by the next result.

Lemma 5.4 *Assume that $\mathcal{H}$ satisfies the relaxed rank condition* $\mathbf{A1}'$ *and that Q is nonsingular and block lower triangular as in (5.3). Let $H = \mathcal{H}Q$ have a singular value decomposition $H = U_1\Sigma V$, and partition V as in (5.5). Then one has*

$$V_1^H V_1 = I_{d_1}, \qquad V_1^H V_2 = 0_{d_1 \times d_2}. \tag{5.7}$$

Therefore under the relaxed rank condition the d_1 columns of V_1 still constitute an orthonormal set, and they are orthogonal to the d_2 columns of V_2. As in chapter IV, consider the matrix

$$R \triangleq \Sigma^{-1}U_1^H C_y(1) U_1 \Sigma^{-1}, \tag{5.8}$$

which satisfies $R = V\bar{C}_s(1)V^H$ as shown in (4.5). Because of (5.7), this gives

$$RV_1 = V\bar{C}_s(1)\begin{bmatrix} I_{d_1} \\ 0_{d_1 \times d_2} \end{bmatrix}, \qquad R^H V_1 = V\bar{C}_s(1)^H \begin{bmatrix} I_{d_1} \\ 0_{d_1 \times d_2} \end{bmatrix}. \tag{5.9}$$

Therefore if one can find conditions under which $\bar{C}_s(1) = J_{d_1} \oplus C$ for some $d_2 \times d_2$ matrix C, the familiar Jordan chains of (4.7) are recovered:

$$RV_1 = V_1 J_{d_1}, \qquad R^H V_1 = V_1 J_{d_1}^H, \tag{5.10}$$

which provide a means to obtain V_1 once its first or last column is available.

In particular, consider the conditions of theorem 3.7, but substituting the full rank requirement of $\mathcal{H}$ by the relaxed rank condition $\mathbf{A1'}$. That is, assume that the symbols are iid and that the memory of the nonlinear part of the channel is strictly less than that of the linear part. Then the normalized lag $d_1 - 1$ source covariance matrix $\bar{C}_s(d_1 - 1)$ still satisfies $\bar{C}_s(d_1 - 1) = e_{d_1} e_1^H \oplus 0_{d_2 \times d_2}$ as shown in the proof of theorem 3.7 (this property is completely independent of $\mathcal{H}$). Therefore the matrix $\tilde{R} \triangleq \Sigma^{-1} U_1^H C_y(d_1 - 1) U_1 \Sigma^{-1}$ still satisfies

$$\tilde{R} = V \bar{C}_s(d_1 - 1) V^H = (V_1 e_{d_1})(V_1 e_1)^H,$$

from which the first and last columns of V_1 can be estimated. Hence Algorithm 4.1 from Chapter IV still provides the desired ZF equalizers.

Consider now the setting of theorem 3.4, in which the symbols $\{a(k)\}$ are iid and satisfy $\mathrm{cov}[S_2(k), a(k - d_1)] = 0$. In this framework, it is still true that $\bar{C}_s(1) = J_{d_1} \oplus C$. Algorithm 4.2 was derived in section 4.3 where it was assumed that $\mathcal{H}$ was full rank. When this requirement is replaced by the relaxed rank condition $\mathbf{A1'}$, some of the steps in the derivation of the algorithm cease to be valid. Specifically, eq. (4.15) does not hold in this case since in general

$$(V_2 C V_2^H)^n \neq V_s C^n V_2^H$$

unless the columns of V_2 are orthonormal, which is not the case under assumption $\mathbf{A1'}$. Nevertheless one has the following result:

Lemma 5.5 *Assume that conditions* $\mathbf{A1'}$ *and* **A2**-**A5** *are satisfied. Then the matrix* R *defined in (5.8) admits a Jordan decomposition of the form*

$$R = [\ V_1 \quad T_0 \quad T_2\ ] \begin{bmatrix} J_{d_1} & & \\ & Y_0 & \\ & & Z \end{bmatrix} \begin{bmatrix} V_1^H \\ T_0^{\#} \\ T_2^{\#} \end{bmatrix}, \tag{5.11}$$

where Z *is nonsingular and* Y_0 *is a direct sum of shift matrices* J_i.

The structure of the Jordan decomposition of R is the same as that found in the case in which $\mathcal{H}$ has full column rank. However, while in that case this Jordan structure was completely determined by the source statistics, now it also depends on the channel coefficients. That is, the matrices Y_0, Z, T_0, T_2 in (5.11) cannot be determined *a priori*, although they can be obtained by the receiver once the matrix R has been computed. In that case, assuming that the matrix Y_0 does not contain any diagonal block of the form J_{d_1}, Algorithm 4.2 from section 4.3 can be employed to determine the ZF equalizers. Thus the price to pay in order to replace the full rank requirement on $\mathcal{H}$ by the relaxed rank condition $\mathbf{A1'}$ is (i) whether the channel is blindly equalizable from $C_y(0)$ and $C_y(1)$ cannot be determined beforehand, and (ii) the receiver must perform a Jordan decomposition of the estimate of the matrix R, which is expected to be very sensitive to effects due to the finite nature of the sample size. The next section provides several examples.

Finally, in the noisy case it is still possible to obtain the MMSE equalizers from the ZF ones even in the case that $\mathcal{H}$ is not full rank but satisfies assumption $\mathbf{A1'}$:

Lemma 5.6 *Assume that* $\mathcal{H}$ *satisfies the relaxed rank condition and* $\mathbf{A1'}$ *and that* $C_s(0)$, $C_y(0) = \mathcal{H}C_s(0)\mathcal{H}^H + C_n(0)$ *are positive definite. Then the delay-d MMSE equalizer* f_d *is related to the delay-d ZF equalizer* g_d *by*

$$f_d = [I - C_y^{-1}(0)C_n(0)]g_d. \tag{5.12}$$

5.3 Simulation examples

We present now the results obtained by the algorithms derived in the preceding section for several numerical examples. For illustration purposes, the phase ambiguity inherent to the method was removed before computing the error rates. Averages were computed based on 100 independent runs.

5.3.1 Example 5

We consider here a complex channel with $q = 2$, $l_1 = 2$, $l_2 = 1$:

$$y(k) = \sum_{j=0}^{2} h_{1j} a(k-j) + \sum_{j=0}^{1} h_{2j} s_2(k-j) + n(k),$$

where the symbols $\{a(k)\}$ are i.i.d., drawn from the QPSK constellation $\{1+j, 1-j, -1+j, -1-j\}$ with equal probabilities (thus $\sigma_a^2 = 2$), and the nonlinear term is $s_2(k) \triangleq a^*(k)a(k-1)a(k-2)$. The channel coefficients are given by

$$h_{10} = \begin{bmatrix} 1+j \\ 1 \\ 1+0.4j \end{bmatrix}, \; h_{11} = \begin{bmatrix} 2-0.5j \\ -1+0.8j \\ 0.2j \end{bmatrix}, \; h_{12} = \begin{bmatrix} 1-j \\ 1-j \\ 1 \end{bmatrix},$$

$$h_{20} = \begin{bmatrix} 0.1-0.2j \\ 0.2-0.4j \\ 0.1-0.2j \end{bmatrix}, \quad h_{21} = \begin{bmatrix} 0.1+0.2j \\ 0.2+0.4j \\ 0.1+0.2j \end{bmatrix}.$$

This yields an LNDR of 8 dB. We chose an equalizer length of $m = 4$. The resulting channel matrix $\mathcal{H}$ has size 12×11 and satisfies

$$10 = \text{rank}(\mathcal{H}) = \text{rank}(\mathcal{H}_1) + \text{rank}(\mathcal{H}_2) = 6 + 4,$$

so that although $\mathcal{H}$ is not full column rank, the relaxed rank condition $\mathbf{A1'}$ holds. The symbols satisfy the condition $\text{cov}[S_2(k), a(k-m-l_1)] = 0$, so that one can attempt to use algorithm 4.2 to find the equalizers. The covariance matrices were estimated and denoised, and once the ZF equalizers were obtained, the MMSE ones were computed using (5.12). The values $r_1 = 6$ and $r_2 = 4$ are assumed known.

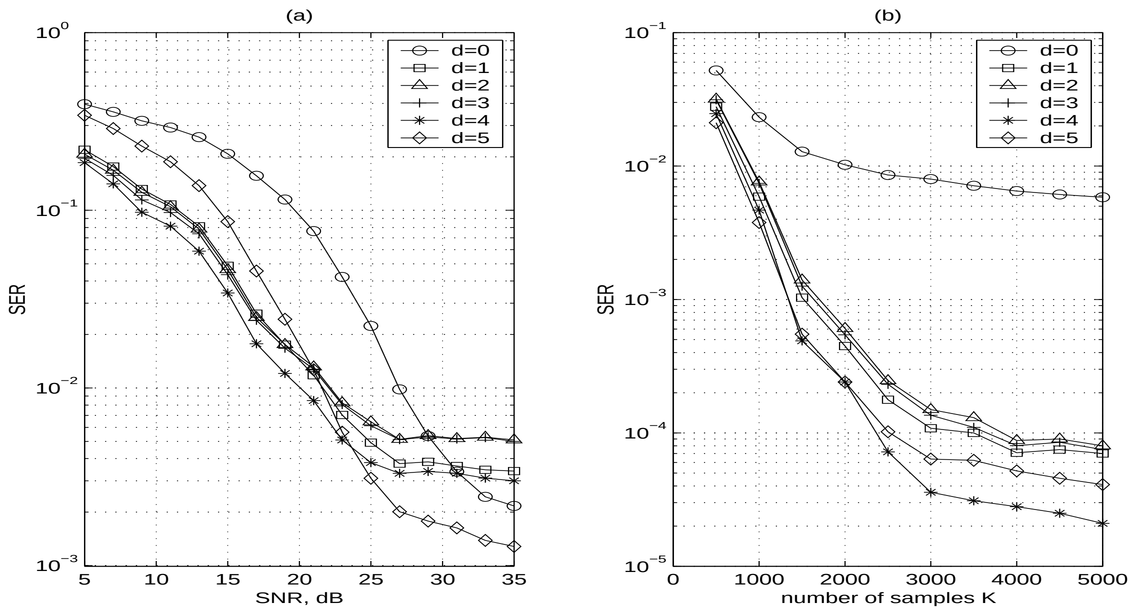

Figure 21: MMSE equalizer performance: Algorithm 4.2, nonlinear channel in Example 5, equalizer length $m = 4$. (a) SER vs. SNR, $K = 1000$ symbols. (b) SER vs. sample size K, SNR = 25 dB.

Figure 21(a) shows the symbol error rate vs. SNR using $K = 1000$ samples for covariance estimation, while figure 21(b) shows the variation of the SER with K when the SNR is fixed at 25 dB, for all possible values of the equalization delay. It is seen that for small values of the SNR, the SER performance is limited by the effect of noise. As the SNR increases, the SER decreases but eventually it flattens out. This indicates that for high SNR the algorithm performance is limited by the accuracy in the estimation of the covariance matrices.

5.3.2 Example 6

Now we consider a real channel with $q = 3$, $l_1 = 4$, $l_2 = l_3 = 1$ and iid symbols taking the values ± 1 with equal probabilities. The number of subchannels is $p = 4$:

$$h_{10} = [\ 1 \quad 0.1 \quad -0.2 \quad 0.3\ ]^T,\ h_{11} = [\ 0.5 \quad 0.6 \quad 0.6 \quad 1\ ]^T,\ h_{12} = [\ 0.4 \quad 1 \quad 0.6 \quad 0.7\ ]^T,$$

$$h_{13} = [\ 0.2 \quad -0.4 \quad 0.1 \quad -0.5\ ]^T, \quad h_{14} = [\ -0.2 \quad 0.2 \quad -0.3 \quad 0.2\ ]^T,$$

$$h_{20} = [\ 0.2 \quad 0.1 \quad 0.2 \quad 0.1\ ]^T, \quad h_{21} = [\ 0.5 \quad 0.25 \quad 0.5 \quad 0.25\ ]^T,$$

$$h_{30} = [\ 0.1 \quad 0.2 \quad 0.2 \quad 0.1\ ]^T, \quad h_{31} = [\ -0.1 \quad -0.2 \quad -0.2 \quad -0.1\ ]^T.$$

The nonlinear terms are $s_2(k) \triangleq a(k)a(k-1)$, $s_3(k) \triangleq a(k)a(k-2)$. The resulting LNDR is 8 dB. The equalizer length that we consider is $m = 6$. Again the corresponding channel matrix $\mathcal{H}$ (which has size 24×24) is not full column rank but it satisfies the relaxed rank condition:

$$23 = \text{rank}(\mathcal{H}) = \text{rank}(\mathcal{H}_1) + \text{rank}([\ \mathcal{H}_2 \quad \mathcal{H}_3\ ]) = 10 + 13.$$

In this case the memory of the nonlinear part is strictly less than that of the linear part, so that both Algorithms 4.1 and 4.2 can be used. The covariance matrices were estimated and denoised, and once the ZF equalizers were obtained, the MMSE ones were computed using (5.12). Observe that the noise power can still be estimated as the smallest eigenvalue of $C_y(0)$ even though the channel matrix $\mathcal{H}$ is square, since $\mathcal{H}$ is rank deficient. The values $r_1 = 10$ and $r_2 = 13$ are assumed known.

First we tested Algorithm 4.1, which exploits the memory dominance of the linear part. Figure 22(a) shows the symbol error rate vs. SNR using $K = 2000$ samples for covariance estimation, while figure 21(b) shows the variation of the SER with K for SNR = 24 dB, for the equalization delays 0, 3, 8 and 9. In this case the equalizer with maximal delay ($d = 9$) provides the poorest performance of all.

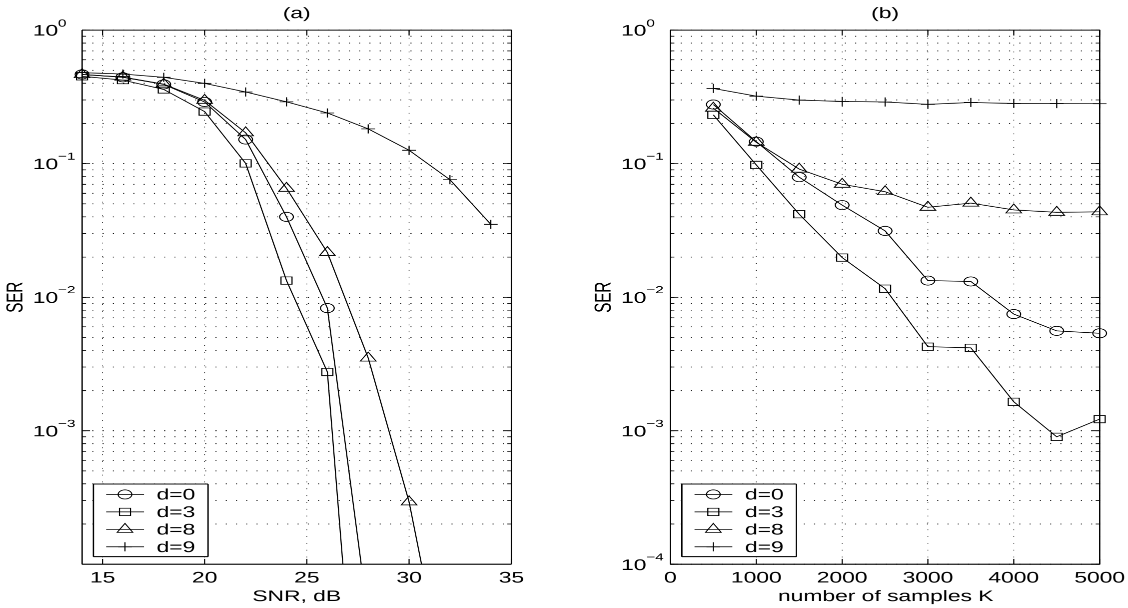

Figure 22: MMSE equalizer performance: Algorithm 4.1, nonlinear channel in Example 6, equalizer length $m = 6$. (a) SER vs. SNR, $K = 2000$ symbols. (b) SER vs. sample size K, SNR = 24 dB.

However the results do not show a limitation due to estimation accuracy for high SNR, in contrast with the behavior of Algorithm 4.2 in the previous example.

The results obtained with Algorithm 4.2 are shown in figure 23. It can be seen how the performance of this approach is much worse than that of Algorithm 4.1. This is due to the high sensitivity of the Jordan decomposition of the matrix R with the number of samples used for estimation of the covariance matrices, as pointed out in section 5.2. This problem is not present in Algorithm 4.1 which makes use of the information contained in $C_y(d_1 - 1)$, information which is not exploited by Algorithm 4.2.

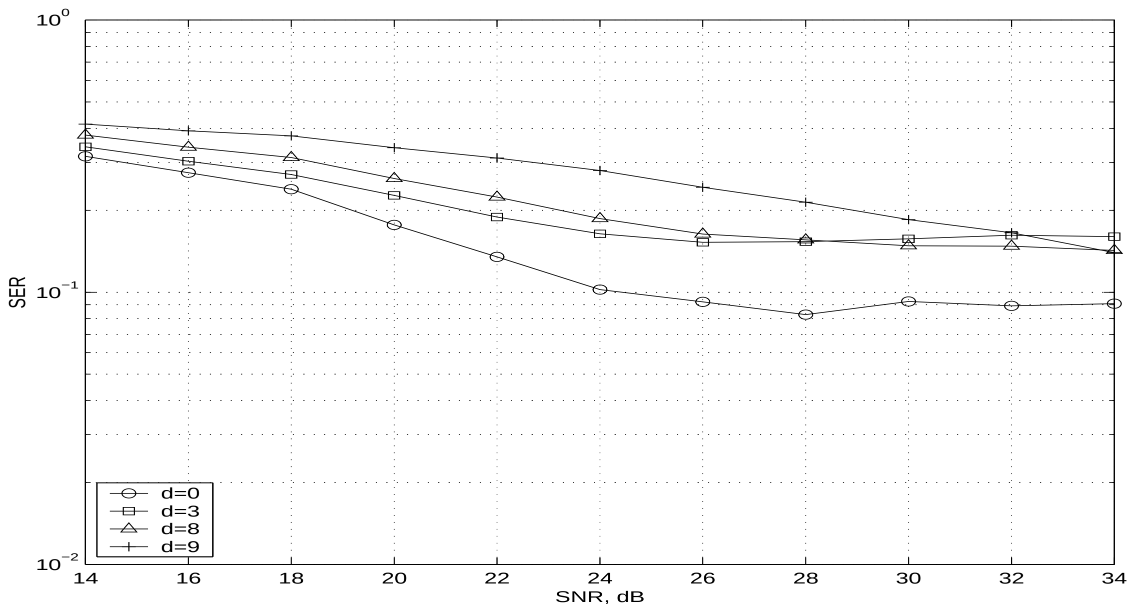

Figure 23: MMSE equalizer performance: Algorithm 4.2, nonlinear channel in Example 6, equalizer length $m = 6$, sample size $K = 2000$ symbols.

CHAPTER VI

EQUALIZATION OF LINEAR CHANNELS WITH CORRELATED SOURCES

In Chapters IV and V we have focused on the development of blind equalization algorithms for nonlinear channels when the input symbols $\{a(k)\}$ are independent. However, the results obtained in Chapter III show that under certain conditions these channels still are blindly equalizable even if the symbols become correlated. Although the problem of developing equalization algorithms for nonlinear channels with correlated inputs remains open, in this chapter we provide a step in this direction by generalizing the original algorithm of Tong, Xu and Kailath [29] (which deals with linear channels and independent sources) in order to accommodate correlated sources. Therefore in the remainder of this chapter it will be assumed that the channel is linear, i.e. we have $q = 1$ in the model (3.1):

$$y(k) = \sum_{j=0}^{l_1} h_{1j} a(k-j) + n(k). \tag{6.1}$$

It is assumed that the number of available subchannels is still p. Correspondingly, the channel matrix $\mathcal{H}$ reduces to $\mathcal{H} = \mathcal{H}_1$ (see (3.7)) and the regressor vector is just

$$S(k) = S_1(k) = [\ a(k) \quad a(k-1) \quad \cdots \quad a(k-d_1+1)\ ]^T,$$

with $d_1 = m + l_1$ and m the equalizer length. In this way the matrix-vector formulation (3.3) is still valid:

$$Y(k) = \mathcal{H} S(k) + N(k), \tag{6.2}$$

with $Y(k)$ and $N(k)$ defined as in (3.2) and (3.4) respectively.

The algorithm from [29] recovers the channel matrix $\mathcal{H}$ from the covariance terms

$$C_y(0) \triangleq \mathrm{cov}[Y(k), Y(k)], \qquad C_y(1) \triangleq \mathrm{cov}[Y(k), Y(k-1)], \tag{6.3}$$

up to an unitary scaling constant, assuming that $\mathcal{H}$ is full column rank and that the symbols are white:

$$C_s(l) \triangleq \mathrm{cov}[S(k), S(k-l)] = \sigma_a^2 J_{d_1}^l. \tag{6.4}$$

This whiteness assumption on $\{a(k)\}$ is crucial for the algorithm from [29]. This was noted in [17] where a modification was proposed in order to deal with weakly correlated sources with unknown correlation (which must then be estimated). Direct extension of [29] to arbitrary colored inputs is currently unavailable. Accordingly, we extend the algorithm from [29] to the case of arbitrary colored sources with known correlation. As will be evident in this chapter such an extension, particularly the proof that the resulting channel estimate is to within a scaling constant of the 'true' channel, is highly nontrivial. To this end we make extensive use of the rich literature on linear prediction theory. *En route* to our main result we derive a singular value decomposition of the normalized lag-1 source covariance matrix which we regard as a contribution of independent significance to linear prediction theory.

A recent attempt to extend the method of [29] to the colored source case can be found in [1], where an algorithm that uses the information contained in $C_y(0)$, $C_y(1)$, $\ldots$, $C_y(\bar{l})$ for some $\bar{l} > 1$ is presented. Besides its greater computational complexity, the method from [1] implicitly relies on the fact that the smallest singular value of certain matrices has multiplicity one; conditions under which this holds were not given. By contrast, the algorithm developed in this section is theoretically sound and makes use of only $C_y(0)$ and $C_y(1)$, so that the computational complexity is comparable to that of the original algorithm from [29].

6.1 Preliminaries

We assume that the source correlation matrices need not satisfy (6.4), and that $C_s(0)$, $C_s(1)$ are known. Let $\sigma_a^2 = E[|a_n|^2]$ and define also the autocorrelation vector

$$w \triangleq C_s(1)^H e_1 = \mathrm{cov}[S(k-1), a(k)]. \tag{6.5}$$

The assumptions of this chapter are as follows:

A1: The channel matrix $\mathcal{H}$ is tall and has full column rank.

A2: The noise $\{n(k)\}$ is zero-mean white with covariance $\sigma_n^2 I_p$.

A3: The $(d_1+1) \times (d_1+1)$ lag-0 source covariance matrix is positive definite:

$$\begin{bmatrix} \sigma_a^2 & w^H \\ w & C_s(0) \end{bmatrix} > 0.$$

In the sequel we will assume that the noise is absent, as the noise component can be subtracted from the output autocorrelation matrices using the approach discussed in section 3.1. In this case one has $C_y(l) = \mathcal{H} C_s(l) \mathcal{H}^H$ for all $l \geq 0$. Thus our goal is to find an estimate of $\mathcal{H}$ from $C_y(0)$ and $C_y(1)$ and from the knowledge of $C_s(0)$ and $C_s(1)$.

As before, it will be useful to consider a square root Q of $C_s(0)$. For this case, we take Q to be the unique square root that is lower triangular with positive diagonal elements; that is,

$$C_s(0) = QQ^H \tag{6.6}$$

is the *Cholesky factorization* of the positive definite matrix $C_s(0)$ [19]. With this, the normalized channel and source covariance matrices are defined as before:

$$H \triangleq \mathcal{H}Q, \qquad \bar{C}_s(1) \triangleq Q^{-1} C_s(1) Q^{-H}. \tag{6.7}$$

Then as usual we find that

$$C_y(0) = HH^H, \qquad C_y(1) = H\bar{C}_s(1)H^H. \tag{6.8}$$

Since Q is known, the problem amounts to identifying H from (6.8).

Here is where the key point of departure from [29] lies. Under the assumption of white $\{a(k)\}$ underlying [29], Q reduces to $\sigma_a I_{d_1}$ and $\bar{C}_s(1)$ reduces to J_{d_1}. These two facts are critically exploited in [29] to obtain the algorithm that estimates H, and also to show that the class of all matrices H that obey (6.8) are scaled versions of each other.

To treat the colored case, we must exploit the structure of $\bar{C}_s(1)$ and its relation to Q. To this end, we now proceed to establish certain connections between these matrices and the optimum forward prediction error filter (FPEF) of order d_1 for the process $\{a(k)\}$. These connections are crucial in resolving the colored problem.

Consider the standard linear prediction problem of finding coefficients θ_i such that the following quantity is minimized:

$$E\left\{\left|a(k) + \sum_{i=1}^{d_1} \theta_i^* a(k-i)\right|^2\right\}.$$

Let $\theta_i = \alpha_i$ be the minimizing parameters. Then $1 + \sum_{i=1}^{d_1} \alpha_i^* z^{-i}$ is the transfer function of the FPEF of order d_1 for the process $\{a(k)\}$. With w as in (6.5), it is well known [14] that the coefficients of the d_1-th order predictor, α_i, are given by

$$\alpha = [\ \alpha_1 \ \ \cdots \ \ \alpha_{d_1}\ ]^T = -C_s^{-1}(0)w. \tag{6.9}$$

Now, since the last (respectively first) $d_1 - 1$ rows (resp. columns) of $C_s(1)$ are the first (resp. last) $d_1 - 1$ rows (resp. columns) of $C_s(0)$, we have that

$$C_s(1) = J_{d_1} C_s(0) + e_1 w^H = C_s(0) J_{d_1} + X_{d_1} w^* e_{d_1}^H, \tag{6.10}$$

which is a simply a reformulation of (3.24)-(3.25). (Recall that X_{d_1} is the $d_1 \times d_1$ exchange matrix with ones in the antidiagonal and zeros elsewhere). Therefore the normalized matrix $\bar{C}_s(1)$ becomes

$$\begin{aligned}
\bar{C}_s(1) &= Q^{-1} C_s(1) Q^{-H} \\
&= Q^{-1}(J_{d_1} Q Q^H + e_1 w^H) Q^{-H} \\
&= Q^{-1}(J_{d_1} Q + e_1 w^H Q^{-H}) \\
&= Q^{-1}(J_{d_1} + e_1 w^H Q^{-H} Q^{-1}) Q \\
&= Q^{-1}(J_{d_1} - e_1 \alpha^H) Q. \qquad (6.11)
\end{aligned}$$

This is the connection between $\bar{C}_s(1)$ and the FPEF of order d_1. Observe that

$$F \triangleq J_{d_1} - e_1 \alpha^H \qquad (6.12)$$

is a companion matrix whose eigenvalues coincide with the zeros of the FPEF transfer function.

Let now the last row of Q^{-1} be

$$\beta^T = [\ \beta_{d_1-1} \ \ \cdots \ \ \beta_1 \ \ \beta_0\ ] \triangleq e_{d_1}^H Q^{-1}. \qquad (6.13)$$

It is known from linear prediction theory [14] that β_i^*/β_0 are the coefficients of the FPEF of order $d_1 - 1$, with β_0 real positive. In view of the order-update property of prediction filters [14], the vectors α, β are related via

$$\begin{bmatrix} 1 \\ \alpha \end{bmatrix} = \frac{1}{\beta_0} \left(\begin{bmatrix} X_{d_1} \beta \\ 0 \end{bmatrix} + \alpha_{d_1} \begin{bmatrix} 0 \\ \beta^* \end{bmatrix} \right). \qquad (6.14)$$

The following fact about the order d_1 FPEF is well known [14] and is very important to the subsequent development.

Theorem 6.1 *Under Assumption* **A3***, all the zeros of* $1+\sum_{i=1}^{d_1}\alpha_i^* z^{-i}$*, the order* d_1 *FPEF for the process* $\{a(k)\}$*, lie strictly inside the unit circle, whence*

$$|\alpha_{d_1}| < 1. \tag{6.15}$$

Another basic property is that $1/\beta_0^2$ is the variance of the forward (or backward) prediction error of order $d_1 - 1$. On the other hand, the variance of the prediction errors of order d_1 is given by [14]

$$\gamma^2 \triangleq \frac{1}{\beta_0^2}(1-|\alpha_{d_1}|^2). \tag{6.16}$$

Finally, it can be shown [3] that $C_s(0)$ and the companion matrix F defined in (6.12) satisfy the following Lyapunov equation:

$$C_s(0) - FC_s(0)F^H = \gamma^2 e_1 e_1^H. \tag{6.17}$$

6.2 Some intermediate results

As in [29], consider an SVD of $C_y(0)$:

$$C_y(0) = \begin{bmatrix} U_1 & U_2 \end{bmatrix} \begin{bmatrix} \Sigma^2 & 0 \\ 0 & 0 \end{bmatrix} \begin{bmatrix} U_1^H \\ U_2^H \end{bmatrix}. \tag{6.18}$$

Here Σ is $d_1 \times d_1$ diagonal. Since H has full column rank (Assumption **A1**), one has $\Sigma > 0$, and it follows from (6.8) that

$$H = U_1 \Sigma V, \tag{6.19}$$

for some $d_1 \times d_1$ unitary V which has to be estimated. For this purpose, consider as usual the matrix

$$R \triangleq \Sigma^{-1} U_1^H C_y(1) U_1 \Sigma^{-1}. \tag{6.20}$$

By direct verification using (6.8) and (6.19), one finds that $R = V\bar{C}_s(1)V^H$, similarly to what was found in (4.5) for the general nonlinear case. Thus, in view of (6.11), one has

$$\begin{aligned} R = V\bar{C}_s(1)V^H &= VQ^{-1}(J_{d_1} - e_1\alpha^H)QV^H \\ &= \tilde{V}(J_{d_1} - e_1\alpha^H)\bar{V}^H, \end{aligned} \tag{6.21}$$

where we have introduced the matrices

$$\tilde{V} \triangleq VQ^{-1}, \qquad \bar{V} \triangleq VQ^H. \tag{6.22}$$

Note that $\bar{V}^H\tilde{V} = I_{d_1}$. Thus, (6.21) implies

$$R\tilde{V} = \tilde{V}(J_{d_1} - e_1\alpha^H), \qquad R^H\bar{V} = \bar{V}(J_{d_1} - e_1\alpha^H)^H.$$

Therefore, partitioning

$$\tilde{V} = [\ \tilde{v}_1 \ \cdots \ \tilde{v}_{d_1}\ ], \tag{6.23}$$

$$\bar{V} = [\ \bar{v}_1 \ \cdots \ \bar{v}_{d_1}\ ], \tag{6.24}$$

columnwise, one has

$$R\tilde{v}_i = \tilde{v}_{i+1} - \alpha_i^*\tilde{v}_1, \quad i = 1, \ldots, d_1 - 1; \tag{6.25}$$

$$R\tilde{v}_{d_1} = -\alpha_{d_1}^*\tilde{v}_1; \tag{6.26}$$

$$R^H\bar{v}_i = \bar{v}_{i-1}, \quad i = 2, \ldots, d_1; \tag{6.27}$$

$$R^H\bar{v}_1 = -\sum_{i=1}^{d_1} \alpha_i\bar{v}_i. \tag{6.28}$$

Note that since Q is known, it suffices to estimate either $\tilde{V}$ or $\bar{V}$. In particular, we shall show how to estimate the vector $\tilde{v}_1$; the remaining columns of $\tilde{V}$ can then be recovered using (6.25). An additional property of this vector which will be exploited in the proof of lemma 6.2 below is as follows.

Lemma 6.1 *With R, $\tilde{v}_i$ and α_{d_1} as above, there holds:*

$$R^H \tilde{v}_1 = -\alpha_{d_1} \tilde{v}_{d_1}. \tag{6.29}$$

Now we expose the structure of the singular values of the matrix R, which are the same as those of $\bar{C}_s(1)$ since $R = V\bar{C}_s(1)V^H$ with V unitary. Therefore these singular values are independent of the channel coefficients, being determined by the source statistics alone.

Theorem 6.2 *There exists a $d_1 \times d_1$ unitary matrix P such that $\bar{C}_s(1) = PD$, where D is $d_1 \times d_1$ diagonal given by*

$$D = \text{diag}(\begin{array}{cccc} 1 & \cdots & 1 & |\alpha_{d_1}| \end{array}). \tag{6.30}$$

The significance of Theorem 6.2 resides in the fact that the smallest singular value of $\bar{C}_s(1)$ (and therefore of R) is given by $|\alpha_{d_1}|$, and it is unique because of Theorem 6.1. This uniqueness allows us to extract the matrix V from R, up to a unitary scaling constant. The fact that, under the nonsingularity assumption on the $(d_1+1) \times (d_1+1)$ lag-0 source covariance matrix, the smallest singular value of the normalized lag-1 covariance matrix has multiplicity one, is in our opinion a result of independent interest. The final result that we need is as follows.

Lemma 6.2 *The vector $\beta_0^{-1}\tilde{v}_1$ is a unit-norm left singular vector of the matrix R associated with its smallest singular value (under Assumption* **A3***) $|\alpha_{d_1}|$.*

6.3 The modified algorithm

In view of the results of the previous section it is possible to estimate the columns of the matrix $\tilde{V}$ as follows: first extract $\tilde{v}_1$ as β_0 times a left singular vector of R associated with the smallest singular value; then use the recurrence (6.25) in order to estimate the remaining columns. For convenience, the algorithm is detailed next:

Algorithm 6.1: Blind equalization of linear channels with correlated sources

---

1. Perform an SVD of $C_y(0)$ as in (6.18) and construct $R = \Sigma^{-1} U_1^H C_y(1) U_1 \Sigma^{-1}$.

2. Let $\hat{v}_1$ be a unit-norm left singular vector of R associated to the smallest singular value.

3. For $i = 1, 2, \ldots, d_1 - 1$, let $\hat{v}_{i+1} = R\hat{v}_i + \alpha_i^* \hat{v}_1$.

4. The normalized channel matrix estimate is then

$$\hat{H} = \beta_0 U_1 \Sigma [\begin{array}{ccc} \hat{v}_1 & \cdots & \hat{v}_{d_1} \end{array}] Q$$

   so that the unnormalized channel matrix estimate $\hat{\mathcal{H}} = \hat{H} Q^{-1}$ is given by

$$\hat{\mathcal{H}} = \beta_0 U_1 \Sigma [\begin{array}{ccc} \hat{v}_1 & \cdots & \hat{v}_{d_1} \end{array}].$$

5. The columns of the matrix $\mathcal{G}_{\mathrm{ZF}}$ given by

$$\mathcal{G}_{\mathrm{ZF}} = \beta_0 U_1 \Sigma^{-1} [\begin{array}{ccc} \hat{v}_1 & \cdots & \hat{v}_{d_1} \end{array}] C_s(0)$$

   constitute zero-forcing equalizers: in the absence of noise,

$$\mathcal{G}_{\mathrm{ZF}}^H Y(k) = \mathrm{e}^{-j\theta} S(k) \tag{6.31}$$

   for some real θ.

Then we have:

Theorem 6.3 *Consider Algorithm 6.1 with the various quantities in Step 1 defined in (6.19). Consider any $\mathcal{H}$ that simultaneously satisfies $C_y(l) = \mathcal{H} C_s(l) \mathcal{H}^H$ for $l = 0, 1$. Then under Assumptions* **A1** *and* **A3***, there exists a real θ such that $\hat{\mathcal{H}}$ obtained in step 4 obeys*

$$\hat{\mathcal{H}} = \mathrm{e}^{j\theta} \mathcal{H}.$$

Further with $N(k) = 0$ in (6.2), the matrix $\mathcal{G}_{\mathrm{ZF}}$ obtained in step 5 obeys (6.31).

Several comments on the algorithm are in order. First note that since the space of left singular vectors of R corresponding to the smallest singular value has dimension 1, $\hat{v}_1$ is easily determined. The chain of equations in Step 3, also determine $[\ \hat{v}_2 \ \cdots \ \hat{v}_{d_1}\ ]$ efficiently (no matrix inversion). The statistics of $\{a(k)\}$ provide β_0 and Q, just as the output statistics provide $C_y(1)$ and U_1, Σ (via a singular value decomposition) and hence R. Note also that when $\{a(k)\}$ is white, i.e. the case covered in [29], one has $\alpha_i = 0$, $\beta_0 = \sigma_a^{-1}$ and $Q = \sigma_a I_{d_1}$, and the algorithm recovers as a special case its counterpart in [29].

6.4 Simulation results

A series of simulation experiments has been performed to test the new algorithm. For comparison purposes, the subspace algorithm (SSA) of Moulines *et al.* [21] was also implemented in the same environment. The subspace algorithm does not require nor exploit any kind of information about the statistics of the symbols $\{a(k)\}$.

6.4.1 Example 7

In this example, the channel impulse response corresponds to a two-ray multipath environment and was taken from [29]. The number of subchannels is $p = 4$ and the corresponding channel order is $l_1 = 5$:

$$[\ h_{10} \ \cdots \ h_{15}\ ] = \begin{bmatrix} -0.0279 & 0.0414 & -0.0703 & 0.3874 & 0.3132 & -0.0837 \\ -0.0156 & 0.0216 & -0.0241 & 0.4931 & 0.1520 & -0.0514 \\ 0.0098 & -0.0196 & 0.0843 & 0.5167 & 0.0138 & -0.0013 \\ 0.0343 & -0.0604 & 0.2351 & 0.4494 & -0.0675 & 0.0368 \end{bmatrix}$$

The input symbols $\{a(k)\}$ are drawn from a QPSK constellation according to the following rule. Let $\{b_k\}$ be the input stream of iid bits, i.e. $b_k \in \{0, 1\}$. Then

$$a(k) = \begin{cases} -1 + j & \text{if} \quad (b_k\, b_{k-2}) = (0\,0) \\ +1 + j & \text{if} \quad (b_k\, b_{k-2}) = (0\,1) \\ -1 - j & \text{if} \quad (b_k\, b_{k-2}) = (1\,0) \\ +1 - j & \text{if} \quad (b_k\, b_{k-2}) = (1\,1) \end{cases}$$

This scheme generates a colored symbol sequence: the autocovariance of the symbols $\{a(k)\}$ is given by

$$\mathrm{cov}[a(k), a(k-l)] = \begin{cases} 2, & l = 0, \\ \pm j, & l = \pm 2, \\ 0, & \text{else.} \end{cases}$$

We consider an equalizer of order $m = 4$, which yields $d_1 = m + l_1 = 9$. The vector α is then given by

$$\alpha = [\ 0 \quad 0.8j \quad 0 \quad -0.6 \quad 0 \quad -0.4j \quad 0 \quad 0.2 \quad 0\ ]^T.$$

Additive white Gaussian noise was added to the channel output, so that the model becomes $Y(k) = \mathcal{H}S(k) + N(k)$. The Signal-to-Noise Ratio (SNR) is defined as

$$\mathrm{SNR} = 10 \log_{10} \frac{\mathrm{trace}\, E[(\mathcal{H}S(k))(\mathcal{H}S(k))^H]}{\mathrm{trace}\, E[N(k)N(k)^H]}.$$

The noise variance estimate $\hat{\sigma}_n^2$ was taken as the smallest eigenvalue of the matrix $C_y(0)$ and then subtracted to provide the algorithms with denoised autocorrelation estimates. Knowledge of the channel length l_1 was assumed.

Once the channel matrix has been estimated by the subspace algorithm, the zero-forcing equalizers are obtained as the rows of the pseudoinverse: $\hat{\mathcal{H}}^{\#} = \mathcal{G}_{\mathrm{ZF}}^H$. For both algorithms the minimum mean-squared error (MMSE) equalizers $\mathcal{G}_{\mathrm{MMSE}}$ are

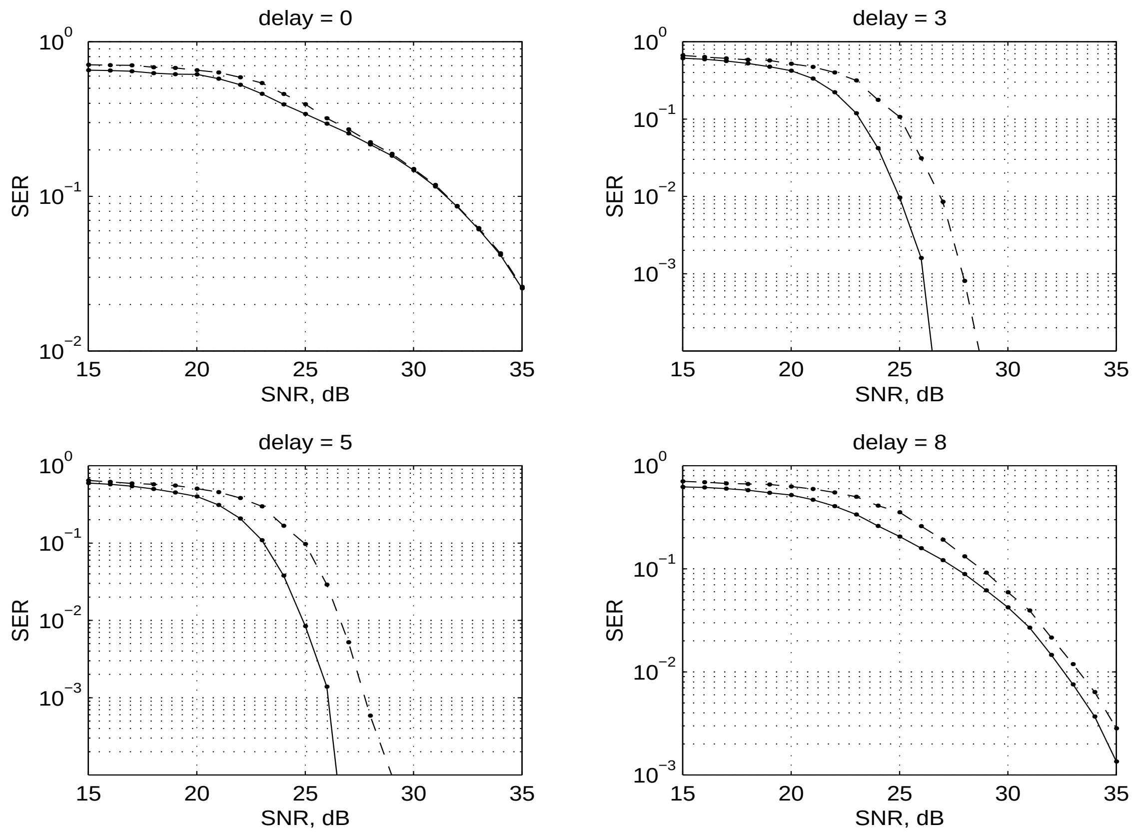

Figure 24: SER vs. SNR, MMSE equalizers from Algorithm 6.1 (solid) and from SSA (dashed), channel from Example 7, $K = 2000$ samples for covariance estimation.

computed via (4.35). The different rows of $\mathcal{G}_{\mathrm{MMSE}}$ correspond to different equalization delays and therefore they present different MSE values at their outputs. Figure 24 shows the symbol error rate (SER), averaged over 200 independent runs, for delays 0, 3, 5 and 8. For the estimation of the covariance matrices, $K = 2000$ symbols were employed. It is seen that for intermediate delays, where the equalizer performance is the best for either approach, Algorithm 6.1 provides an advantage of about 2 dB compared to the subspace algorithm.

In figure 25 the normalized root-mean-square error (NRMSE) of the channel

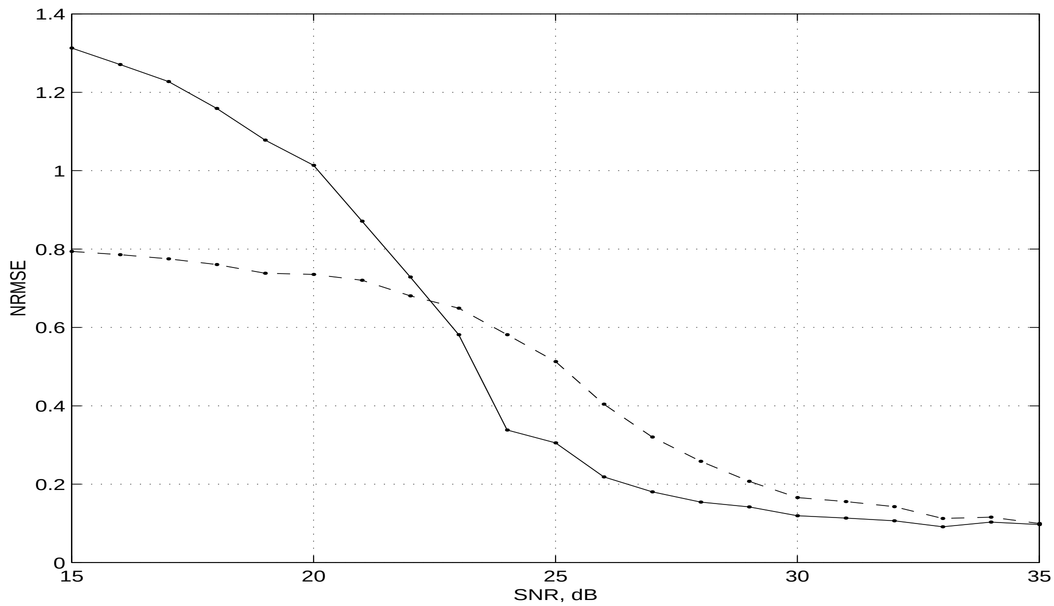

Figure 25: NRMSE versus SNR for Algorithm 6.1 (solid) and SSA (dashed); $K = 2000$ data samples.

estimate as a function of the SNR is depicted. The NRMSE is defined as

$$\text{NRMSE} = \frac{1}{||h||}\sqrt{\frac{1}{T}\sum_{t=1}^{T}||\hat{h}(t) - h||^2},$$

where h is the vector of channel coefficients and T is the number of runs (200 for our experiment). $K = 2000$ symbols were used. The subspace method seems to present a smaller error for low values of the SNR, although for intermediate values the new estimate is more accurate.

Figure 26 shows the variation of the NRMSE with the number of samples K for a fixed value of SNR = 25 dB. At this noise level, the new algorithm clearly outperforms the subspace approach. This is as expected since the subspace method does not exploit knowledge about the symbol statistics.

It could seem paradoxical at first that even though the new algorithm presents

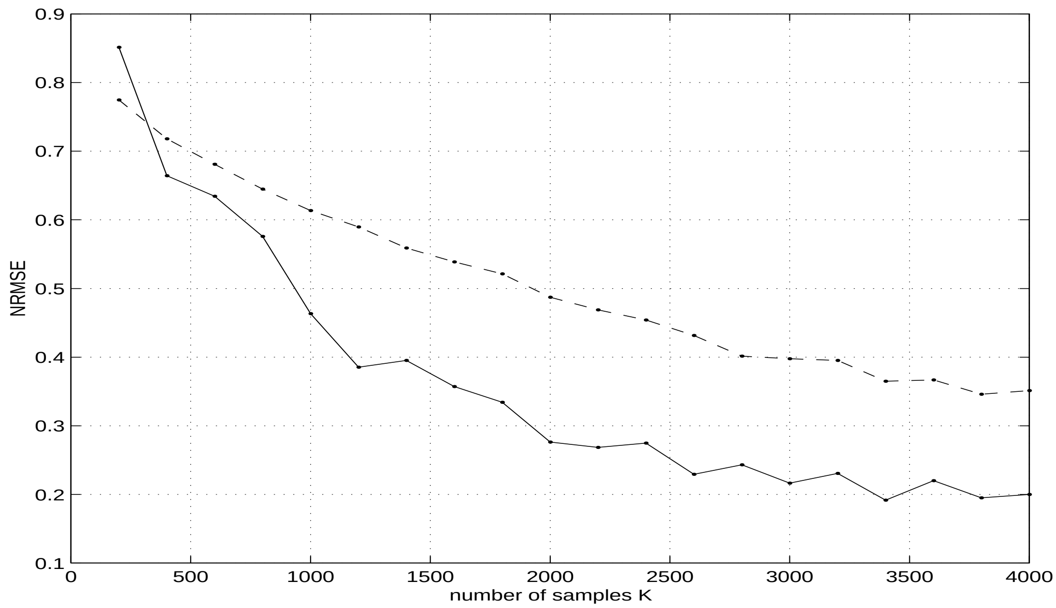

Figure 26: NRMSE versus number of samples K for Algorithm 6.1 (solid) and SSA (dashed); SNR = 25 dB.

a higher NRMSE for low SNR, it still yields a SER lower than that of the subspace method. However, we must recall that the subspace approach computes the zero-forcing equalizers by obtaining the pseudoinverse of the channel matrix. If this channel matrix is ill-conditioned, the obtained equalizers need not be close to the true ones, even if the channel estimation NRMSE is not too high. On the other hand, the new algorithm explicitly uses the statistical information about the symbols (in the form of the matrix $C_s(0)$) when computing $\mathcal{G}_{\mathrm{ZF}}$, which is the reason for its greater accuracy. This can be seen in figure 27, which shows the normalized root-mean-squared error between the "true" zero-forcing equalizer and those computed by the new algorithm and the subspace approach, for a delay of 3.

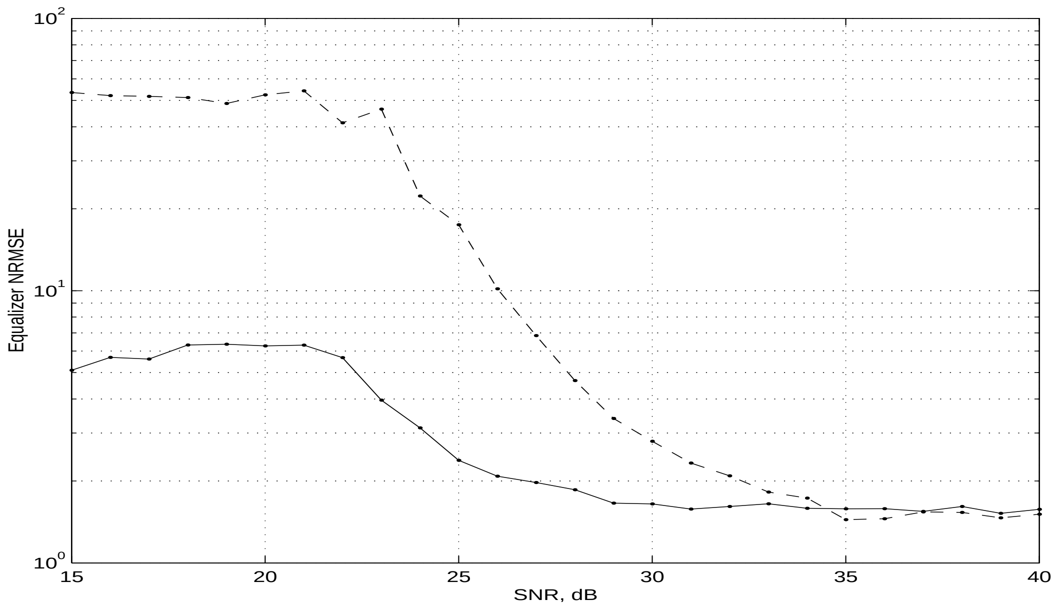

Figure 27: Equalizer (delay 3) NRMSE versus SNR for Algorithm 6.1 (solid) and SSA (dashed); $K = 2000$ data samples.

6.4.2 Example 8

We consider now a linear channel with $p = 2$ subchannels and order $l_1 = 5$. The channel coefficients are given by

$$[\ h_{10} \quad \cdots \quad h_{15}\ ] = \begin{bmatrix} 0.3 & -0.2 & 0.4 & 0.1 & 0.2 & 0.3 \\ 0.5 & 0.4 & -0.7 & 0.2 & -0.5 & -0.2 \end{bmatrix}.$$

The modulation type is Offset QPSK (OQPSK) with rectangular pulses, so that the symbols can be considered to be generated via

$$a(k) = \begin{cases} b_{k-1} + jb_k & \text{for } k \text{ even,} \\ b_k + jb_{k-1} & \text{for } k \text{ odd,} \end{cases}$$

where now $\{b_k\}$ is a stream of independent random variables taking the values ± 1 with equal probabilities. The resulting symbol sequence is correlated, its covariance being given by

$$\text{cov}[a(k), a(k-n)] = \begin{cases} 2, & n = 0, \\ 1, & n = \pm 1, \\ 0, & \text{else.} \end{cases}$$

We consider an equalizer of length $m = 6$, which yields $d_1 = m + l_1 = 11$. The corresponding vector α for this process $\{a(k)\}$ is given by

$$\alpha = \frac{1}{12} \begin{bmatrix} -11 & 10 & -9 & 8 & -7 & 6 & -5 & 4 & -3 & 2 & -1 \end{bmatrix}^T.$$

Figure 28 shows the symbol error rate obtained by using the MMSE equalizers with associated delays 0, 2, 4, 6, 8 and 10, using $K = 1000$ symbols for covariance estimation for both Algorithm 6.1 and the subspace method. It is seen how the equalizers with high values of the delay perform worse than those with lower values. The two algorithms yield very similar results for those 'poor' delay values, while for the 'better' delays the new approach clearly outperforms the subspace method.

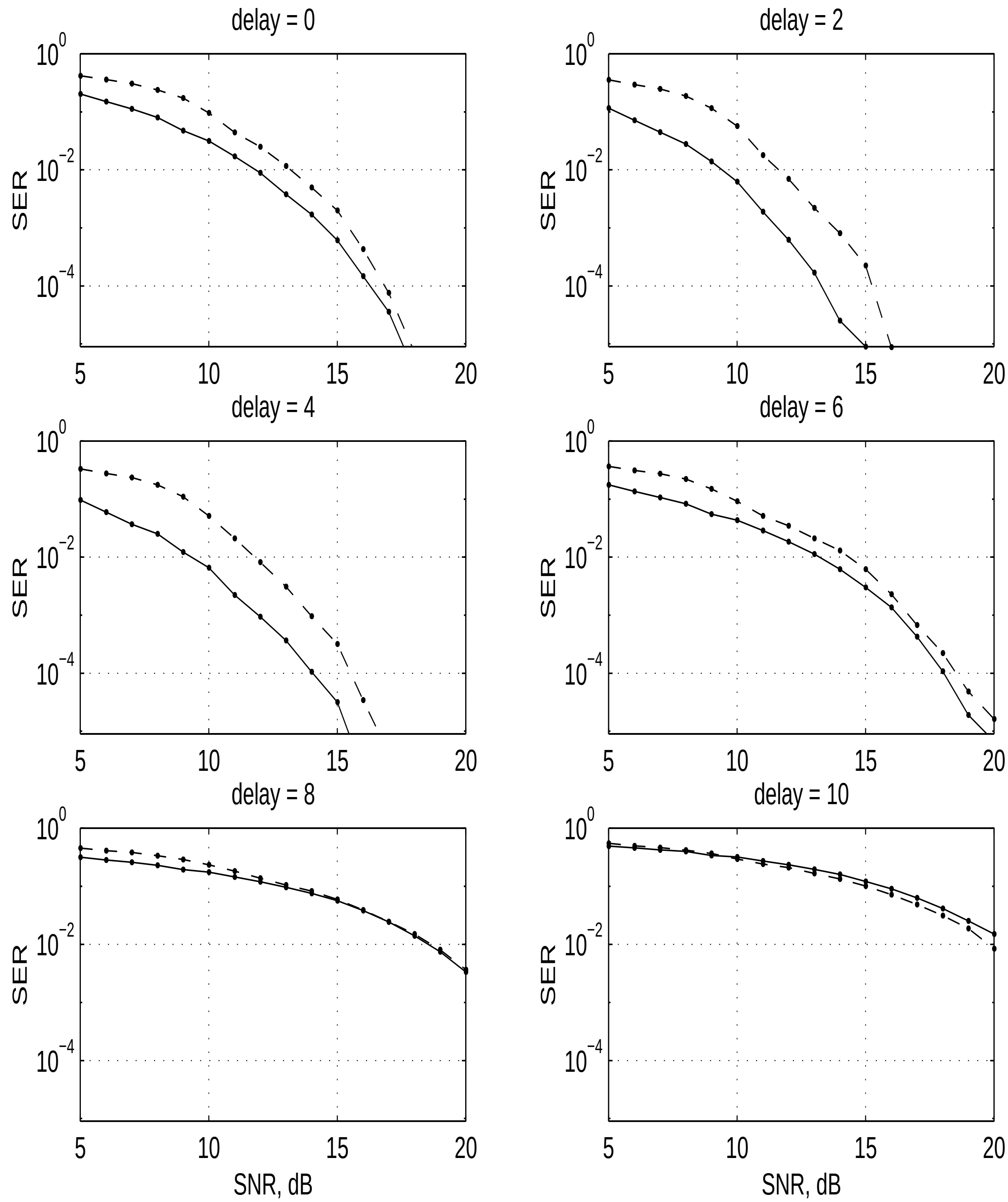

Figure 28: SER vs. SNR, MMSE equalizers from Algorithm 6.1 (solid) and SSA (dashed), channel from Example 8, $K = 1000$ data samples.

CHAPTER VII

CONCLUSIONS AND OPEN PROBLEMS

It is a fact that in most engineering fields a wide gap between linear and nonlinear problems exists. Sophisticated mathematical tools and comprehensive theories are often available in the linear case, but only very special kinds of problems can be analyzed in nonlinear situations. This is also the case in the field of digital communications, where no well established procedure exists for the design of a digital transmission system over a nonlinear channel.

In this thesis we have considered the following question. Given a nonlinear digital communication system, is it possible to exploit channel diversity in order to eliminate the distortion (linear and nonlinear intersymbol interference) introduced by the channel?

Channel diversity can be obtained by sampling the continuous-time received signal at a rate faster than the symbol rate and/or from the use of an array of sensors at the receiver. In that case the channel can be regarded as a single-input multiple-output (SIMO) system. A major breakthrough in this context was achieved by [29], where it was shown that under the so-called *zero and length* conditions, linear finite impulse response SIMO channels can be identified/equalized using the second-order statistics (SOS) of the observed signal, that is, blindly. This result has spawned intensive research in the area of blind system identification and equalization, although most of this effort has focused on the linear channel case.

Recently, it has been pointed out [12] that at least certain classes of *nonlinear* SIMO channels (namely, channels that are linear in the parameters; for example, truncated Volterra series approximations) can be perfectly equalized by means of a bank of *linear* filters, as in the linear channel case. Further, although identification of the channel parameters may not be feasible, at least the equalizers can be computed blindly (under certain conditions) without aid from the transmitter end. The approach used in [12] was deterministic in nature and presented several drawbacks, but it opened the door to the nonlinear channel case for blind equalization techniques.

We have investigated the applicability of SOS based methods to this problem. Specifically, a systematic search for sufficient conditions on the channel and on the input statistics for blind equalizability has been conducted. The results obtained cover a wide class of symbol sources, and they allow to check *a priori* whether the channel is blindly equalizable or not, since the conditions do not depend on the unknown channel parameters.

We have also developed blind algorithms for the computation of the equalizers for the particular but important case in which the transmitted symbols are statistically independent. These algorithms exploit the knowledge of the symbol statistics and therefore are expected to perform better than previous deterministic approaches, which neither require nor exploit such information. This was confirmed via simulations. Computation of both zero-forcing and minimum mean-squared error equalizers was considered. An additional advantage of the new algorithms is that they are able to provide the equalizers for all possible associated delays, while the deterministic method of [12] only yields those of minimal and maximal delays. This issue is of importance since the performance of equalizers with different associated delay can vary considerably in the presence of noise. Also, the new approach does not require that the linear kernel of the channel be the longest, as was the case for the algorithm in [12].

Both the deterministic and SOS-based approaches hinge on the assumption that certain matrix constructed from the channel coefficients (the *channel matrix*) has full column rank, as this is a sufficient condition for the existence of linear equalizers. However, this requirement is not necessary: We have given an alternative relaxed rank condition on the channel matrix, which was shown to be necessary and sufficient. The blind algorithms can be extended to cover the class of nonlinear channels satisfying this condition; however, SOS-based equalizability becomes dependent on the channel parameters and consequently cannot be checked *a priori* as in the full rank case. In addition the computation of the equalizers becomes very sensitive to the channel output SOS estimation accuracy. An exception is found for those channels in which the memory of the linear part exceeds that of the nonlinear part, for which the algorithms remain more robust to this sensitivity problem.

The problem of developing blind equalization algorithms for nonlinear channels with correlated sources still remains open. We have provided a step in this direction by generalizing the original approach of [29], which applies to linear channels with uncorrelated sources, to the case of linear channels and colored symbols. The extension is fairly natural and the complexity of the resulting algorithm is comparable to that of [29]. The algorithm handles all kinds of correlation in the transmitted symbols as long as knowledge of this correlation is available at the receiver. The new method compares favorably to other approaches capable of dealing with colored symbols, such as the subspace approach of [21], but which do not exploit the information about the symbol statistics.

One drawback of the approaches considered in this thesis for the equalization of nonlinear SIMO channels is that the required number of subchannels has to exceed the number of kernels in the channel. In the linear case only one kernel is present, and therefore 2 subchannels generally suffice. When the number of kernels needed to accurately describe the channel input-output behavior increases, the corresponding number of subchannels required could become prohibitively large. Here we have considered polynomial approximations of nonlinear channels as our basic model, which are widely used in practice. It is conceivable, however, that by selecting other types of basis functions (rather than monomials) for the model, the number of kernels required in order to model the channel with the same accuracy could be smaller. Another drawback of the method is that the kernel lengths are assumed known. If this condition is not met, the algorithms may fail to provide the adequate equalizers. This lack of robustness to channel undermodeling or overmodeling is inherited from the original algorithm in [29] for which this problem is well known. Although some techniques are available in order to determine the order of a linear channel blindly [20], to the author's knowledge the problem of blind kernel length determination for nonlinear channels is still open.

APPENDIX

PROOFS

A.1 Proof of Lemma 2.1

Since H is time invariant, $Hz^{-1} = z^{-1}H$. Then

$$\begin{aligned} D_p H U_p z^{-1} &= D_p H z^{-p} U_p \\ &= D_p z^{-p} H U_p \\ &= z^{-1} D_p H U_p, \end{aligned}$$

where use has been made of the noble identities (2.10)-(2.11). ■

A.2 Proof of Lemma 2.2

Let the operators F and G be given by

$$\begin{aligned} Fu(k) &= f[\cdots, u(k+2), u(k+1), u(k), \cdots], \\ Gu(k) &= g[\cdots, u(k+2), u(k+1), u(k), \cdots]. \end{aligned}$$

Let $x(k) = Gu(k)$. Then $Hu(k) = FGu(k) = Fx(k)$ so that

$$\begin{aligned} Hu(k) &= f[\cdots, x(k+2), x(k+1), x(k), \cdots] \\ &= f\begin{bmatrix} \vdots \\ g[\cdots, u(k+4), u(k+3), u(k+2), \cdots] \\ g[\cdots, u(k+3), u(k+2), u(k+1), \cdots] \\ g[\cdots, u(k+2), u(k+1), u(k), \cdots] \\ \vdots \end{bmatrix}. \end{aligned}$$

Therefore the sequence $H^{[p]}u(k)$ becomes

$$H^{[p]}u(k) = f\begin{bmatrix} \vdots \\ g[\cdots, u(k+4p), u(k+3p), u(k+2p), \cdots] \\ g[\cdots, u(k+3p), u(k+2p), u(k+p), \cdots] \\ g[\cdots, u(k+2p), u(k+p), u(k), \cdots] \\ \vdots \end{bmatrix}$$

$$= f[\cdots, G^{[p]}u(k+2p), G^{[p]}u(k+p), G^{[p]}u(k), \cdots]$$

$$= F^{[p]}G^{[p]}u(k),$$

as was to be proved. ■

A.3 Proof of Lemma 2.3

Let H be defined via $Hu(k) = f[\cdots, u(k+2), u(k+1), u(k), \cdots]$. Then

$$HD_pu(k) = Hu(kp) = f[\cdots, u(kp+2p), u(kp+p), u(kp), \cdots]. \tag{A.1}$$

On the other hand,

$$\begin{aligned} D_pH^{[p]}u(k) &= D_pf[\cdots, u(k+2), u(k+1), u(k), \cdots] \\ &= f[\cdots, u(kp+2p), u(kp+p), u(kp), \cdots] \\ &= HD_pu(k) \end{aligned}$$

in view of (A.1), proving the first noble identity. To prove the second one, note that

$$\begin{aligned} U_pHu(k) &= U_pf[\cdots, u(k+2p), u(k+p), u(k), \cdots] \\ &= \begin{cases} f[\cdots, u(k/p+2), u(k/p+1), u(k/p), \cdots], & n \bmod p = 0, \\ 0, & \text{otherwise.} \end{cases} \end{aligned} \tag{A.2}$$

On the other hand, if we let $x(k) = U_pu(k)$, we have

$$H^{[p]}U_pu(k) = H^{[p]}x(k)$$

$$
\begin{aligned}
&= f[\cdots, x(k+2p), x(k+p), x(k), \cdots] \\
&= \begin{cases} f[\cdots, u(k/p+2), u(k/p+1), u(k/p), \cdots], & n \bmod p = 0, \\ f[\cdots, 0, 0, 0, \cdots], & \text{otherwise.} \end{cases}
\end{aligned} \tag{A.3}
$$

Since $f[\cdots, 0, 0, 0, \cdots] = 0$ by assumption, comparing (A.2) and (A.3) the second noble identity is proven. ■

A.4 Proof of Lemma 2.4

Since by assumption the p-input 1-output operator T is linear, we can write $T = [\ T^{(0)}\ \ T^{(1)}\ \ \ldots\ \ T^{(p-1)}\ ]$, where each $T^{(j)}$ is linear. Then $H = \sum_{j=0}^{p-1} T^{(j)} H_j^{[p]}$, so that for $0 \le i \le p-1$ the p-fold polyphase components of H become

$$
\begin{aligned}
D_p z^i H U_p &= \sum_{j=0}^{p-1} D_p z^i T^{(j)} H_j^{[p]} U_p \\
&= \sum_{j=0}^{p-1} D_p z^i T^{(j)} U_p H_j \\
&= \sum_{j=0}^{p-1} T_i^{(j)} H_j,
\end{aligned} \tag{A.4}
$$

where we have used the second noble identity and the definition of the polyphase components of $T^{(j)}$. Now since each $T^{(j)}$ is linear, one has $T^{(j)} = \sum_{i=0}^{p-1} z^{-i} (T_i^{(j)})^{[p]}$. Using this,

$$
\begin{aligned}
\sum_{j=0}^{p-1} T^{(j)} H_j^{[p]} &= \sum_{j=0}^{p-1} \sum_{i=0}^{p-1} z^{-i} (T_i^{(j)})^{[p]} H_j^{[p]} \\
&= \sum_{i=0}^{p-1} z^{-i} \sum_{j=0}^{p-1} (T_i^{(j)} H_j)^{[p]} \\
&= \sum_{i=0}^{p-1} z^{-i} H_i^{[p]},
\end{aligned}
$$

where the second line follows from lemma (2.2) and the third line follows from (A.4). This shows that there is no loss of generality in setting $T^{(j)} = z^{-j}$. ■

A.5 Proof of Lemma 2.5

Let us define the operator

$$R_p \triangleq \begin{bmatrix} 0 & I_{p-1} \\ z^{-1} & 0 \end{bmatrix}.$$

Before proving lemma 2.5, we present several properties of the operators L_p, B_p, R_p:

$$B_p z^{-1} = R_p B_p, \tag{A.5}$$

$$z^{-1} L_p = L_p R_p, \tag{A.6}$$

$$(zR_p) B_p L_p = I_p, \tag{A.7}$$

$$B_p L_p (zR_p) = I_p, \tag{A.8}$$

$$L_p (zR_p) B_p = I. \tag{A.9}$$

To show (A.5), note that

$$\begin{aligned} B_p z^{-1} &= D_p Z_p z^{-1} \\ &= [\ D_p z^{-1} \ \cdots \ D_p z^{-p+1} \ D_p z^{-p}\ ]^T \\ &= [\ D_p z^{-1} \ \cdots \ D_p z^{-p+1} \ z^{-1} D_p\ ]^T \\ &= R_p [\ D_p \ D_p z^{-1} \ \cdots \ D_p z^{-p+1}\ ]^T \\ &= R_p B_p, \end{aligned}$$

where we have used the noble identity $D_p z^{-p} = z^{-1} D_p$. Eq. (A.6) is proven in the same way. To show (A.7),

$$(zR_p) B_p L_p = (zR_p) D_p Z_p Z_p^T U_p X_p$$

$$
\begin{aligned}
&= (zR_p) \begin{bmatrix} 1 & 0 & \cdots & 0 \\ 0 & 0 & \cdots & z^{-1} \\ \vdots & \vdots & \ddots & \vdots \\ 0 & z^{-1} & \cdots & 0 \end{bmatrix} X_p \\
&= \begin{bmatrix} 0 & zI_{p-1} \\ 1 & 0 \end{bmatrix} \begin{bmatrix} 0 & 1 \\ z^{-1}I_{p-1} & 0 \end{bmatrix} \\
&= I_p,
\end{aligned}
$$

where the second line follows from property (2.14). Eq. (A.8) is proven analogously. Finally, to show (A.9), observe that

$$
\begin{aligned}
L_p(zR_p)B_p &= Z_p^T U_p X_p (zR_p) D_p Z_p \\
&= Z_p^T U_p \begin{bmatrix} 1 & 0 \\ 0 & zX_{p-1} \end{bmatrix} D_p Z_p \\
&= \begin{bmatrix} U_p & z^{-1}U_p & \cdots & z^{-p+1}U_p \end{bmatrix} \begin{bmatrix} D_p \\ zD_p z^{-p+1} \\ \vdots \\ zD_p z^{-1} \end{bmatrix} \\
&= \begin{bmatrix} U_p & z^{-1}U_p & \cdots & z^{-p+1}U_p \end{bmatrix} \begin{bmatrix} D_p \\ D_p z \\ \vdots \\ D_p z^{p-1} \end{bmatrix} \\
&= I,
\end{aligned}
$$

where the fourth line follows from the noble identity $zD_p = D_p z^p$ and the last line follows from (2.13). Now using (2.12), we can write the expression of the filterbank

(2.22) as

$$\begin{aligned} G &= \left(\sum_{i=0}^{p-1} z^{-i} U_p D_p z^i\right) F U_p D_p \begin{bmatrix} H^{(0)} & \cdots & H^{(p-1)} \end{bmatrix}^T \\ &= \sum_{i=0}^{p-1} z^{-i} U_p F_i D_p \begin{bmatrix} H^{(0)} & H^{(1)} & \cdots & H^{(p-1)} \end{bmatrix}^T \\ &= L_p \tilde{F} D_p \begin{bmatrix} H^{(0)} & H^{(1)} & \cdots & H^{(p-1)} \end{bmatrix}^T \end{aligned}$$

with $\tilde{F} = \begin{bmatrix} F_{p-1} & \cdots & F_1 & F_0 \end{bmatrix}^T$, and F_i the p-fold i-th polyphase components of F. Note that every $F_i = D_p z^i F U_p$ is a p-input 1-output operator. Further, if we let

$$\tilde{H} = D_p \begin{bmatrix} H^{(0)} & \cdots & H^{(p-1)} \end{bmatrix}^T L_p z R_p,$$

then in view of (A.9) one has $\tilde{H} B_p = D_p \begin{bmatrix} H^{(0)} & \cdots & H^{(p-1)} \end{bmatrix}^T$, and thus,

$$G = L_p \tilde{F} \tilde{H} B_p,$$

which proves the first part of the lemma. Now assume that the analysis filters $H^{(j)}$ are linearly p-separable: $H^{(j)} = \sum_{i=0}^{p-1} [H_i^{(j)}]^{[p]} z^{-i}$. Then

$$\begin{bmatrix} H^{(0)} \\ \vdots \\ H^{(p-1)} \end{bmatrix} = \underbrace{\begin{bmatrix} H_0^{(0)} & H_1^{(0)} & \cdots & H_{p-1}^{(0)} \\ H_0^{(1)} & H_1^{(1)} & \cdots & H_{p-1}^{(1)} \\ \vdots & \vdots & \ddots & \vdots \\ H_0^{(p-1)} & H_1^{(p-1)} & \cdots & H_{p-1}^{(p-1)} \end{bmatrix}^{[p]}}_{\triangleq\; K^{[p]}} Z_p,$$

so that $\tilde{H}$ becomes

$$\begin{aligned} \tilde{H} &= D_p K^{[p]} Z_p L_p z R_p \\ &= K D_p Z_p L_p z R_p \\ &= K(D_p Z_p Z_p^T U_p) X_p z R_p \end{aligned}$$

$$
\begin{aligned}
&= K \begin{bmatrix} 1 & 0 \\ 0 & z^{-1}X_{p-1} \end{bmatrix} \begin{bmatrix} 1 & 0 \\ 0 & zX_{p-1} \end{bmatrix} \\
&= K,
\end{aligned}
$$

as was to be proven. ■

A.6 Proof of Lemma 2.6

By properties (A.5) and (A.6), one has

$$
Gz^{-1} = L_p(\tilde{F}\tilde{H})R_pB_p, \qquad z^{-1}G = L_pR_p(\tilde{F}\tilde{H})B_p.
$$

Now note that properties (A.7) and (A.8) show that L_p is left-invertible while B_p is right-invertible. Thus

$$
\begin{aligned}
Gz^{-1} = z^{-1}G \quad &\Leftrightarrow \quad L_p(\tilde{F}\tilde{H})R_pB_p = L_pR_p(\tilde{F}\tilde{H})B_p \\
&\Leftrightarrow \quad (\tilde{F}\tilde{H})R_p = R_p(\tilde{F}\tilde{H}),
\end{aligned}
$$

which proves the lemma. ■

A.7 Proof of Lemma 2.7

G has the perfect reconstruction property iff $L_p(\tilde{F}\tilde{H})B_p = cz^{-d}$. In view of properties (A.7) and (A.8) which show the left and right invertibility of L_p and B_p respectively, this implies

$$
\tilde{F}\tilde{H} = (zR_p)B_pcz^{-d}L_p(zR_p)
$$

which is a *linear* operator. Then the condition of lemma 2.7 for perfect reconstruction follows from [31, p. 253]. ■

A.8 Proof of Lemma 2.8

By using property (2.13), one can write the overall system as

$$\begin{aligned} D_pGHU_p &= (D_pG)\left(\sum_{j=0}^{p-1} z^{-j}U_pD_pz^j\right)(HU_p) \\ &= (D_pG)\left[\sum_{j=0}^{p-1} z^{-j}U_p(D_pz^jHU_p)\right] \\ &= (D_pG)\left(\sum_{j=0}^{p-1} z^{-j}U_pH_j\right) \\ &= D_pGZ_p^TU_p\left[\begin{array}{ccc} H_0 & \cdots & H_{p-1}\end{array}\right]^T \\ &= \tilde{G}\left[\begin{array}{ccc} H_0 & \cdots & H_{p-1}\end{array}\right]^T, \end{aligned}$$

which proves the result. ■

A.9 Proof of Theorem 3.1

Assume that W and $\bar{C}_s(l)$ commute; then W^k and $\bar{C}_s(l)$ also commute for all k. Since any function of a matrix can be expressed as a polynomial in that matrix [19], one has

$$P = \mathrm{e}^{jW} = \gamma_{d_1+d_2-1}W^{d_1+d_2-1} + \cdots + \gamma_1 W + \gamma_0 I_{d_1+d_2}$$

for some constants γ_i. Thus

$$P\bar{C}_s(l) = \sum_{k=0}^{d_1+d_2-1} \gamma_k W^k \bar{C}_s(l) = \sum_{k=0}^{d_1+d_2-1} \gamma_k \bar{C}_s(l) W^k = \bar{C}_s(l)P.$$

Now assume that $P = \mathrm{e}^{jW}$ and $\bar{C}_s(l)$ commute. Let $\lambda_1, \ldots, \lambda_r$ be the distinct eigenvalues of W with respective multiplicities $m_1, \ldots, m_r$. As W is Hermitian, it is diagonalizable, so let $W = T\Lambda T^{-1}$ with $\Lambda = \lambda_1 I_{m_1} \oplus \cdots \oplus \lambda_r I_{m_r}$. Then

$$\begin{aligned} \mathrm{e}^{jW}\bar{C}_s(l) = \bar{C}_s(l)\mathrm{e}^{jW} &\Leftrightarrow T\mathrm{e}^{j\Lambda}T^{-1}\bar{C}_s(l) = \bar{C}_s(l)T\mathrm{e}^{j\Lambda}T^{-1} \\ &\Leftrightarrow \mathrm{e}^{j\Lambda}(T^{-1}\bar{C}_s(l)T) = (T^{-1}\bar{C}_s(l)T)\mathrm{e}^{j\Lambda}. \qquad \text{(A.10)} \end{aligned}$$

Thus $e^{j\Lambda}$ and $T^{-1}\bar{C}_s(l)T$ commute. Partition $T^{-1}\bar{C}_s(l)T = [D_{ik}]_{1\le i,k\le r}$ with each D_{ik} $m_i \times m_k$. Since $e^{j\Lambda} = e^{j\lambda_1}I_{m_1} \oplus \cdots \oplus e^{j\lambda_r}I_{m_r}$, (A.10) reads as $e^{j\lambda_i}D_{ik} = D_{ik}e^{j\lambda_k}$ for $1 \le i,k \le r$, giving $D_{ik} = 0$ for $i \ne k$ since $\lambda_i \ne \lambda_k$ implies $e^{j\lambda_i} \ne e^{j\lambda_k}$. Thus $T^{-1}\bar{C}_s(l)T$ is block diagonal and therefore it commutes with Λ, as can be readily checked. Then

$$\begin{aligned}(T^{-1}\bar{C}_s(l)T)\Lambda = \Lambda(T^{-1}\bar{C}_s(l)T) \quad &\Leftrightarrow \quad \bar{C}_s(l)T\Lambda T^{-1} = T\Lambda T^{-1}\bar{C}_s(l) \\ &\Leftrightarrow \quad \bar{C}_s(l)W = W\bar{C}_s(l),\end{aligned}$$

as was to be shown. ■

A.10 Proof of Theorem 3.2

Let $C_{11} = SMS^{-1}$, $C_{22} = TNT^{-1}$ be Jordan decompositions of C_{11}, C_{22}. Assume that these have no common eigenvalues. Then the matrix equation $C_{22}TL - TLC_{11} = C_{21}$ has a solution L [19, p. 414], so that

$$\bar{C}_s(1) = \begin{bmatrix} S & 0 \\ -TLS & T \end{bmatrix} \begin{bmatrix} M & 0 \\ 0 & N \end{bmatrix} \begin{bmatrix} S^{-1} & 0 \\ L & T^{-1} \end{bmatrix} \tag{A.11}$$

constitutes a Jordan decomposition of $\bar{C}_s(1)$. Let now

$$W = \begin{bmatrix} W_{11} & W_{12} \\ W_{12}^H & W_{22} \end{bmatrix}, \qquad W_{ij} \text{ of size } d_i \times d_j, \tag{A.12}$$

be a Hermitian matrix commuting with $\bar{C}_s(1)$. Then W must be of the form [19, pp. 417-418]

$$W = \begin{bmatrix} S & 0 \\ -TLS & T \end{bmatrix} \begin{bmatrix} \times & G \\ H^H & \times \end{bmatrix} \begin{bmatrix} S^{-1} & 0 \\ L & T^{-1} \end{bmatrix} \tag{A.13}$$

where the blocks marked '×' are of no concern. Note that $W_{12} = SGT^{-1}$. But since C_{11}, C_{22} have no common eigenvalues, it follows from [19, pp. 417-418] that $G = 0$ and hence $W_{12} = 0$, which proves the first part of the theorem.

Before proving the second part, let us introduce the following definition:

Definition A.1 (Set $\mathcal{U}$) *An $n \times m$ matrix is said to belong to the set $\mathcal{U}$ if it is of the form $[\ U \quad 0\ ]$ when $n < m$, $[\ 0 \quad U^H\ ]^H$ when $n > m$, or $\bar{U}$ when $n = m$, with U any square upper triangular matrix and $\bar{U}$ any square upper triangular matrix with zeros on the diagonal.*

The following fact is readily verified:

Lemma A.1 *The set $\mathcal{U}$ is closed under addition and multiplication.*

Now assume $C_{21} = 0$ and that C_{11}, C_{22} do not have common Jordan blocks. Then (A.11) with $L = 0$ is a Jordan decomposition of $\bar{C}_s(1)$. Let W as in (A.12) be a Hermitian matrix commuting with $\bar{C}_s(1)$. Then W satisfies (A.13) with $L = 0$. Let $M = M_1 \oplus \cdots \oplus M_t$, $N = N_1 \oplus \cdots \oplus N_c$, with $M_i = \alpha_i I_{r_i} + J_{r_i}^H$, $N_j = \lambda_j I_{s_j} + J_{s_j}^H$ elementary Jordan blocks, and partition $G = [G_{ij}]_{1 \le i \le t}^{1 \le j \le c}$, $H = [H_{ij}]_{1 \le i \le t}^{1 \le j \le c}$ accordingly, where each G_{ij}, H_{ij} have size $r_i \times s_j$. By assumption, if $\alpha_i = \lambda_j$ then $r_i \neq s_j$. Therefore, from [19, pp. 417-418] it follows that all G_{ij}, H_{ij}^H are in $\mathcal{U}$.

Observe that $W_{12} = SGT^{-1}$ and $W_{12}^H = TH^H S^{-1}$. Then $GH^H = S^{-1} W_{12} W_{12}^H S$ is similar to the Hermitian positive semidefinite matrix $W_{12} W_{12}^H$. If one shows that GH^H is nilpotent then all the eigenvalues of $W_{12} W_{12}^H$ will be zero and thus $W_{12} = 0$. This we proceed to show.

Write $D \triangleq GH^H = [D_{ij}]_{1 \le i,j \le t}$, with each D_{ij} $r_i \times r_j$. Then from lemma A.1, each D_{ij} is in $\mathcal{U}$. Without loss of generality, assume $r_i \ge r_{i+1}$. We prove the nilpotence of D by induction on t.

Clearly when $t = 1$, D_{11} being square and in $\mathcal{U}$ is zero diagonal upper triangular; hence all its eigenvalues are zero so that D is nilpotent. Now suppose nilpotence holds for $t = \tau - 1$. Then for $t = \tau$, write

$$D = \begin{bmatrix} \bar{D}_0 & \bar{D}_1 \\ \bar{D}_2 & D_{\tau\tau} \end{bmatrix}$$

where $\bar{D}_1 \triangleq [\ D_{1\tau}^H \ \cdots \ D_{\tau-1,\tau}^H\ ]^H$ and $\bar{D}_2 \triangleq [\ D_{\tau 1} \ \cdots \ D_{\tau,\tau-1}\ ]$. Then

$$\begin{aligned} \det(\lambda I - D) &= \det(\lambda I - D_{\tau\tau}) \det[(\lambda I - \bar{D}_0) - \bar{D}_1(\lambda I - D_{\tau\tau})^{-1}\bar{D}_2] \\ &= \lambda^{r_\tau} \det\{\lambda I - [\bar{D}_0 + \bar{D}_1(\lambda I - D_{\tau\tau})^{-1}\bar{D}_2]\}. \end{aligned}$$

As $\lambda I - D_{\tau\tau}$ is $r_\tau \times r_\tau$ upper triangular, and each $D_{\tau i}$, $1 \leq i < \tau$, is $r_\tau \times r_i$ and in $\mathcal{U}$, it follows that $(\lambda I - D_{\tau\tau})^{-1}\bar{D}_2$ is $r_\tau \times r_i$ and in $\mathcal{U}$. Thus $\bar{D}_1(\lambda I - D_{\tau\tau})^{-1}\bar{D}_2$ and hence also $\bar{D}_0 + \bar{D}_1(\lambda I - D_{\tau\tau})^{-1}\bar{D}_2$ can be partitioned into $r_i \times r_j$ blocks, $1 \leq i, j < \tau$, all in $\mathcal{U}$. Thus by the induction hypothesis,

$$\det\{\lambda I - [\bar{D}_0 + \bar{D}_1(\lambda I - D_{\tau\tau})^{-1}\bar{D}_2]\} = \lambda^{r_1 + \cdots + r_{\tau-1}}.$$

Hence the result. ■

A.11 Proof of Theorem 3.3

If $\{a(k)\}$ is generated via (3.43), then the forward prediction error is just $f(k) = w(k)$, which by assumption is an iid process. Since $S_2(k-1)$ is a function of $\{f(i),\ i < k\}$, this means that the random variables $S_2(k-1)$ and $f(k)$ are independent and therefore $\text{cov}[S_2(k-1), f(k)] = 0$. Thus with Q as in (3.29), $\bar{C}_s(1)$ is lower triangular as in (3.42). We can apply the result of theorem 3.2 to conclude that if the diagonal blocks of $\bar{C}_s(1)$, which are similar to $J_{d_1} - e_1\alpha^H$ and $A_0^{-1}(B_0 - ve_{d_1}^H A_{11}^{-1}A_{12})$, do not share any eigenvalues, then any Hermitian W commuting with $\bar{C}_s(1)$ is block diagonal as in (3.20). Hence QWQ^{-1} is block lower triangular, being given by

$$QWQ^{-1} = \begin{bmatrix} A_{11}^{1/2} W_{11} A_{11}^{-1/2} & 0 \\ \times & \times \end{bmatrix}. \tag{A.14}$$

Hence for QWQ^{-1} to be admissible it only remains to be shown that $A_{11}^{1/2}W_{11}A_{11}^{-1/2}$ is diagonal. Observe that because W commutes with $\bar{C}_s(1)$, W_{11} must commute with $A_{11}^{-1/2}(J_{d_1} - e_1\alpha^H)A_{11}^{1/2}$. Lemma A.2 below provides this final step. ■

Lemma A.2 *Any Hermitian matrix W_{11} commuting with $A_{11}^{-1/2}(J_{d_1} - e_1\alpha^H)A_{11}^{1/2}$ is of the form $W_{11} = \theta I_{d_1}$ for some real θ, provided (3.44) is satisfied.*

Proof: Let $\lambda_1, \ldots, \lambda_s$ be the distinct eigenvalues of $J_{d_1} + e_1\alpha^H$ with multiplicities $m_1, \ldots, m_s$ ($m_1 + \cdots + m_s = d_1$). Note that these are the zeros of the transfer function of the FPEF of order d_1. Since $\Upsilon > 0$ from (3.44), the FPEF is minimum phase [15] i.e. $|\lambda_i| < 1$ for $1 \leq i \leq s$. Because $J_{d_1} + e_1\alpha^H$ is a companion matrix, it has a Jordan decomposition of the form

$$J_{d_1} + e_1\alpha^H = KNK^{-1} = K(N_1 \oplus \cdots \oplus N_s)K^{-1}$$

such that $N_i = \lambda I_{m_i} + J_{m_i}^H$, i.e. there is only one Jordan block per distinct eigenvalue [19, p. 69]. In addition, K is a generalized Vandermonde matrix given by $K = \begin{bmatrix} K_1 & \cdots & K_s \end{bmatrix}$ where $K_i = \begin{bmatrix} K_{i,1} & \cdots & K_{i,m_i} \end{bmatrix}$ and

$$K_{i,k} = \frac{1}{(k-1)!}\left\{\frac{\mathrm{d}^{k-1}}{\mathrm{d}z^{k-1}}\begin{bmatrix} z^{d_1-1} & \cdots & z & 1 \end{bmatrix}^T\right\}_{z=\lambda_i} \tag{A.15}$$

(see, e.g. [19, pp. 69-70]). Now since W_{11} and $A_{11}^{-1/2}KNK^{-1}A_{11}^{1/2}$ commute, one must have

$$W_{11} = A_{11}^{-1/2}K(Y_1 \oplus \cdots \oplus Y_s)K^{-1}A_{11}^{1/2} \tag{A.16}$$

with each Y_i $m_i \times m_i$ upper triangular Toeplitz [19, pp. 416-418]. Since W_{11} is Hermitian, it is diagonalizable with real eigenvalues; in view of (A.16), this must be true also for $Y_1, \ldots, Y_s$. Because Y_i is upper triangular Toeplitz, it only has a distinct eigenvalue, say θ_i (the elements of its diagonal). Thus diagonalizability of Y_i means that for some T, $Y_i = T(\theta_i I_{m_i})T^{-1} = \theta_i TT^{-1} = \theta_i I_{m_i}$. This holds for $i = 1, \ldots, s$.

We shall show that all the θ_i are equal: $\theta_1 = \cdots = \theta_s \triangleq \theta$, yielding $W_{11} = \theta I_{d_1}$ as desired.

Let $\Theta \triangleq \theta_1 I_{m_1} \oplus \cdots \oplus \theta_s I_{m_s}$. Since $W_{11} = W_{11}^H$, one has

$$A_{11}^{-1/2} K \Theta K^{-1} A_{11}^{1/2} = A_{11}^{H/2} K^{-H} \Theta K^H A_{11}^{-H/2} \qquad \Leftrightarrow \qquad (K^H A_{11}^{-1} K)\Theta = \Theta(K^H A_{11}^{-1} K)$$

which reads as $(\theta_i - \theta_j)(K_i^H A_{11}^{-1} K_j) = 0$ for $1 \leq i, j \leq s$. It suffices to show that $K_i^H A_{11}^{-1} K_j$ has at least one nonzero element for every i, j. In particular, from (A.15) the (1,1) element of $K_i^H A_{11}^{-1} K_j$ is given by $K_{i,1}^H A_{11}^{-1} K_{j,1} = P(\lambda_i, \lambda_j)$ where the bivariate polynomial $P(z, w)$ is defined as

$$P(z,w) \triangleq [\ (z^*)^{d_1-1} \quad \cdots \quad z^* \quad 1\ ] A_{11}^{-1} [\ w^{d_1-1} \quad \cdots \quad w \quad 1\ ]^T.$$

Using the Christoffel-Darboux formula [18], the polynomial $P(z, w)$ can also be written as

$$P(z,w) = \frac{\alpha(1/z^*)\alpha^*(1/w^*) - \bar{\alpha}(1/z^*)\bar{\alpha}^*(1/w^*)}{\gamma^2(1 - z^* w)}$$

where γ is a real constant, $\alpha(z) \triangleq z^{-d_1} \det[zI - (J - e_1 \alpha^H)]$ and $\bar{\alpha}(z) \triangleq z^{-d_1} \alpha^*(1/z^*)$. (Specifically, $\alpha(z)$ and $\bar{\alpha}(z)$ are the transfer functions of the FPEF and BPEF of order d_1 for the process $\{a(k)\}$, and γ^2 is the variance of the corresponding prediction errors).

Since both λ_i, λ_j are roots of $\alpha(z)$, one has $\bar{\alpha}(1/\lambda_i^*) = \bar{\alpha}^*(1/\lambda_j^*) = 0$ so that

$$P(\lambda_i, \lambda_j) = \frac{\alpha(1/\lambda_i^*)\alpha^*(1/\lambda_j^*)}{\gamma^2(1 - \lambda_i^* \lambda_j)}. \tag{A.17}$$

Now all roots of $\alpha(z)$ lie strictly inside the unit circle, while both $1/\lambda_i^*$ and $1/\lambda_j^*$ lie strictly outside the unit circle. Therefore in view of (A.17), $P(\lambda_i, \lambda_j)$ cannot be zero. This concludes the proof. ∎

A.12 Proof of Theorem 3.4

Since $\bar{C}_s(1)$ is as in (3.46), and noting that $A_0^{-1/2} B_0 A_0^{-H/2}$ is similar to $A_0^{-1} B_0$, by theorem 3.2 any Hermitian W commuting with $\bar{C}_s(1)$ is as in (3.20). As the characteristic polynomial of J_{d_1} is just λ^{d_1} which is minimum phase, the result follows from lemma A.2 above. ■

A.13 Proof of Theorem 3.5

Since the linear and nonlinear terms are uncorrelated, the source covariance matrices $C_s(l)$ are block diagonal: referring to (3.22), one has $A_{12} = 0$, $B_{12} = 0$, $B_{21} = 0$. Hence A_0 in (3.28) reduces to $A_0 = A_{22}$, while B_0 in (3.31) reduces to $B_0 = B_{22}$, so that from (3.30),

$$\bar{C}_s(1) = (A_{11}^{-1/2} B_{11} A_{11}^{-H/2}) \oplus (A_{22}^{-1/2} B_{22} A_{22}^{-H/2}).$$

According to theorem 3.2, if the matrices $A_{11}^{-1/2} B_{11} A_{11}^{-H/2}$ and $A_{22}^{-1/2} B_{22} A_{22}^{-H/2}$, which are respectively similar to $A_{11}^{-1} B_{11}$ and $A_{22}^{-1} B_{22}$, do not share any elementary Jordan blocks in their Jordan decompositions then any Hermitian W commuting with $\bar{C}_s(1)$ is as in (3.20): $W = W_{11} \oplus W_{22}$. In addition, because W commutes with $\bar{C}_s(1)$, W_{11} must commute with $A_{11}^{-1/2}(J_{d_1} - e_1 \alpha^H) A_{11}^{1/2}$, and admissibility of QWQ^{-1} follows from lemma A.2. ■

A.14 Proof of Theorem 3.6

By the orthogonality principle, $\mathrm{cov}[S_1(k-1), f(k)] = 0$ and $\mathrm{cov}[S_1(k), b(k)] = 0$, so that $(S_1(k-1),\ f(k))$ are uncorrelated random variables and so are $(S_1(k),\ b(k))$. Since the process $\{a(k)\}$ is Gaussian, so are the processes $\{S_1(k)\}$, $\{f(k)\}$, $\{b(k)\}$. Therefore the random variables $(\phi(S_1(k-1)),\ f(k))$ and $(\phi(S_1(k)),\ b(k))$, are independent, so that $\mathrm{cov}[S_2(k-1), f(k)] = \mathrm{cov}[S_2(k), b(k)] = 0$, i.e. $v = 0$. Thus with Q as in (3.29), $\bar{C}_s(1)$ is block diagonal as in (3.45) with $(2,2)$ block equal to

$A_0^{-1/2} B_0 A_0^{1/2}$, which is similar to $A_0^{-1} B_0$. Since the Jordan forms of $J_{d_1} + e_0 \alpha^H$ and $A_0^{-1} B_0$ do not share any elementary Jordan blocks, by theorem 3.2 any Hermitian W commuting with $\bar{C}_s(1)$ is block diagonal. Then QWQ^{-1} has the form shown in (A.14), and its admissibility follows from lemma A.2. ■

A.15 Proof of Theorem 3.7

In view of the equalizability test of section 3.2, we shall look at the structure of any Hermitian W commuting with $\bar{C}_s(d_1 - 1)$. The iid assumption and stationarity yield

$$\operatorname{cov}[S_1(k), S_1(k - d_1 + 1)] = \sigma_a^2 e_{d_1} e_1^H, \tag{A.18}$$

$$\operatorname{cov}[S_1(k), S_2(k - d_1 + 1)] = e_{d_1} e_1^H A_{12}, \tag{A.19}$$

$$\operatorname{cov}[S_2(k), S_1(k - d_1 + 1)] = 0, \tag{A.20}$$

$$\operatorname{cov}[S_2(k), S_2(k - d_1 + 1)] = 0, \tag{A.21}$$

with A_{12} defined in (3.21) and $\sigma_a^2 \triangleq E[|a(n)|^2]$. Therefore

$$C_s(d_1 - 1) = \begin{bmatrix} \sigma_a^2 e_{d_1} e_1^H & e_{d_1} e_1^H A_{12} \\ 0 & 0 \end{bmatrix}. \tag{A.22}$$

Take Q as in (3.29) with $A_{11}^{1/2} = \sigma_a I_{d_1}$. Noting that $e_{d_1}^H A_{12} = \operatorname{cov}[a(k-d_1+1), S_2(k)] = 0$ from (A.20), it follows from (A.22) that $\bar{C}_s(d_1 - 1)$ has only one nonzero element:

$$\begin{aligned} \bar{C}_s(d_1 - 1) &= Q^{-1} C_s(d_1 - 1) Q^{-H} \\ &= \begin{bmatrix} \frac{1}{\sigma_a} I_{d_1} & 0 \\ -\frac{1}{\sigma_a^2} A_0^{-1/2} A_{12}^H & A_0^{-1/2} \end{bmatrix} \begin{bmatrix} \sigma_a^2 e_{d_1} e_1^H & e_{d_1} e_1^H A_{12} \\ 0 & 0 \end{bmatrix} Q^{-H} \\ &= \begin{bmatrix} \sigma_a e_{d_1} e_1^H & \frac{1}{\sigma_a} e_{d_1} e_1^H A_{12} \\ -\sigma_a A_0^{-1/2} A_{12}^H e_{d_1} e_1^H & -\frac{1}{\sigma_a^2} A_0^{-1/2} A_{12}^H e_{d_1} e_1^H A_{12} \end{bmatrix} Q^{-H} \end{aligned}$$

$$
\begin{aligned}
&= \begin{bmatrix} \sigma_a e_{d_1} e_1^H & \frac{1}{\sigma_a} e_{d_1} e_1^H A_{12} \\ 0 & 0 \end{bmatrix} \begin{bmatrix} \frac{1}{\sigma_a} I_{d_1} & -\frac{1}{\sigma_a^2} A_{12} A_0^{-H/2} A_{12}^H \\ 0 & A_0^{-H/2} \end{bmatrix} \\
&= \begin{bmatrix} e_{d_1} e_1^H & (\frac{1}{\sigma_a} e_{d_1} e_1^H A_{12} A_0^{-H/2} - \frac{1}{\sigma_a} e_{d_1} e_1^H A_{12} A_0^{-H/2}) \\ 0 & 0 \end{bmatrix} \\
&= (e_{d_1} e_1^H) \oplus 0_{d_2 \times d_2}. \qquad \text{(A.23)}
\end{aligned}
$$

Now let $W = [W_{ij}]_{i,j=1,2}$ be a Hermitian matrix commuting with $\bar{C}_s(d_1 - 1)$, with each W_{ij} $d_i \times d_j$. From (A.23), we must then have

$$
W_{11} e_{d_1} e_1^H = e_{d_1} e_1^H W_{11}, \qquad e_{d_1} e_1^H W_{12} = 0, \qquad W_{12}^H e_{d_1} e_1^H = 0.
$$

These imply that, with θ a scalar,

$$
W_{11} = \theta \oplus \bar{W}_{11} \oplus \theta, \qquad W_{12}^H = \begin{bmatrix} 0 & \bar{W}_{12}^H & 0 \end{bmatrix}, \qquad \text{(A.24)}
$$

where $\bar{W}_{11}$ is $(d_1 - 2) \times (d_1 - 2)$ Hermitian and $\bar{W}_{12}$ is $(d_1 - 2) \times d_2$. The matrix QWQ^{-1} is

$$
QWQ^{-1} = \begin{bmatrix} W_{11} - \frac{1}{\sigma_a} W_{12} A_0^{-1/2} A_{12}^H & \sigma_a W_{12} A_0^{-1/2} \\ \times & \times \end{bmatrix}, \qquad \text{(A.25)}
$$

with '×' indicating irrelevant values. Therefore, in view of (A.24), the rows 1 and d_1 of QWQ^{-1} are just θe_1^H and $\theta e_{d_1}^H$ respectively. Thus, the rows 1 and d_1 of $\mathrm{e}^{-jQWQ^{-1}}$ are $\mathrm{e}^{-j\theta} e_1^H$ and $\mathrm{e}^{-j\theta} e_{d_1}^H$. Now recall from (3.16) that any $\tilde{\mathcal{H}}$ that is compatible must satisfy $\mathcal{H} = \tilde{\mathcal{H}} \mathrm{e}^{-jQWQ^{-1}}$. Thus for $d = 0$ and $d = d_1 - 1$, (3.12) holds. ■

A.16 Proof of Lemma 3.1

Observe that in the noiseless case the ZF equalizers of delays 0 and d satisfy $g_0^H Y(k) = a(k)$ and $g_d^H Y(k) = a(k-d)$, so that $g_d^H Y(k) = g_0^H Y(k-d)$. Therefore

$$
\mathrm{cov}[Y(k), g_d^H Y(k)] = \mathrm{cov}[Y(k), g_0^H Y(k-d)]
$$

$$\begin{aligned} \Rightarrow \quad \mathrm{cov}[Y(k), Y(k)]g_d &= \mathrm{cov}[Y(k), Y(k-d)]g_0 \\ \Rightarrow \quad C_y(0)g_d &= C_y(d)g_0. \end{aligned} \tag{A.26}$$

Now $C_y(0) = \mathcal{H}C_s(0)\mathcal{H}^H$, $C_y(d) = \mathcal{H}C_s(d)\mathcal{H}^H$; observe that $C_y(0)$ is singular. Since $\mathcal{H}$ has full column rank, $\mathcal{H}^{\#}\mathcal{H} = I$ so that the equalizer g_d is given by $g_d = (\mathcal{H}^H)^{\#}e_{d+1}$. Thus (A.26) reads as

$$\begin{aligned} \mathcal{H}C_s(0)\mathcal{H}^H g_d &= \mathcal{H}C_s(d)\mathcal{H}^H g_0 \\ \Rightarrow \quad C_s(0)\mathcal{H}^H g_d &= C_s(d)\mathcal{H}^H g_0 \\ \Rightarrow \quad \mathcal{H}^H g_d &= C_s^{-1}(0)C_s(d)\mathcal{H}^H g_0 \\ \Rightarrow \quad (\mathcal{H}^H)^{\#}\mathcal{H}^H g_d &= (\mathcal{H}^H)^{\#}C_s^{-1}(0)C_s(d)\mathcal{H}^H g_0. \end{aligned} \tag{A.27}$$

Now since $\mathcal{H}^H(\mathcal{H}^H)^{\#} = I$, one has

$$(\mathcal{H}^H)^{\#}\mathcal{H}^H g_d = (\mathcal{H}^H)^{\#}\mathcal{H}^H(\mathcal{H}^H)^{\#}e_{d+1} = (\mathcal{H}^H)^{\#}e_{d+1} = g_d. \tag{A.28}$$

In addition, observe that

$$\begin{aligned} C_y(0)^{\#}C_y(d) &= [\mathcal{H}C_s(0)\mathcal{H}^H]^{\#}[\mathcal{H}C_s(d)\mathcal{H}^H] \\ &= (\mathcal{H}^H)^{\#}C_s^{-1}(0)\mathcal{H}^{\#}\mathcal{H}C_s(d)\mathcal{H}^H \\ &= (\mathcal{H}^H)^{\#}C_s^{-1}(0)C_s(d)\mathcal{H}^H. \end{aligned} \tag{A.29}$$

Substituting (A.28) and (A.29) in (A.27), the result follows. ■

A.17 Proof of Lemma 3.2

Given two terms $s_i(k)$, $s_j(k)$ of the form (3.50), they can be written as

$$\begin{aligned} s_i(k) &= a^{p_0}(k)a^{p_1}(k-1)\cdots a^{p_t}(k-t)[a^{p_0'}(k)]^*[a^{p_1'}(k-1)]^*\cdots[a^{p_t'}(k-t)]^*, \\ s_j(k) &= a^{q_0}(k)a^{q_1}(k-1)\cdots a^{q_t}(k-t)[a^{q_0'}(k)]^*[a^{q_1'}(k-1)]^*\cdots[a^{q_t'}(k-t)]^*, \end{aligned}$$

for some integers t and p_i, p_i', q_i, q_i' such that

$$(p_0 - p_0') + \cdots + (p_t - p_t') = 1, \qquad (q_0 - q_0') + \cdots + (q_t - q_t') = 1. \tag{A.30}$$

(Some p_i, p_i', q_i, q_i' may be zero). We shall show that if $\mathrm{cov}[s_i(k), s_j(k-d)] \neq 0$ for some d, then $s_i(k)$ must be a scaled version of $s_j(k-d)$. To do so, note that for all integers $l > 0$, the circular symmetry of the M-ary PSK constellation gives

$$E[a^l(k)] = \frac{R^l}{M} \sum_{n=0}^{M-1} \mathrm{e}^{j2\pi nl/M} = \frac{R^l}{M} \frac{1 - \mathrm{e}^{j2\pi l}}{1 - \mathrm{e}^{j2\pi l/M}} = \begin{cases} 0, & l \bmod M \neq 0, \\ R^l, & l \bmod M = 0. \end{cases}$$

But if $l \bmod M = 0$ then $a^l(k) = R^l$ reduces to a constant. Thus without loss of generality we can assume that none of the p_i, p_i', q_i, q_i' are multiples of M, since any multiplicative constants in the terms $s_i(k)$, $s_j(k)$ can be absorbed in the corresponding channel coefficients. As a consequence, since

$$E\left\{a^l(k)[a^{l'}(k)]^*\right\} = \begin{cases} R^{2l'} E\left\{a^{l-l'}(k)\right\}, & l > l', \\ R^{2l}, & l = l', \\ R^{2l} E\left\{[a^{l'-l}(k)]^*\right\}, & l < l', \end{cases} \tag{A.31}$$

we have that for all l, l' with $l, l' \bmod M \neq 0$,

$$E\left\{a^l(k)[a^{l'}(k)]^*\right\} \neq 0 \qquad \text{only if } l = l', \tag{A.32}$$

in which case the term $a^l(k)[a^l(k)]^*$ is constant:

$$a^l(k)[a^l(k)]^* = R^{2l}. \tag{A.33}$$

Now observe that due to the independence and stationarity of the symbols $\{a(k)\}$,

$$E[s_i(k)] = \prod_{n=0}^{t} E\left\{a^{p_n}(k)[a^{p_n'}(k)]^*\right\},$$

which is zero in view of (A.32) since (A.30) precludes having $p_j = p'_j$ for all $0 \leq j \leq t$; similarly, $E[s_j(k)] = 0$. Hence the nonlinear terms have zero mean, so that

$$\mathrm{cov}[s_i(k), s_j(k-d)] = E[s_i(k)s_j^*(k-d)].$$

Suppose that $E[s_i(k)s_j^*(k-d)] \neq 0$. Then we must have $0 \leq d \leq t$, or otherwise $s_i(k)$, $s_j(k-d)$ are independent and their covariance becomes zero automatically. Due to the independence of the symbols, one has

$$\begin{aligned}
&E[s_i(k)s_j^*(k-d)] = \\
&\quad E\left\{a^{p_0}(k)\cdots a^{p_{d-1}}(k-d+1)[a^{p'_0}(k)]^*\cdots[a^{p'_{d-1}}(k-d+1)]^*\right\} \\
&\quad \times E\left\{a^{p_d}(k-d)\cdots a^{p_t}(k-t)[a^{p'_d}(k-d)]^*\cdots[a^{p'_t}(k-t)]^*\right. \\
&\qquad \left. a^{q'_0}(k-d)\cdots a^{q'_{t-d}}(k-t)[a^{q_0}(k-d)]^*\cdots[a^{q_{t-d}}(k-t)]^*\right\} \\
&\quad \times E\left\{a^{q'_{t-d+1}}(k-t-1)\cdots a^{q'_t}(k-t-d)\right. \\
&\qquad \left.[a^{q_{t-d+1}}(k-t-1)]^*\cdots[a^{q_t}(k-t-d)]^*\right\}.
\end{aligned} \tag{A.34}$$

If (A.34) is nonzero, then the three factors in the right hand side must be nonzero. Using the stationarity of the symbol sequence, the first factor can be rewritten as

$$\prod_{n=0}^{d-1} E\left\{a^{p_n}(k)[a^{p'_n}(k)]^*\right\} \neq 0 \qquad \Rightarrow \qquad p_n = p'_n, \qquad 0 \leq n \leq d-1, \tag{A.35}$$

in view of (A.32). Similarly, for the third factor,

$$\prod_{n=t-d+1}^{t} E\left\{a^{q'_n}(k)[a^{q'_n}(k)]^*\right\} \neq 0 \qquad \Rightarrow \qquad q_n = q'_n, \qquad t-d+1 \leq n \leq t. \tag{A.36}$$

From (A.33), it follows that we must have

$$\begin{aligned}
s_i(k) &= R^{2(p_0+\cdots+p_{d-1})}a^{p_d}(k-d)\cdots a^{p_t}(k-t)[a^{p'_d}(k-d)]^*\cdots[a^{p'_t}(k-t)]^*, \\
s_j(k) &= R^{2(q_{t-d+1}+\cdots+q_t)}a^{q_0}(k)\cdots a^{q_{t-d}}(k-t+d)[a^{q'_0}(k)]^*\cdots[a^{q'_{t-d}}(k-t+d)]^*.
\end{aligned}$$

In addition, the second factor in the right hand side of (A.34) must be nonzero. Therefore

$$\prod_{n=d}^{t} E\left\{a^{p_n}(k)a^{q'_{n-d}}(k)[a^{p'_n}(k)]^*[a^{q'_{n-d}}(k)]^*\right\} \neq 0$$
$$\Rightarrow \quad q_n - q'_n = p_{n-d} - p'_{n-d}, \qquad d \leq n \leq t. \tag{A.37}$$

Now observe that

$$a^{p_n}(k)[a^{p'_n}(k)]^* = R^{2\bar{p}_n}[b_n(k)]^{|p_n - p'_n|}$$

where

$$\bar{p}_n \triangleq \min\{p_n, p'_n\}, \qquad b_n(k) \triangleq \begin{cases} a(k), & p_n \geq p'_n, \\ a^*(k), & p_n < p'_n. \end{cases}$$

Then we can write

$$\begin{aligned} s_i(k) &= R^{2(p_0+\cdots+p_{d-1}+\bar{p}_d+\cdots+\bar{p}_t)}[b_d(k-d)]^{|p_d-p'_d|}\cdots[b_t(k-t)]^{|p_t-p'_t|}, \\ s_j(k) &= R^{2(\bar{q}_0+\cdots+\bar{q}_{t-d}+q_{t-d+1}+\cdots+q_t)}[c_0(k)]^{|q_0-q'_0|}\cdots[c_{t-d}(k-t+d)]^{|q_{t-d}-q'_{t-d}|}, \end{aligned}$$

where

$$\bar{q}_n \triangleq \min\{q_n, q'_n\}, \qquad c_n(k) \triangleq \begin{cases} a(k), & q_n \geq q'_n, \\ a^*(k), & q_n < q'_n. \end{cases}$$

But since for $d \leq n \leq t$ we have $p_n - p'_n = q_n - q'_n$ in view of (A.37), it follows that

$$b_0(k) = c_d(k), \quad b_1(k) = c_{d+1}(k), \quad \ldots, \quad b_{t-d}(k) = c_t(k).$$

Therefore $s_i(k) = \bar{c} \cdot s_j(k-d)$ where $\bar{c}$ is a constant, as was to be proven. ∎

A.18 Proof of Lemma 4.1

The delay-d ZF equalizer, g_d, is given by

$$g_d = (\mathcal{H}^{\#})^H e_{d+1} = (\mathcal{H}^H)^{\#} e_{d+1}. \tag{A.38}$$

On the other hand, the delay-d MMSE equalizer, f_d, is the minimizer of the quadratic cost (4.34), given by

$$\begin{aligned} f_d &= C_y^{-1}(0) \cdot \text{cov}[Y(k), a(k-d)] \\ &= C_y^{-1}(0)\mathcal{H}\,\text{cov}[S(k), a(k-d)] \\ &= C_y^{-1}(0)\mathcal{H}C_s(0)e_{d+1}, \end{aligned} \tag{A.39}$$

where now $C_y(0)$ is the *undenoised* covariance matrix of the received signal, i.e. $C_y(0) = \mathcal{H}C_s(0)\mathcal{H} + \sigma_n^2 I$. Let us define the matrix Ω and the vector η_d as

$$\Omega \triangleq \mathcal{H}C_s(0)\mathcal{H}^H = C_y(0) - C_n(0), \qquad \eta_d \triangleq \mathcal{H}C_s(0)e_{d+1}.$$

Recall that since $\mathcal{H}$ has full column rank, $\mathcal{H}^\#\mathcal{H} = I$. Therefore one has

$$\begin{aligned} \Omega^\#\eta_d &= [\mathcal{H}C_s(0)\mathcal{H}^H]^\#\mathcal{H}C_s(0)e_{d+1} \\ &= (\mathcal{H}^\#)^H C_s^{-1}(0)\mathcal{H}^\#\mathcal{H}C_s(0)e_{d+1} \\ &= (\mathcal{H}^\#)^H e_{d+1}, \end{aligned} \tag{A.40}$$

so that we can write

$$g_d = \Omega^\#\eta_d, \tag{A.41}$$

$$f_d = C_y^{-1}(0)\eta_d. \tag{A.42}$$

Also note that, in view of (A.40),

$$\begin{aligned} \Omega\Omega^\#\eta_d &= \mathcal{H}C_s(0)\mathcal{H}^H(\mathcal{H}^\#)^H e_{d+1} \\ &= \mathcal{H}C_s(0)e_{d+1} \\ &= \eta_d. \end{aligned}$$

Therefore, from (A.41)-(A.42),

$$\begin{aligned} f_d &= C_y^{-1}(0)\eta_d \\ &= C_y^{-1}(0)\Omega\Omega^{\#}\eta_d \\ &= C_y^{-1}(0)\Omega g_d \\ &= C_y^{-1}(0)[C_y(0) - C_n(0)]g_d \\ &= [I - C_y^{-1}(0)C_n(0)]g_d, \end{aligned}$$

which proves the result. ∎

A.19 Proof of Theorem 5.1

Suppose a matrix $\mathcal{G}$ satisfying (5.2) exists. Then $\mathcal{G}^H\mathcal{H}_1 = I_{d_1}$ which shows that $\mathcal{H}_1$ has full column rank. Also (5.2) shows that the rows of the matrix $[\ I_{d_1} \quad 0_{d_1\times d_2}\ ]$ are linear combinations of the rows of $\mathcal{H}$. Hence

$$\operatorname{rank}(\mathcal{H}) = \operatorname{rank}\left(\begin{bmatrix} \mathcal{H}_1 & \mathcal{H}_{\text{nl}} \\ I_{d_1} & 0_{d_1\times d_2} \end{bmatrix}\right). \tag{A.43}$$

On the other hand, the columns of the matrix $[\ \mathcal{H}_1^T \quad I_{d_1}\ ]^T$ are not linear combinations of the columns of $[\ \mathcal{H}_{\text{nl}}{}^T \quad 0_{d_1\times d_2}^T\ ]^T$. Therefore

$$\begin{aligned} \operatorname{rank}\left(\begin{bmatrix} \mathcal{H}_1 & \mathcal{H}_{\text{nl}} \\ I_{d_1} & 0_{d_1\times d_2} \end{bmatrix}\right) &= \operatorname{rank}\left(\begin{bmatrix} \mathcal{H}_1 \\ I_{d_1} \end{bmatrix}\right) + \operatorname{rank}\left(\begin{bmatrix} \mathcal{H}_{\text{nl}} \\ 0_{d_1\times d_2} \end{bmatrix}\right) \\ &= d_1 + \operatorname{rank}(\mathcal{H}_{\text{nl}}). \end{aligned} \tag{A.44}$$

Thus from (A.43) and (A.44), and since $\operatorname{rank}(\mathcal{H}_1) = d_1$,

$$\operatorname{rank}(\mathcal{H}) = \operatorname{rank}(\mathcal{H}_1) + \operatorname{rank}(\mathcal{H}_{\text{nl}}) = r_1 + r_2.$$

Now assume that the relaxed rank condition **A1′** holds. Consider SVDs of $\mathcal{H}_1$, $\mathcal{H}_{\text{nl}}$:

$$\mathcal{H}_1 = P_1\Sigma_1F_1^H, \qquad \mathcal{H}_{\text{nl}} = P_2\Sigma_2F_2^H,$$

where for $i = 1, 2$, the matrices P_i, Σ_i, F_i have sizes $pm \times r_i$, $r_i \times r_i$ and $d_i \times r_i$ respectively. Then one has

$$\begin{aligned} \mathcal{H} &= [\ P_1\Sigma_1 F_1^H \quad P_2\Sigma_2 F_2^H\ ] \\ &= [\ P_1 \quad P_2\ ] \begin{bmatrix} \Sigma_1 F_1^H & 0 \\ 0 & \Sigma_2 F_2^H \end{bmatrix}. \end{aligned} \tag{A.45}$$

Observe that the $pm \times (r_1 + r_2)$ matrix $[\ P_1 \quad P_2\ ]$ must be full column rank in view of (A.45) and Sylvester's inequality [19] since $\text{rank}(\mathcal{H}) = r_1 + r_2$. Therefore its pseudoinverse satisfies

$$[\ P_1 \quad P_2\ ]^{\#}[\ P_1 \quad P_2\ ] = I_{r_1+r_2}.$$

Then the matrix $\mathcal{G}$ defined by

$$\mathcal{G}^H \triangleq [\ F_1\Sigma_1^{-1} \quad 0\ ][\ P_1 \quad P_2\ ]^{\#}$$

satisfies

$$\begin{aligned} \mathcal{G}^H\mathcal{H} &= [\ F_1\Sigma_1^{-1} \quad 0\ ][\ P_1 \quad P_2\ ]^{\#}[\ P_1 \quad P_2\ ] \begin{bmatrix} \Sigma_1 F_1^H & 0 \\ 0 & \Sigma_2 F_2^H \end{bmatrix} \\ &= [\ F_1\Sigma_1^{-1} \quad 0\ ] \begin{bmatrix} \Sigma_1 F_1^H & 0 \\ 0 & \Sigma_2 F_2^H \end{bmatrix} \\ &= [\ I_{d_1} \quad 0_{d_1\times d_2}\ ] \end{aligned}$$

as desired. The last line follows from the fact that F_1 is $d_1 \times d_1$ unitary. ■

A.20 Proof of Lemma 5.1

Let $\text{rank}(\mathcal{H}_1) = r_1$ and $\text{rank}(\mathcal{H}_{\text{nl}}) = r_2$. Consider the SVDs $\mathcal{H}_1 = P_1\Sigma_1 F_1^H$, $\mathcal{H}_{\text{nl}} = P_2\Sigma_2 F_2^H$, where for $i = 1, 2$, the matrices P_i, Σ_i, F_i have sizes $pm \times r_i$, $r_i \times r_i$

and $d_i \times r_i$ respectively. Then

$$\mathcal{H} = \begin{bmatrix} P_1 & P_2 \end{bmatrix} \begin{bmatrix} \Sigma_1 F_1^H & 0 \\ 0 & \Sigma_2 F_2^H \end{bmatrix}. \tag{A.46}$$

Assume that $\text{rank}(\mathcal{H}) = \text{rank}(\mathcal{H}_1) + \text{rank}(\mathcal{H}_{\text{nl}}) = r_1 + r_2$; then $\text{rank}(\begin{bmatrix} P_1 & P_2 \end{bmatrix}) = r_1 + r_2$ as well. Now let x_1, x_2 be two vectors such that $\mathcal{H}_1 x_1 = \mathcal{H}_{\text{nl}} x_2$. Then

$$P_1 \Sigma_1 F_1^H x_1 = P_2 \Sigma_2 F_2^H x_2$$

or equivalently

$$\begin{bmatrix} P_1 & P_2 \end{bmatrix} \begin{bmatrix} \Sigma_1 F_1^H x_1 \\ -\Sigma_2 F_2^H x_2 \end{bmatrix} = 0,$$

or, since $\begin{bmatrix} P_1 & P_2 \end{bmatrix}$ is full column rank,

$$\begin{bmatrix} \Sigma_1 F_1^H x_1 \\ -\Sigma_2 F_2^H x_2 \end{bmatrix} = 0 \quad \Rightarrow \quad \Sigma_1 F_1^H x_1 = 0, \quad \Sigma_2 F_2^H x_2 = 0,$$

which gives $\mathcal{H}_1 x_1 = P_1 \Sigma_1 F_1^H x_1 = 0$ and $\mathcal{H}_{\text{nl}} x_2 = P_2 \Sigma_2 F_2^H x_2 = 0$. Therefore $\text{range}(\mathcal{H}_1) \bigcap \text{range}(\mathcal{H}_{\text{nl}}) = \{0\}$.

Now assume that $\text{rank}(\mathcal{H}) < \text{rank}(\mathcal{H}_1) + \text{rank}(\mathcal{H}_{\text{nl}}) = r_1 + r_2$. In that case $\text{rank}(\begin{bmatrix} P_1 & P_2 \end{bmatrix}) < r_1 + r_2$ as well, i.e. $\begin{bmatrix} P_1 & P_2 \end{bmatrix}$ does not have full column rank. Therefore there exists a nonzero vector $y = \begin{bmatrix} y_1^T & -y_2^T \end{bmatrix}^T$ such that $\begin{bmatrix} P_1 & P_2 \end{bmatrix} y = 0$, i.e. $P_1 y_1 = P_2 y_2$. Now let $x_1 = F_1 \Sigma_1^{-1} y_1$ and $x_2 = F_2 \Sigma_2^{-1} y_2$. Then

$$\begin{aligned} \mathcal{H}_1 x_1 &= P_1 \Sigma_1 F_1^H x_1 = P_1 y_1, \\ \mathcal{H}_{\text{nl}} x_2 &= P_2 \Sigma_2 F_2^H x_2 = P_2 y_2, \end{aligned}$$

so that $\mathcal{H}_1 x_1 = \mathcal{H}_{\text{nl}} x_2 \neq 0$ since both P_1, P_2 have full column rank and y_1, y_2 cannot both be zero. This shows that $\text{range}(\mathcal{H}_1) \bigcap \text{range}(\mathcal{H}_{\text{nl}})$ has a nonzero element. ■

A.21 Proof of Lemma 5.2

Let x be a vector such that $H_1 x = 0$. Then

$$\mathcal{H}_1 Q_{11} x = \mathcal{H}_{\rm nl}(-Q_{21} x).$$

Since by assumption $\text{rank}(\mathcal{H}) = \text{rank}(\mathcal{H}_1) + \text{rank}(\mathcal{H}_{\rm nl})$, or, in view of lemma 5.1, $\text{range}(\mathcal{H}_1) \bigcap \text{range}(\mathcal{H}_{\rm nl}) = \{0\}$, we must have

$$\mathcal{H}_1 Q_{11} x = \mathcal{H}_{\rm nl}(-Q_{21} x) = 0.$$

In particular, since $\mathcal{H}_1$ has full column rank, and Q_{11} is invertible, it follows that $x = 0$. In other words, $H_1 x = 0$ implies $x = 0$; which means that H_1 has full column rank.

Now let x_1, x_2 be two vectors satisfying $H_1 x_1 = H_2 x_2$. Then

$$(\mathcal{H}_1 Q_{11} + \mathcal{H}_{\rm nl} Q_{21}) x_1 = \mathcal{H}_{\rm nl} Q_{22} x_2,$$

that is,

$$\mathcal{H}_1 Q_{11} x_1 = \mathcal{H}_{\rm nl}(Q_{22} x_2 - Q_{21} x_1).$$

Again, since $\text{range}(\mathcal{H}_1) \bigcap \text{range}(\mathcal{H}_{\rm nl}) = \{0\}$, this gives

$$\mathcal{H}_1 Q_{11} x_1 = 0 \qquad \Rightarrow \qquad x_1 = 0.$$

Thus $H_2 x_2 = H_1 x_1 = 0$ which implies $\text{range}(H_1) \bigcap \text{range}(H_2) = \{0\}$ or equivalently $\text{rank}(H) = \text{rank}(H_1) + \text{rank}(H_2)$. ■

A.22 Proof of Lemma 5.3

Let $\text{rank}(\mathcal{H}_1) = r_1$ and $\text{rank}(\mathcal{H}_{\rm nl}) = r_2$. Consider the SVDs $\mathcal{H}_1 = P_1 \Sigma_1 F_1^H$, $\mathcal{H}_{\rm nl} = P_2 \Sigma_2 F_2^H$, where for $i = 1, 2$, the matrices P_i, Σ_i, F_i have sizes $pm \times r_i$, $r_i \times r_i$

and $d_i \times r_i$ respectively. It was shown in the proof of theorem 5.1 that the ZF equalizers are given by

$$\mathcal{G}^H = [\ F_1\Sigma_1^{-1} \quad 0\ ][\ P_1 \quad P_2\ ]^{\#}.$$

Now let $H = U_1 \Sigma V$ be an SVD of H, with U_1, Σ, V having sizes $pm \times (r_1 + r_2)$, $(r_1 + r_2) \times (r_1 + r_2)$ and $(d_1 + d_2) \times (r_1 + r_2)$ respectively. Since $H = \mathcal{H}Q$, we have

$$U_1 \Sigma V = [\ P_1 \quad P_2\ ] \begin{bmatrix} \Sigma_1 F_1^H & 0 \\ 0 & \Sigma_2 F_2^H \end{bmatrix} Q$$

or, since $VV^H = I$,

$$U_1 = [\ P_1 \quad P_2\ ]T, \tag{A.47}$$

where

$$T \triangleq \begin{bmatrix} \Sigma_1 F_1^H & 0 \\ 0 & \Sigma_2 F_2^H \end{bmatrix} QV^H \Sigma^{-1}.$$

Observe that since both U_1 and $[\ P_1 \quad P_2\ ]$ have full column rank, in view of (A.47) T is invertible. Thus

$$[\ P_1 \quad P_2\ ] = U_1 T^{-1} \qquad \Rightarrow \qquad [\ P_1 \quad P_2\ ]^{\#} = TU_1^H,$$

since $U_1^H U_1 = I_{r_1+r_2}$. Therefore the equalizers are given by

$$\begin{aligned} \mathcal{G}^H &= [\ F_1\Sigma_1^{-1} \quad 0\ ][\ P_1 \quad P_2\ ]^{\#} \\ &= [\ F_1\Sigma_1^{-1} \quad 0\ ]TU_1^H \\ &= [\ F_1\Sigma_1^{-1} \quad 0\ ] \begin{bmatrix} \Sigma_1 F_1^H & 0 \\ 0 & \Sigma_2 F_2^H \end{bmatrix} QV^H \Sigma^{-1} U_1^H \\ &= [\ I_{d_1} \quad 0\ ]QH^{\#} \\ &= Q_{11}[\ I_{d_1} \quad 0\ ]H^{\#}, \end{aligned}$$

as was to be shown. ■

A.23 Proof of Lemma 5.4

Observe that under the conditions of the lemma, the equalizers $\mathcal{G}$ are given by (5.6) and satisfy $\mathcal{G}^H\mathcal{H} = [\ I_{d_1} \quad 0_{d_1 \times d_2}\ ]$. Therefore,

$$\begin{aligned} \mathcal{G}^H\mathcal{H} &= \mathcal{G}^H H Q^{-1} \\ &= Q_{11} V_1^H \Sigma^{-1} U_1^H U_1 \Sigma V Q^{-1} \\ &= Q_{11} V_1^H V Q^{-1}, \end{aligned}$$

since $U_1^H U_1 = I_{r_1+r_2}$. Thus,

$$Q_{11} V_1^H V Q^{-1} = [\ I_{d_1} \quad 0_{d_1 \times d_2}\ ],$$

that is,

$$\begin{aligned} V_1^H V &= Q_{11}^{-1} [\ I_{d_1} \quad 0_{d_1 \times d_2}\ ] Q \\ &= Q_{11}^{-1} [\ Q_{11} \quad 0_{d_1 \times d_2}\ ] \\ &= [\ I_{d_1} \quad 0_{d_1 \times d_2}\ ], \end{aligned}$$

which proves the result. ■

A.24 Proof of Lemma 5.5

Let $A \triangleq V_2 C V_2^H$. Observe that $AV_1 = 0$ in view of (5.7), so that A has at least $d_1 = r_1$ eigenvalues equal to zero. In addition, for any nonzero $d_1 \times 1$ vector x, there is no vector y such that $Ay = V_1 x$ since

$$\begin{aligned} Ay &= V_1 x \\ \Rightarrow \quad V_2 C V_2^H y &= V_1 x \\ \Rightarrow \quad V_1^H V_2 C V_2^H y &= V_1^H V_1 x \end{aligned}$$

$$\Rightarrow \quad 0 = x,$$

where the last line follows from (5.7); this contradicts the assumption $x \neq 0$. Therefore there is no Jordan chain for the zero eigenvalue of A starting with a vector in the range space of V_1 and with length greater than 1. As a consequence, A admits a Jordan decomposition of the form

$$A = [\; V_1 \quad T_0 \quad T_2 \;] \begin{bmatrix} 0_{d_1 \times d_1} & & \\ & Y_0 & \\ & & Z \end{bmatrix} \begin{bmatrix} V_1^H \\ T_0^{\#} \\ T_2^{\#} \end{bmatrix}, \tag{A.48}$$

with Y_0, Z as in the statement of the lemma. Since $R = V_1 J_{d_1} V_1^H + A$, we have in view of (A.48) that

$$R = [\; V_1 \quad T_0 \quad T_2 \;] \begin{bmatrix} J_{d_1} & & \\ & Y_0 & \\ & & Z \end{bmatrix} \begin{bmatrix} V_1^H \\ T_0^{\#} \\ T_2^{\#} \end{bmatrix},$$

which constitutes a Jordan decomposition of R. ■

A.25 Proof of Lemma 5.6

We can always choose the square root matrix Q to be lower triangular as in (5.3). It was shown in the proof of lemma 4.1 that the MMSE equalizer with associated delay d is given by

$$\begin{aligned} f_d &= C_y^{-1}(0)\mathcal{H}C_s(0)e_{d+1} \\ &= C_y^{-1}(0)HQ^H e_{d+1} \\ &= C_y^{-1}(0)U_1 \Sigma V Q^H e_{d+1} \end{aligned} \tag{A.49}$$

(see (A.39)). On the other hand, in view of (5.6), the corresponding ZF equalizer is

$$g_d = \mathcal{G} e_{d+1}$$

$$
\begin{aligned}
&= U_1 \Sigma^{-1} V \begin{bmatrix} Q_{11}^H \\ 0_{d_2 \times d_1} \end{bmatrix} e_{d+1} \\
&= U_1 \Sigma^{-1} V Q^H e_{d+1}.
\end{aligned}
$$

Premultiplying this by $U_1 \Sigma^2 U_1^H$, one gets

$$
U_1 \Sigma^2 U_1^H g_d = U_1 \Sigma V Q^H e_{d+1}, \tag{A.50}
$$

and since $U_1 \Sigma^2 U_1^H = C_y(0) - C_n(0)$, (A.49) and (A.50) yield

$$
[C_y(0) - C_n(0)] g_d = C_y(0) f_d,
$$

as was to be proven. ■

A.26 Proof of Lemma 6.1

Observe that (6.28) yields

$$
R^H \bar{V} \begin{bmatrix} 1 \\ \alpha_1 \\ \vdots \\ \alpha_{d_1 - 1} \end{bmatrix} = -\alpha_{d_1} \bar{v}_d. \tag{A.51}
$$

In view of (6.13) and (6.14), the vector in brackets in (A.51) is

$$
\begin{bmatrix} 1 \\ \alpha_1 \\ \vdots \\ \alpha_{d_1 - 1} \end{bmatrix} = \frac{1}{\beta_0} \left(X_{d_1} \beta + \alpha_{d_1} J_{d_1} \beta^* \right) = \frac{1}{\beta_0} \left(X_{d_1} Q^{-T} + \alpha_{d_1} J_{d_1} Q^{-H} \right) e_{d_1}. \tag{A.52}
$$

Substituting (A.52) into (A.51) yields

$$
R^H \bar{V} (X_{d_1} Q^{-T} + \alpha_{d_1} J_{d_1} Q^{-H}) e_{d_1} = -\alpha_{d_1} \beta_0 \bar{v}_{d_1}
$$

from which

$$R^H V Q^H X_{d_1} Q^{-T} e_d = -\alpha_{d_1}(\beta_0 \bar{v}_{d_1} + R^H \bar{V} J_{d_1} Q^{-H} e_{d_1}), \tag{A.53}$$

where we have substituted $\bar{V} = VQ^H$ in the left hand side. Now since $C_s(0)$ is Hermitian Toeplitz, it satisfies $X_{d_1} C_s(0) = C_s^*(0) X_{d_1}$. Because of (6.6), this yields

$$Q^H X_{d_1} Q^{-T} = Q^{-1} X_{d_1} Q^*. \tag{A.54}$$

Further, from (6.13), and the fact that the diagonal elements of the lower triangular matrix Q, the Cholesky factor of $C_s(0)$, are positive real,

$$\begin{aligned} [\, 0 \ \cdots \ 0 \ \ \bar{v}_{d_1} \,] Q^{-H} e_{d_1} &= [\, 0 \ \cdots \ 0 \ \ \bar{v}_{d_1} \,] \beta^* \\ &= \beta_0 \bar{v}_{d_1}. \end{aligned} \tag{A.55}$$

Also, (6.27) shows that

$$R^H \bar{V} J_{d_1} = [\, \bar{v}_1 \ \cdots \ \bar{v}_{d_1-1} \ \ 0 \,].$$

Thus because of (A.54) and (A.55), (A.53) reads as

$$\begin{aligned} R^H V Q^{-1} X_{d_1} Q^* e_{d_1} &= -\alpha_{d_1} \left(\beta_0 \bar{v}_{d_1} + [\, \bar{v}_1 \ \cdots \ \bar{v}_{d_1-1} \ \ 0 \,] Q^{-H} e_{d_1} \right) \\ &= -\alpha_{d_1} \bar{V} Q^{-H} e_{d_1}. \end{aligned} \tag{A.56}$$

Observe from (6.13), and the fact that Q is lower triangular with positive real diagonal elements that

$$X_{d_1} Q^* e_{d_1} = \beta_0^{-1} e_1 \qquad \text{and} \qquad \beta_0 e_{d_1} = Q^{-1} e_{d_1}. \tag{A.57}$$

Thus from (A.57) and the definitions of $\tilde{V}$ and $\bar{V}$, one has

$$\begin{aligned} R^H V Q^{-1} X_{d_1} Q^* e_{d_1} &= \beta_0^{-1} R^H V Q^{-1} e_1 \\ &= \beta_0^{-1} R^H \tilde{V} e_1, \end{aligned} \tag{A.58}$$

and

$$\begin{aligned} -\alpha_{d_1}\bar{V}Q^{-H}e_{d_1} &= -\beta_0^{-1}\alpha_{d_1}\bar{V}Q^{-H}Q^{-1}e_{d_1} \\ &= -\beta_0^{-1}\alpha_{d_1}\tilde{V}e_{d_1}. \end{aligned} \tag{A.59}$$

In view of (A.56), (A.58) equals (A.59):

$$\beta_0^{-1}R^H\tilde{V}e_1 = -\beta_0^{-1}\alpha_{d_1}\tilde{V}e_{d_1},$$

i.e. $R^H\tilde{v}_1 = -\alpha_{d_1}\tilde{v}_{d_1}$, which proves the lemma. ■

A.27 Proof of Theorem 6.2

Suppose first that $\alpha_{d_1} \neq 0$. In that case it suffices to show that $P \triangleq \bar{C}_s(1)D^{-1}$ is unitary. One has

$$PP^H = \bar{C}_s(1)D^{-2}\bar{C}_s(1)^H, \tag{A.60}$$

and, because of (6.16), D^{-2} can be written as

$$D^{-2} = I_{d_1} - (1 - |\alpha_{d_1}|^{-2})e_{d_1}e_{d_1}^H = I_{d_1} + \frac{\gamma^2\beta_0^2}{|\alpha_{d_1}|^2}e_{d_1}e_{d_1}^H.$$

Recall from (6.12) that $F \triangleq J_{d_1} - e_1\alpha^H$; then from (6.11), $\bar{C}_s(1) = Q^{-1}FQ$. One has from (6.6) and (A.57)

$$\begin{aligned} PP^H &= Q^{-1}FQ\left(I_{d_1} + \frac{\gamma^2\beta_0^2}{|\alpha_{d_1}|^2}e_{d_1}e_{d_1}^H\right)Q^HF^HQ^{-H} \\ &= Q^{-1}\left(FQQ^HF^H + \frac{\gamma^2\beta_0^2}{|\alpha_{d_1}|^2}F(Qe_{d_1})(Qe_{d_1})^HF^H\right)Q^{-H} \\ &= Q^{-1}\left(FC_s(0)F^H + \frac{\gamma^2}{|\alpha_{d_1}|^2}Fe_{d_1}e_{d_1}^HF^H\right)Q^{-H}. \end{aligned} \tag{A.61}$$

Now from (6.17) one has $FC_s(0)F^H = C_s(0) - \gamma^2e_1e_1^H$. Also, $Fe_{d_1} = -\alpha_{d_1}^*e_1$. Substituting these in (A.61), from (6.6),

$$PP^H = Q^{-1}\left(C_s(0) - \gamma^2e_1e_1^H + \frac{\gamma^2}{|\alpha_{d_1}|^2}|\alpha_{d_1}|^2e_1e_1^H\right)Q^{-H}$$

$$
\begin{aligned}
&= Q^{-1} C_s(0) Q^{-H} \\
&= I_{d_1},
\end{aligned}
$$

so that P is unitary.

Now suppose $\alpha_{d_1} = 0$. In that case we shall show that with u the vector given by

$$u \triangleq \gamma Q^{-1} e_1, \tag{A.62}$$

the matrix $P = \bar{C}_s(1) + u e_{d_1}^H$ satisfies the requirements of the lemma. First, note that the last column of $\bar{C}_s(1)$ is the zero vector: Indeed, from (A.57),

$$\bar{C}_s(1) e_{d_1} = Q^{-1} F Q e_{d_1} = \frac{1}{\beta_0} Q^{-1} F e_{d_1} = 0, \tag{A.63}$$

since $F e_{d_1} = -\alpha_{d_1}^* e_1 = 0$. Then

$$
\begin{aligned}
PD &= (\bar{C}_s(1) + u e_{d_1}^H)(I_{d_1} - e_{d_1} e_{d_1}^H) \\
&= \bar{C}_s(1) - \bar{C}_s(1) e_{d_1} e_{d_1}^H + u e_{d_1}^H - u(e_{d_1}^H e_{d_1}) e_{d_1}^H \\
&= \bar{C}_s(1) - 0 + u e_{d_1}^H - u e_{d_1}^H \\
&= \bar{C}_s(1).
\end{aligned}
$$

Thus it remains to show that P is unitary. To do so, observe that in view of (6.17) and (6.6),

$$
\begin{aligned}
\bar{C}_s(1) \bar{C}_s(1)^H &= Q^{-1} F C_s(0) F^H Q^{-H} \\
&= Q^{-1} (C_s(0) - \gamma^2 e_1 e_1^H) Q^{-H} \\
&= I_{d_1} - \gamma^2 (Q^{-1} e_1)(Q^{-1} e_1)^H \\
&= I_{d_1} - u u^H.
\end{aligned}
$$

Therefore,

$$PP^H = (\bar{C}_s(1) + u e_{d_1}^H)(\bar{C}_s(1)^H + e_{d_1} u^H)$$

$$\begin{aligned} &= \bar{C}_s(1)\bar{C}_s(1)^H + \bar{C}_s(1)e_{d_1}u^H + ue_{d_1}^H\bar{C}_s(1)^H + u(e_{d_1}^H e_{d_1})u^H \\ &= \bar{C}_s(1)\bar{C}_s(1)^H + uu^H \\ &= I_{d_1}, \end{aligned}$$

since, from (A.63), one has $\bar{C}_s(1)e_{d_1} = 0$. Thus P is unitary. ■

A.28 Proof of Lemma 6.2

First, observe that since $\tilde{v}_1 = VQ^{-1}e_1$ with V unitary, the norm of $\tilde{v}_1$ is the same as that of $Q^{-1}e_1$. One has $(Q^{-1}e_1)^H(Q^{-1}e_1) = e_1^H C_s^{-1}(0)e_1$, which is the (1, 1) element of $C_s^{-1}(0)$. Since $C_s(0)$ is Toeplitz, its inverse $C_s^{-1}(0)$ is symmetric about the antidiagonal, so that its (1, 1) and (d_1, d_1) elements coincide. But it is easily seen that as Q is lower triangular, because of (6.13) one has $e_{d_1}^H C_s^{-1}(0)e_{d_1} = \beta_0^2$. Thus $\beta_0^{-1}\tilde{v}_1$ has unit norm. Similarly, the (squared) norm of $\tilde{v}_{d_1}$ is $\tilde{v}_{d_1}^H\tilde{v}_{d_1} = (Q^{-1}e_{d_1})^H(Q^{-1}e_{d_1}) = \beta_0^2$.

From (6.26), one has $R\tilde{v}_{d_1} = -\alpha_{d_1}^*\tilde{v}_1$. Premultiply this by R^H and use the result from lemma 6.1 to obtain

$$R^H R\tilde{v}_{d_1} = |\alpha_{d_1}|^2\tilde{v}_{d_1}, \tag{A.64}$$

which shows that $\beta_0^{-1}\tilde{v}_{d_1}$ is a *right* singular vector of R associated to the smallest singular value. But then, using (6.26),

$$R(\beta_0^{-1}\tilde{v}_{d_1}) = -\alpha_{d_1}^*(\beta_0^{-1}\tilde{v}_1)$$

which must equal $|\alpha_{d_1}|v$ with v a unit-norm left singular vector. This shows that $\beta_0^{-1}\tilde{v}_1$ is a unit-norm left singular vector of R associated to its smallest singular value.

■

A.29 Proof of Theorem 6.3

Because of Theorem 6.1, $|\alpha_{d_1}| < 1$. Thus, from Theorem 6.2 the smallest singular value of R has multiplicity one. Hence, the left singular vectors of R corresponding to this singular value span a space of dimension one. Because of Lemma 6.2, the vector $\beta_0^{-1}\tilde{v}_1$ is one such unit-norm left singular vector of R. Since by construction, $\hat{v}_1$ is also a unit-norm left singular vector of R corresponding to this singular value, it follows that there exists a real θ such that

$$\hat{v}_1 = \beta_0^{-1} \mathrm{e}^{j\theta} \tilde{v}_1.$$

Because of Step 3 and (6.25)

$$\hat{V} = [\begin{array}{ccc} \hat{v}_1 & \cdots & \hat{v}_{d_1} \end{array}] = \beta_0^{-1} \mathrm{e}^{j\theta} \tilde{V}.$$

Thus, because of (6.7), (6.19), (6.22) and Step 4,

$$\begin{aligned} \hat{\mathcal{H}} &= \beta_0 U_1 \Sigma \left(\beta_0^{-1} \mathrm{e}^{j\theta} \tilde{V}\right) \\ &= \mathrm{e}^{j\theta} U_1 \Sigma V Q^{-1} \\ &= \mathrm{e}^{j\theta} H Q^{-1} \\ &= \mathrm{e}^{j\theta} \mathcal{H}. \end{aligned}$$

Further, the matrix $\mathcal{G}_{\mathrm{ZF}}$ obtained in Step 5 satisfies

$$\begin{aligned} \mathcal{G}_{\mathrm{ZF}}^H &= \beta_0 C_s(0) \beta_0^{-1} \mathrm{e}^{-j\theta} \tilde{V}^H \Sigma^{-1} U_1^H \\ &= \mathrm{e}^{-j\theta} C_s(0) Q^{-H} V^H \Sigma^{-1} U_1^H \\ &= \mathrm{e}^{-j\theta} Q V^H \Sigma^{-1} U_1^H. \end{aligned}$$

Therefore if $N(k) = 0$ in (6.2), from (6.6), (6.7), (6.19), and (6.22) one obtains

$$\begin{aligned} \mathcal{G}_{\mathrm{ZF}}^H Y(k) &= \mathcal{G}_{\mathrm{ZF}}^H \mathcal{H} S(k) \\ &= (\mathrm{e}^{-j\theta} Q V^H \Sigma^{-1} U_1^H)(U_1 \Sigma V Q^{-1}) S(k) \\ &= \mathrm{e}^{-j\theta} S(k). \end{aligned}$$

This concludes the proof. ■

REFERENCES

[1] K. H. Afkhamie and Z.-Q. Luo, "Blind identification of FIR systems driven by Markov-like input signals", *IEEE Trans. on Signal Processing,* vol. 48 no. 6, pp. 1726-1736, June 2000.

[2] L. Agarossi, S. Bellini, A. Canella and P. Migliorati, "A Volterra model for the high density optical disc", *Proc. 1998 IEEE Int. Conf. Acoustic, Speech, Signal Processing*, vol. 3, pp. 1605-1608, Seattle, WA.

[3] B. D. O. Anderson and J. B. Moore, *Optimal Filtering,* Prentice Hall, Englewwod Cliffs, NJ, 1979.

[4] S. Benedetto, E. Biglieri and V. Castellani, *Digital Transmission Theory*, Prentice Hall, Englewwod Cliffs, NY, 1987.

[5] S. Benedetto, E. Biglieri and R. Daffara, 'Modeling and performance evaluation of nonlinear satellite links – A Volterra series approach', *IEEE Trans. Aerospace and Electronics Systems*, vol. 15 no. 4, pp. 494-506, July 1979.

[6] E. Biglieri, E. Chiaberto, G. P. Maccone and E. Viterbo, "Compensation of nonlinearities in high-density magnetic recording channels", *IEEE Trans. Magnetics*, vol. 30 no. 6, pp. 5079-5086, November 1994.

[7] J. A. C. Bingham, "Multicarrier modulation for data transmission: An idea whose time has come", *IEEE Communications Mag.*,vol. 28 no. 5, pp. 5-14, May 1990.

[8] D. Brillinger, *Time Series: Data Analysis and Theory*, Holden-Day, San Francisco, CA, 1981.

[9] O. Egger, W. Li and M. Kunt, 'High compression image coding using an adaptive morphological subband decomposition', *Proc. IEEE*, vol. 83 no. 2, pp. 272-287, February 1995.

[10] K. Feher, *Digital Communications – Satellite/Earth Station Engineering*, Prentice Hall, Englewood Cliffs, NY, 1993.

[11] W. A. Gardner and T. L. Archer, "Exploitation of cyclostationarity for identifying the Volterra kernels of nonlinear systems", *IEEE Trans. Information Theory*, vol. 39 no. 2, pp. 535-542, March 1993.

[12] G. B. Giannakis and E. Serpedin, "Linear multichannel blind equalizers of non-linear FIR Volterra channels", *IEEE Trans. Signal Processing*, vol. 45 no. 1, pp. 67-81, January 1997.

[13] F. J. Hampton and J. C. Pesquet, 'M-band nonlinear subband decompositions with perfect reconstruction', *IEEE Trans. Image Processing*, vol. 7 no. 11, pp. 1547-1560, November 1998.

[14] S. Haykin, *Adaptive Filter Theory, 3rd ed.,* Prentice Hall, Upper Saddle River, NJ, 1996.

[15] R. Hermann, "Volterra modeling of digital magnetic saturation recording channels", *IEEE Trans. Magnetics*, vol. 26 no. 5, pp. 2125-2127, September 1990.

[16] H. H. Hopkins, 'Diffraction theory of laser readout system for optical video disc', *J. Opt. Soc. Amer.*, vol. 69, pp. 4-24, 1979.

[17] Y. Hua, H. Yang and W. Qiu, "Source correlation compensation for blind channel identification based on second-order statistics", *IEEE Signal Processing Letters,* vol. 1 no. 8, pp. 119-120, August 1994.

[18] T. Kailath, A. Vieira and M. Morf, "Inverses of Toeplitz operators, innovations, and orthogonal polynomials", *SIAM Review,* vol. 20 no. 1, pp. 106-119, January 1978.

[19] P. Lancaster and M. Tismenetsky, *The theory of matrices*, Academic Press, 1985.

[20] A. Liavas, P. A. Regalia and J.-P. Delmas, "Blind channel approximation: effective channel order determination", *IEEE Trans. Signal Processing,* vol. 47 no. 12, pp. 3336-3344, December 1999.

[21] E. Moulines, P. Duhamel, J.-F. Cardoso and S. Mayrargue, "Subspace methods for the blind identification of multichannel FIR filters", *IEEE Trans. Signal Processing,* vol. 43 no. 2, pp. 516-525, February 1995.

[22] C. B. Papadias and D. T. M. Slock, "Fractionally spaced equalization of linear polyphase channels and related blind techniques based on multichannel linear prediction", *IEEE Trans. Signal Processing*, vol. 47 no. 3, pp. 641-654, March 1999.

[23] S. Pasupathy, "Minimum shift keying: A spectrally efficient modulation", *IEEE Communications Magazine*, pp.14-22, July 1979.

[24] J. G. Proakis, *Digital Communications*, 2nd ed., McGraw-Hill, New York, 1989.

[25] S. U. H. Qureshi, "Adaptive equalization", *Proc. IEEE*, vol. 37 no. 9, pp. 1340-1387, September 1985.

[26] G. M. Raz and B. D. Van Veen, "Blind equalization and identification of nonlinear and IIR systems–A Least Squares approach", *IEEE Trans. Signal Processing*, vol. 48 no. 1, pp. 192-200, January 2000.

[27] A. A. M. Saleh, "Frequency-independent and frequency-dependent nonlinear models of TWT amplifiers", *IEEE Trans. Communications*, vol. 29 no. 11, pp. 1715-1720, November 1981.

[28] L. Tong and S. Perreau, "Multichannel blind identification: from subspace to maximum likelihood methods", *Proc. IEEE*, vol. 86 no. 10 , pp. 1951-1968, October 1998.

[29] L. Tong, G. Xu and T. Kailath, "Blind identification and equalization based on second-order statistics: a time-domain approach", *IEEE Trans. Information Theory*, vol. 40, no. 2, pp. 340-350, March 1994.

[30] M. Tsatsanis and H. Cirpan, "Blind identification of nonlinear channels excited by discrete alphabet inputs", *Proc. 1996 IEEE Signal Proc. Workshop Statistical Signal Array Processing*, vol. 1, pp. 176-179, Corfu, Greece.

[31] P. P. Vaidyanathan, *Multirate Systems and Filter Banks*, Prentice-Hall, Englewood Cliffs, NY, 1993.

[32] G. Xu, H. Liu, L. Tong and T. Kailath, "A Least-Squares approach to blind channel identification" *IEEE Trans. Signal Processing*, vol. 43, no. 12, pp. 2982-2993, December 1995.

[33] E. Zervas, J. Proakis and V. Eyuboglu, "Effects of constellation shaping on blind equalization", *SPIE vol. 1565 Adaptive Signal Processing*, pp. 178–187, August 1991.